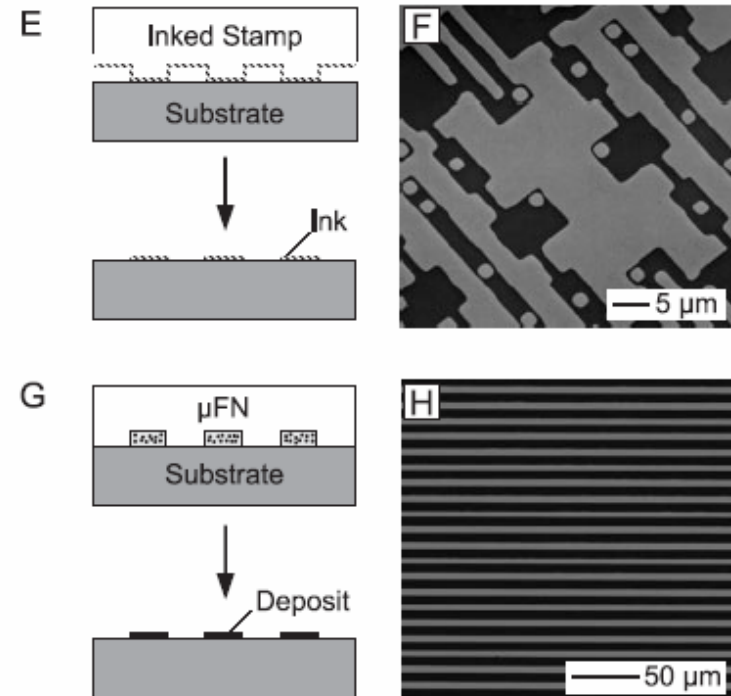
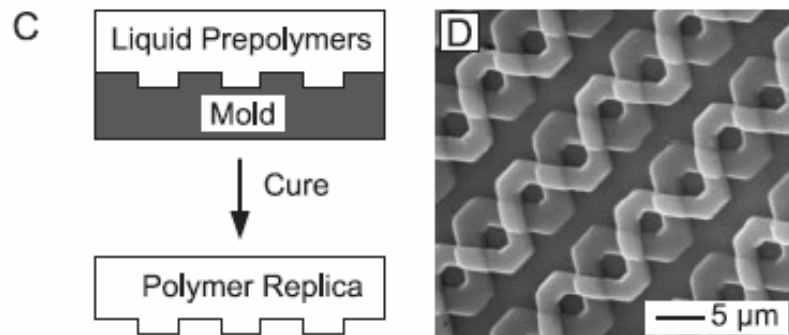
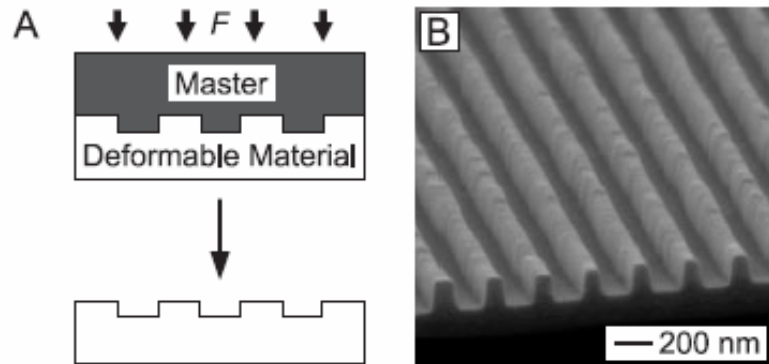
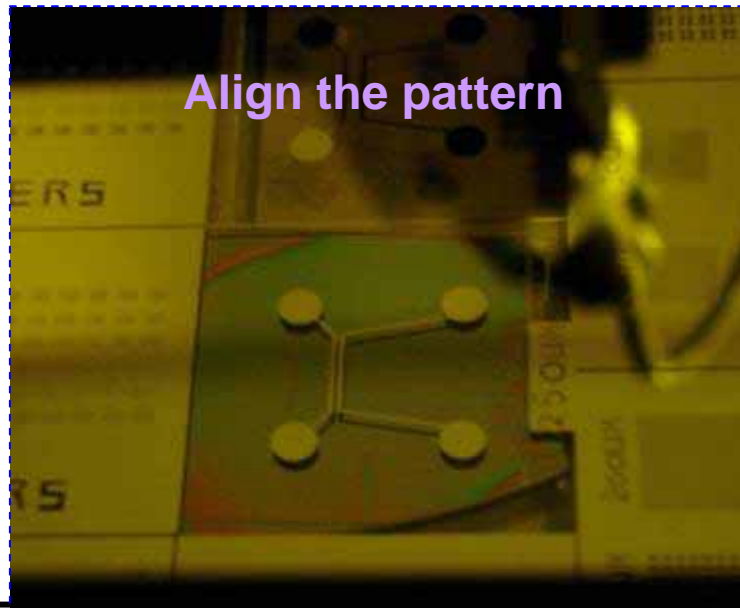
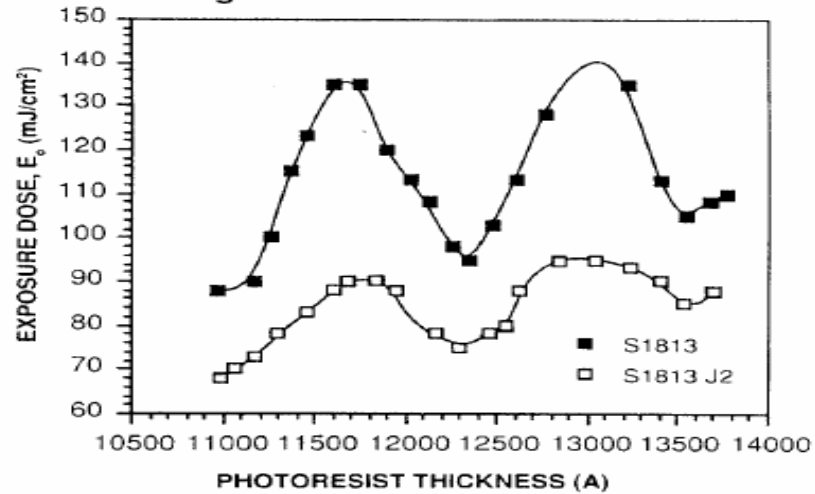


Replication

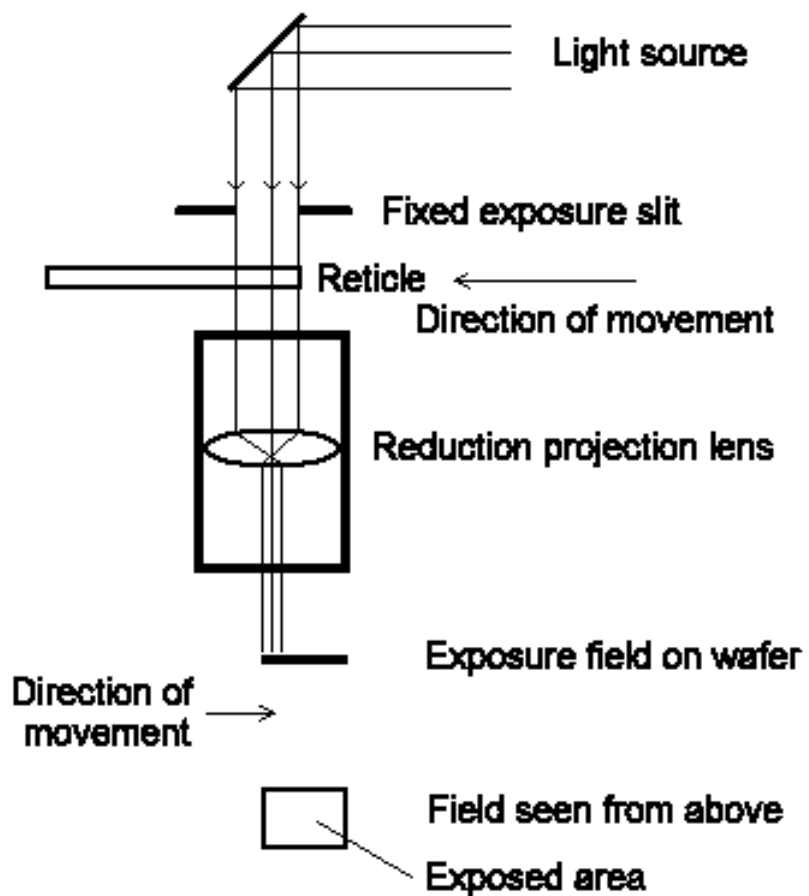
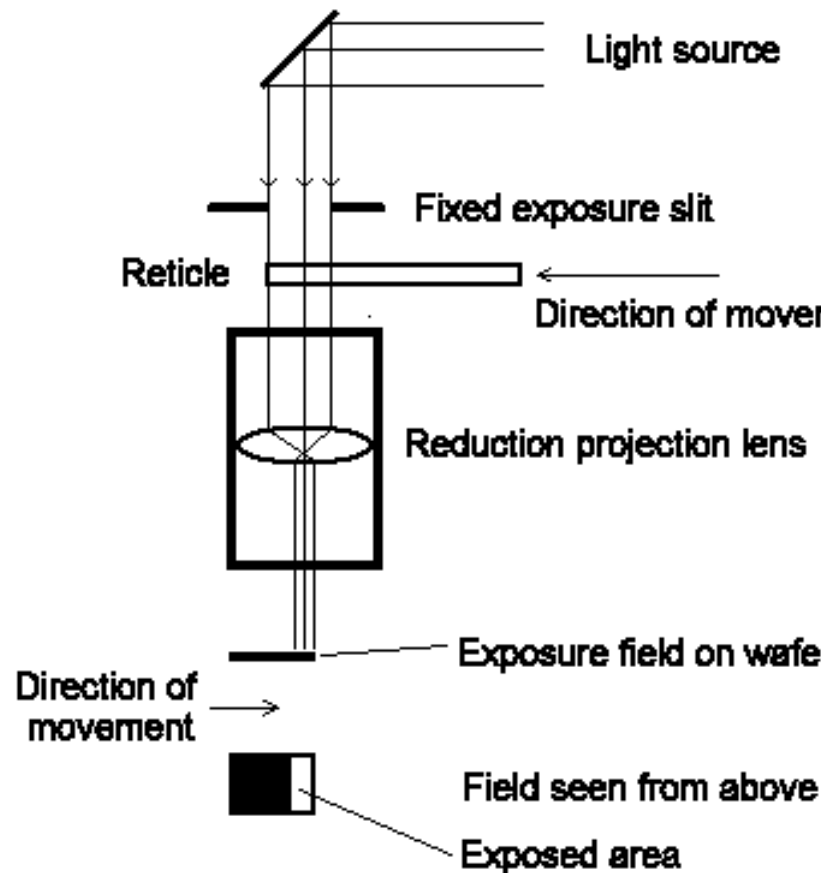


Align the pattern and Exposure

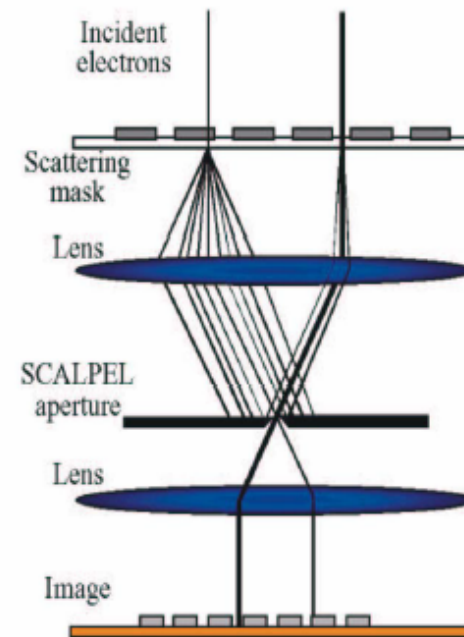
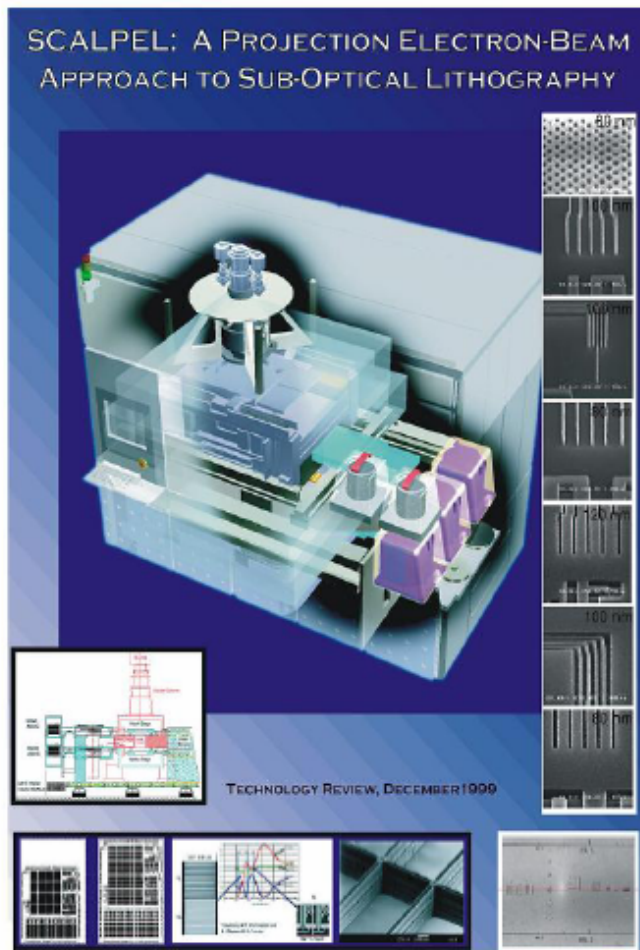
MICROPOSIT S1813 and S1813 J2 PHOTO RESISTS
Figure 4. Interference Curves



Stepper

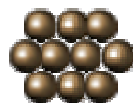


E-beam Projection



Bell Lab (1999)

There 'was' a consortium including Applied Materials, Inc. and ASM Lithography Holding N.V.; Lucent Technologies Inc.; Motorola, Semiconductor Products Sector; Samsung Electronics Co., Ltd.; and Texas Instruments Incorporated (TI).



Imprint Lithography with 25-Nanometer Resolution

Stephen Y. Chou; Peter R. Krauss; Preston J. Renstrom

Science, New Series, Volume 272, Issue 5258 (Apr. 5, 1996), 85-87.

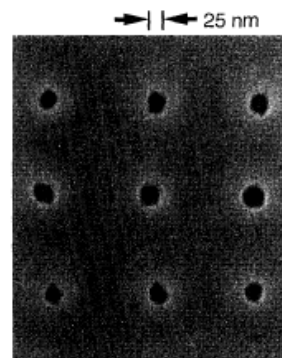


Fig. 2. SEM micrograph of a top view of holes 25 nm in diameter with a period of 120 nm, formed by compression molding into a PMMA film.

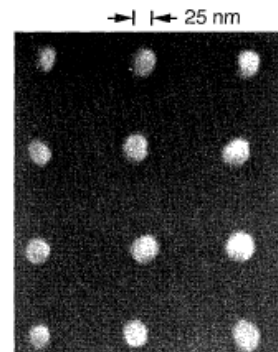


Fig. 5. SEM micrograph of the substrate in Fig. 2, after deposition of metal and a lift-off process. The diameter of the metal dots is 25 nm, the same as that of the original holes created in the PMMA.

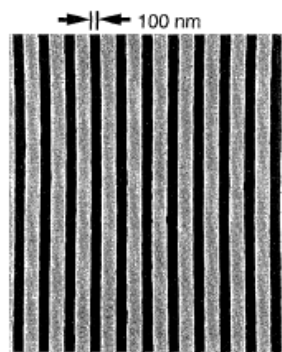


Fig. 3. SEM micrograph of a top view of trenches 100 nm wide with a period of 250 nm, formed by compression molding into a PMMA film.

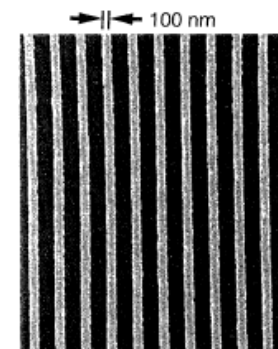
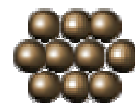
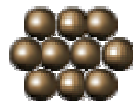
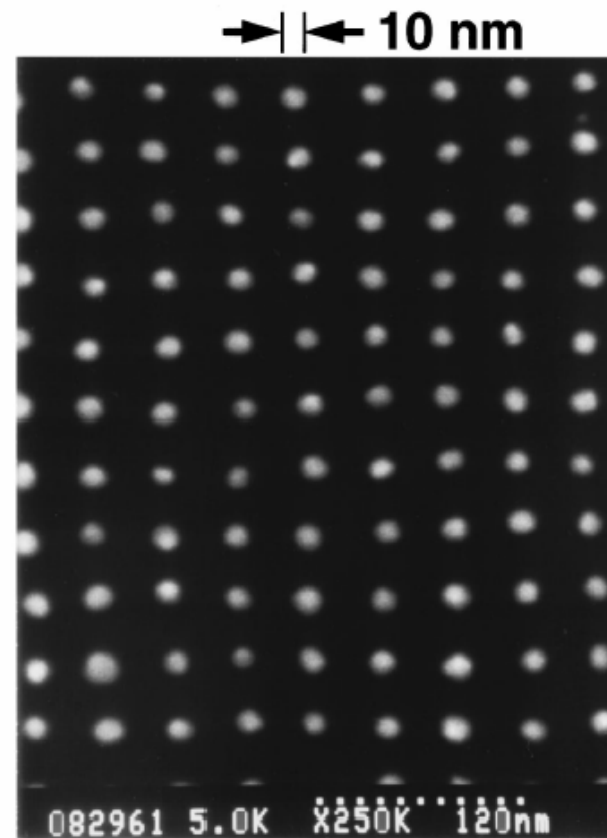
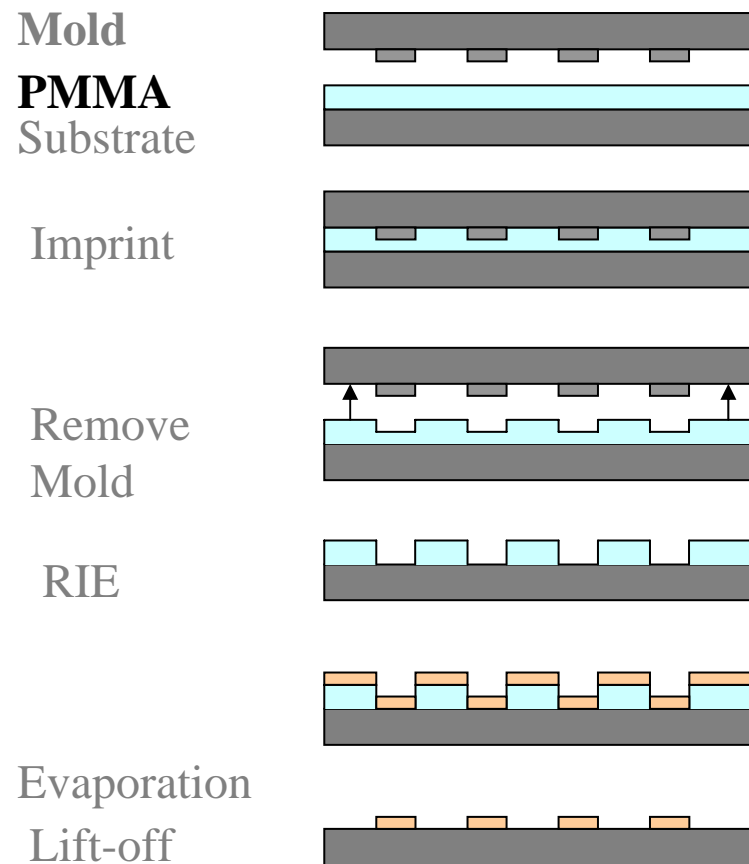


Fig. 6. SEM micrograph of the substrate in Fig. 3, after deposition of metal and a lift-off process. The metal linewidth is 100 nm, the same as the width of the original PMMA trenches.



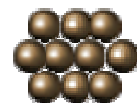
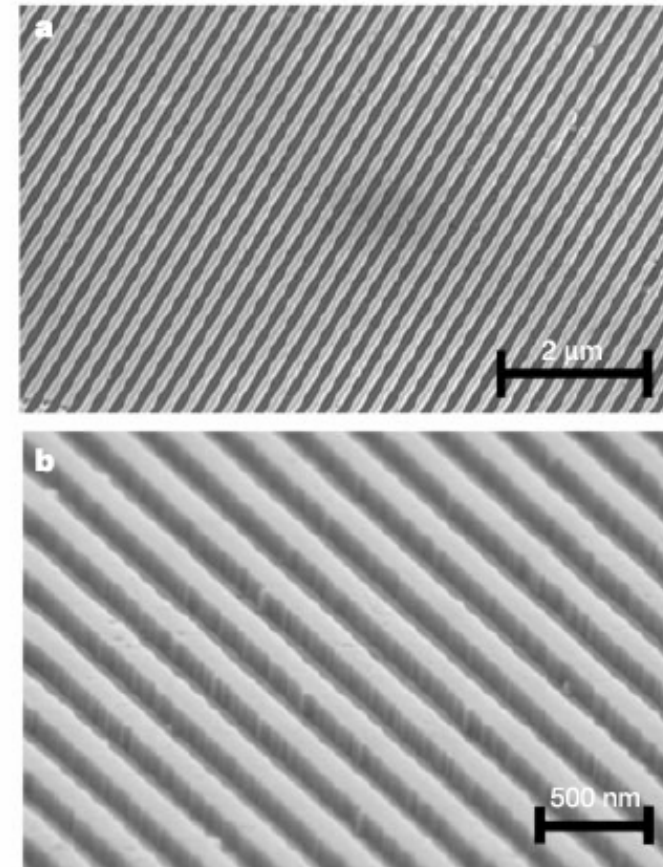
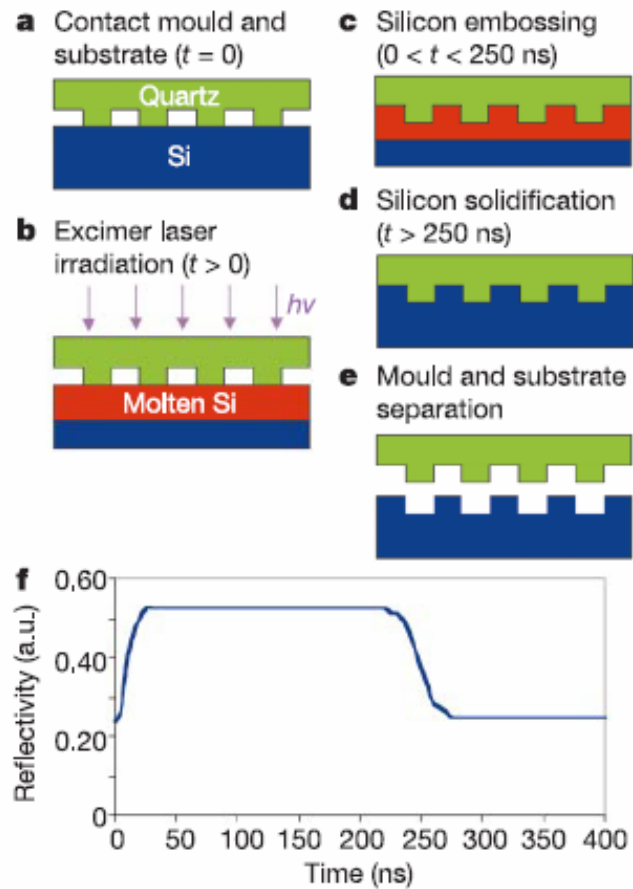
Nanoimprint Lithography



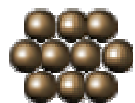
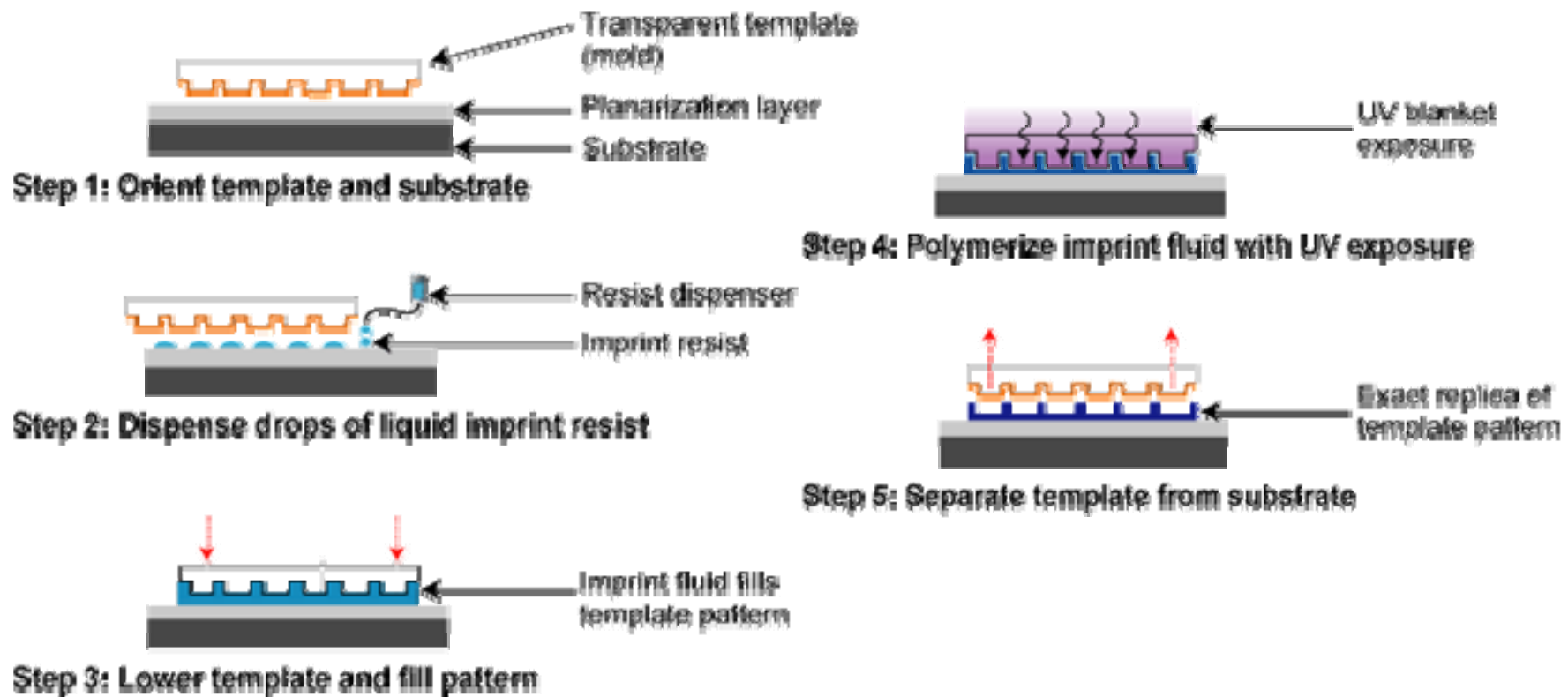
Ultrafast and direct imprint of nanostructures in silicon

NATURE | VOL 417 | 20 JUNE 2002 |

Stephen Y. Chou*, Chris Keimel & Jian Gu



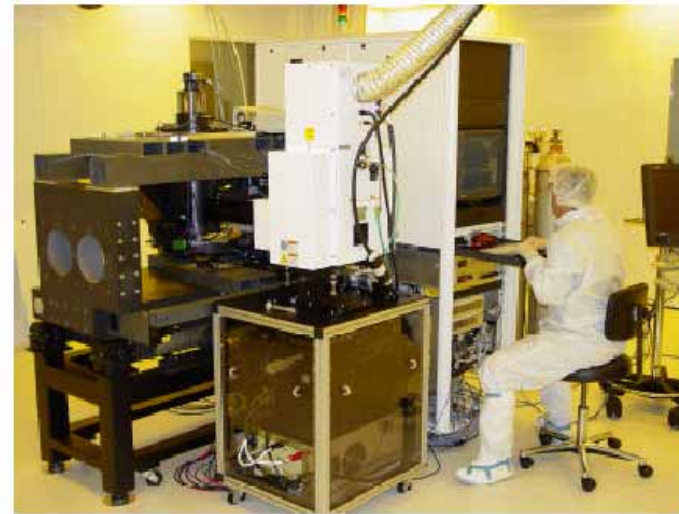
Step and Flash Imprint Lithography



Nanoimprintors



NX-2000, Nanoimprintor, Nanonex



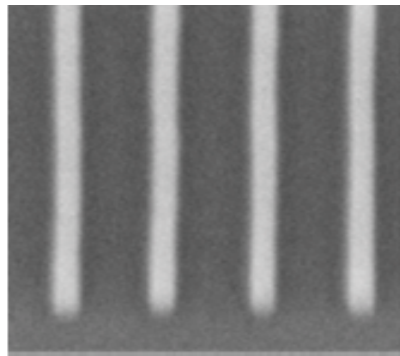

IMPRIO
100



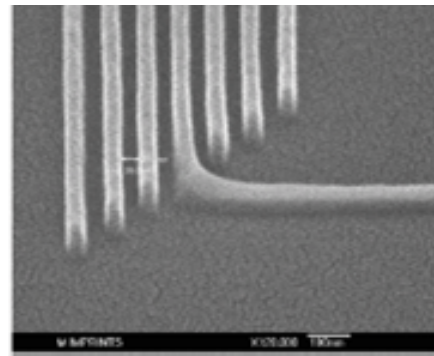
- Resolution: Sub-50 nanometers, imprint template (mold) limited.
- Alignment: < 500 nm, 3σ (X, Y, and Rotation).
- Flexibility: Handles up to 8 inch wafers, including fragile substrates.
- Field size: 25 x 25 mm full active print area, 100 μ m street width.



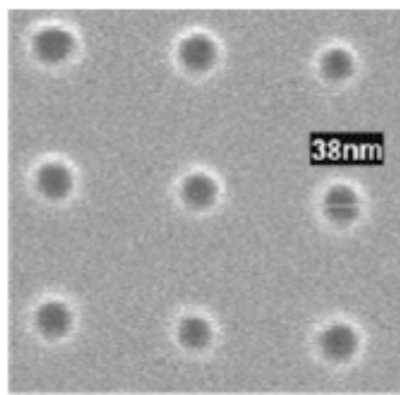
Imprinting Result



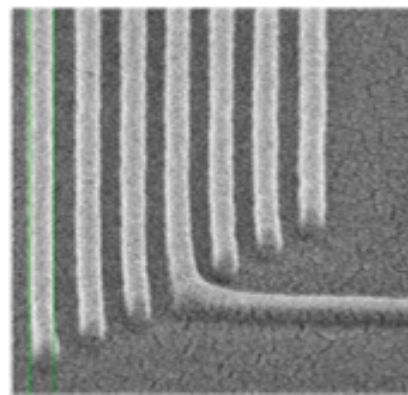
Imprinted 20 nm isolated lines



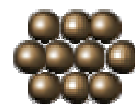
Imprinted 30 nm dense lines



Imprinted sub-40 nm contacts



Imprinted 50 nm dense lines



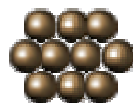
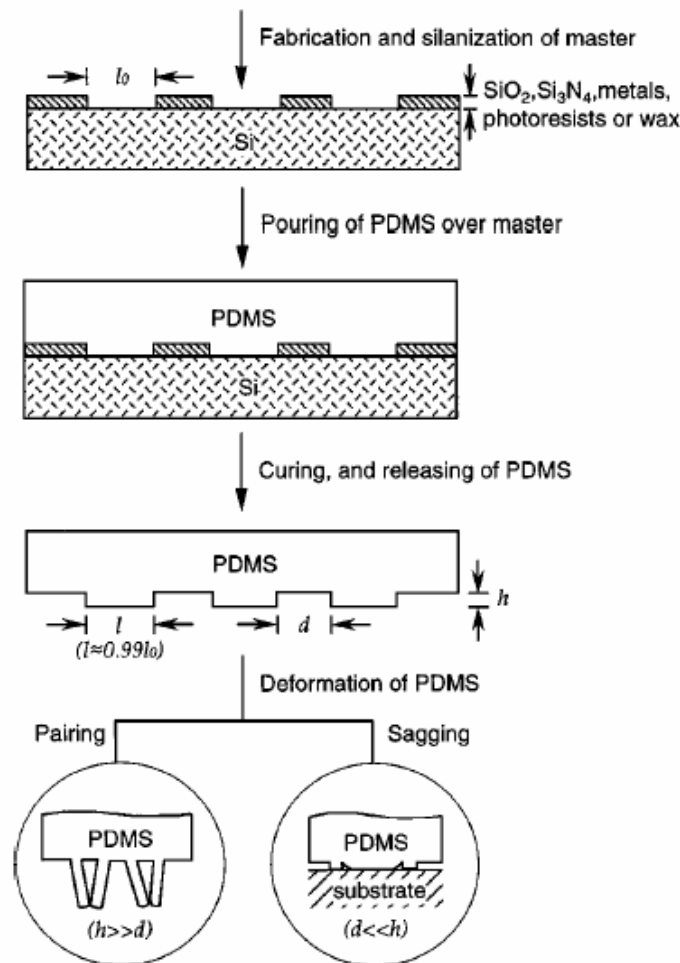
Challenges

- Mask Fabrication (1:1)
- Lift-off process
- Resist
- Mask Design



Soft Lithography

Annu. Rev. Mater. Sci. 1998. 28:153–84



Soft Lithography

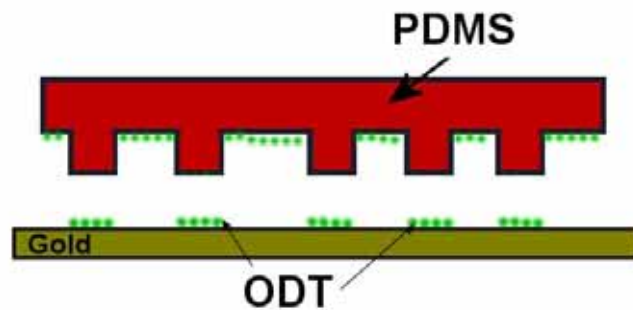
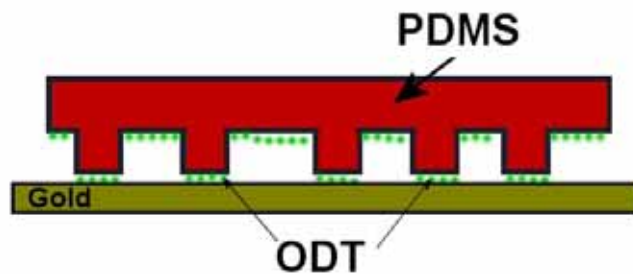
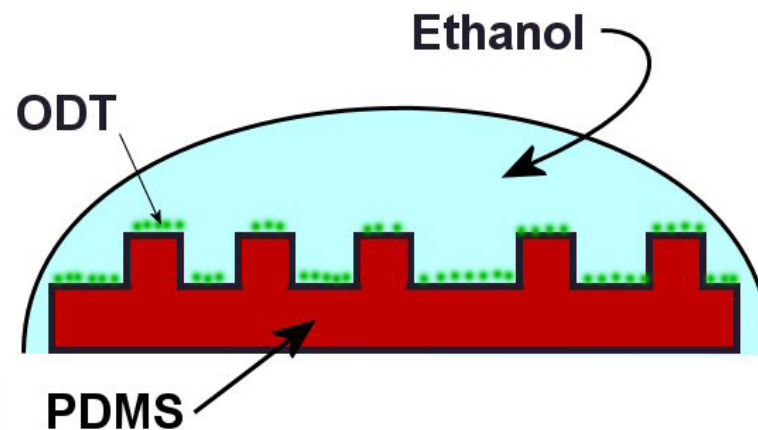
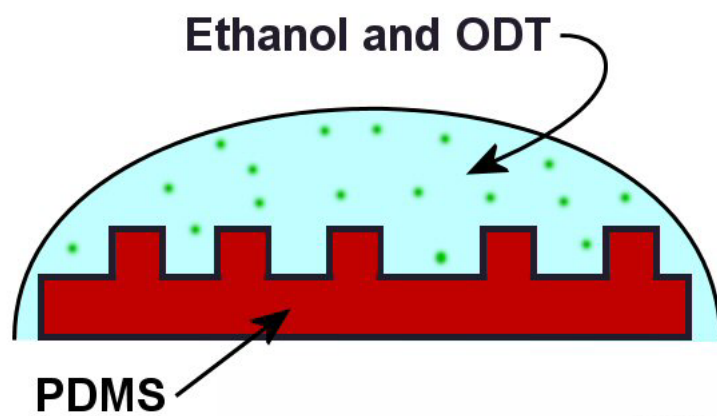
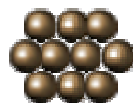


Table 1 Comparison between photolithography and soft lithography

| | Photolithography | Soft lithography |
|--|--|---|
| Definition of patterns | Rigid photomask (patterned Cr supported on a quartz plate) | Elastomeric stamp or mold (a PDMS block patterned with relief features) |
| Materials that can be patterned directly | Photoresists (polymers with photo- sensitive additives) SAMs on Au and SiO ₂ | Photoresists ^{a,e} SAMs on Au, Ag, Cu, GaAs, Al, Pd, and SiO ₂ ^a Unsensitized polymers ^{b-e} (epoxy, PU, PMMA, ABS, CA, PS, PE, PVC) Precursor polymers ^{c,d} (to carbons and ceramics) Polymer beads ^d Conducting polymers ^d Colloidal materials ^{a,d} Sol-gel materials ^{c,d} Organic and inorganic salts ^d Biological macromolecules ^d |
| Surfaces and structures that can be patterned | Planar surfaces 2-D structures | Both planar and nonplanar Both 2-D and 3-D structures |
| Current limits to resolution | ~250 nm (projection) ~100 nm (laboratory) | ~30 nm ^{a,b} , ~60 nm ^e , ~1 μ m ^{d,e} (laboratory) |
| Minimum feature size | ~100 nm (?) | 10 (?) - 100 nm |

^{a-e}Made by (a) μ CP, (b) REM, (c) μ TM, (d) MIMIC, (e) SAMIM. PU:polyurethane; PMMA: poly(methyl methacrylate); ABS: poly(acrylonitrile-butadiene-styrene); CA: cellulose acetate; PS: polystyrene; PE: polyethylene; and PVC: poly(vinyl chloride)



Micro-contact Printing

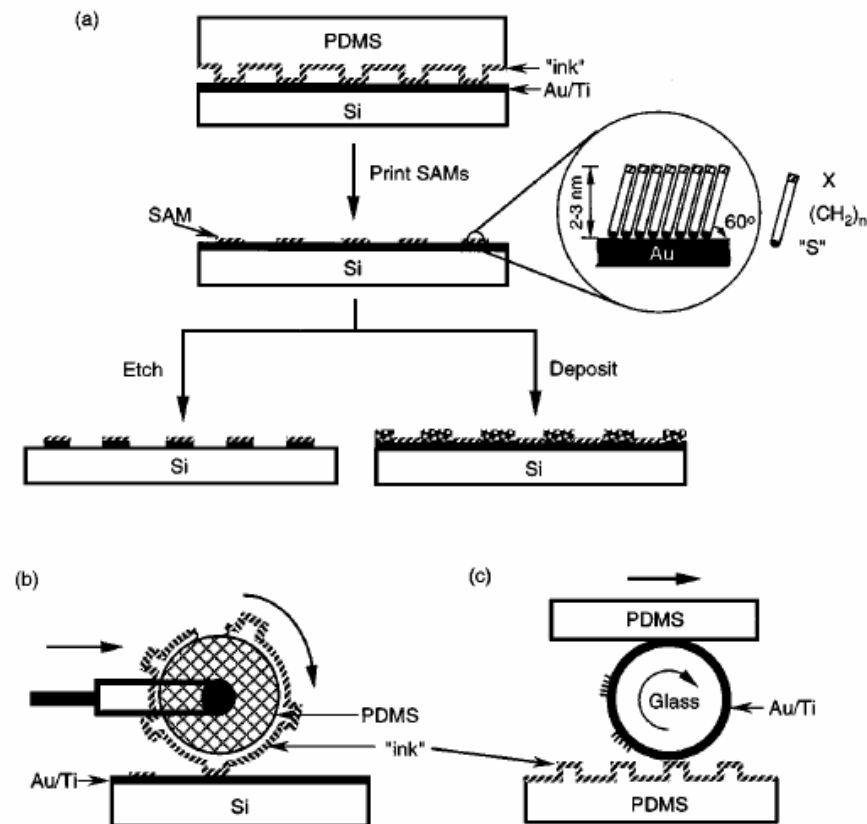
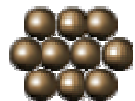


Figure 2 Schematic procedures for μ CP of hexadecanethiol (HDT) on the surface of gold: (a) printing on a planar surface with a planar stamp (21), (b) printing on a planar surface over large areas with a rolling stamp (128), and (c) printing on a nonplanar surface with a planar stamp (174).



Micro-contact Printing

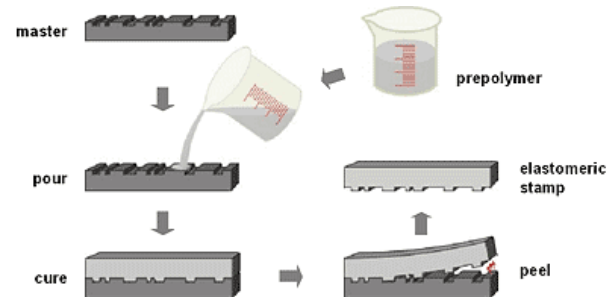


Fig.2 The stamp replication process: A master with a negative of the desired pattern is cast with a pre-polymer. After curing the polymer, the elastomeric stamp is peeled off the master and ready for microcontact printing.

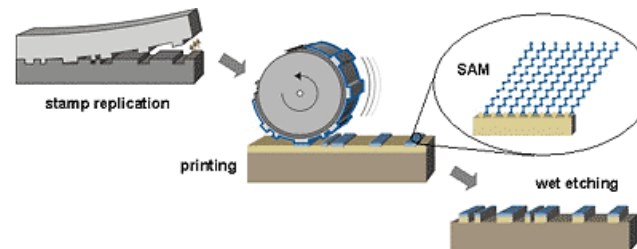
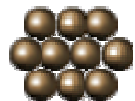
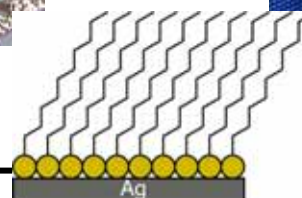
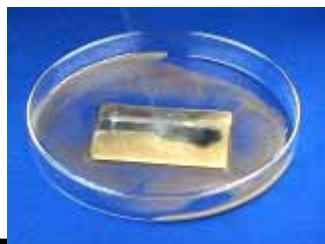
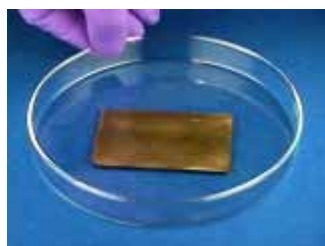
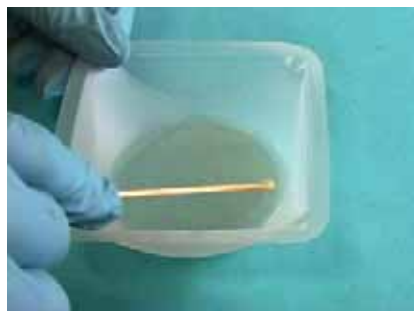
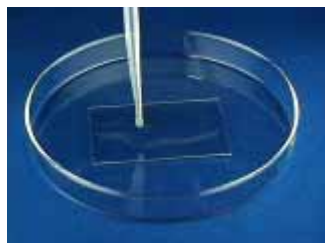


Fig.1 The microcontact printing (μ CP) process: An elastomeric stamp is replicated from a master. After inking of the stamp with a suitable ink, it is fixated on a printing machine with help of which it is brought into conformal contact with a substrate. There the ink forms a self-assembled monolayer (SAM) which can be used as a resist in a subsequent wet etching step.

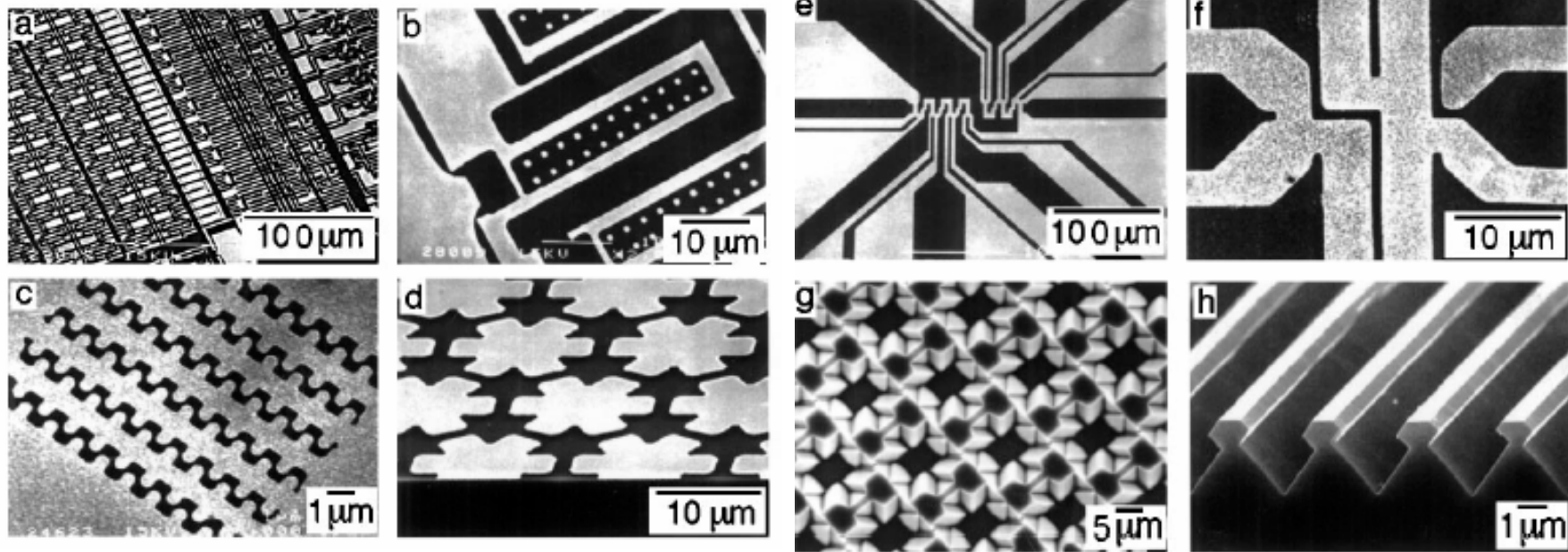


Micro-contact Printing

<http://mrsec.wisc.edu/Edetc/nanolab/print/text.html>

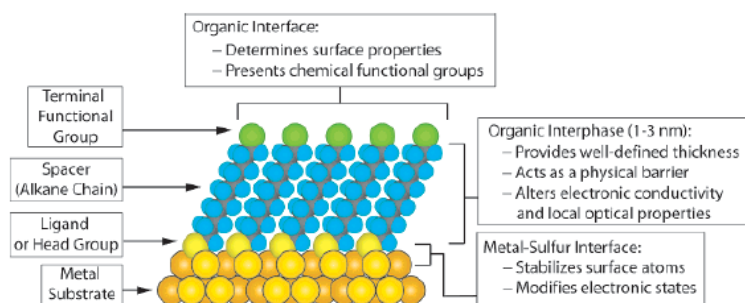


Micro-contact Printing



Self-Assemble Monolayer (SAM)

Chem. Rev. 2005, 105, 1103–1169



S-Au 25-30 Kcal/mole
Si-O 190 kcal/mole

| Morphology of Substrate | | | | Morphology of Substrate | | | |
|---------------------------------------|---|-----------------------------|---------------------------------------|--|--|-----------------------------|---------------------------------------|
| Ligand | Substrates | Thin Films or Bulk Material | Nanoparticles or Other Nanostructures | Ligand | Substrates | Thin Films or Bulk Material | Nanoparticles or Other Nanostructures |
| ROH | Fe ₂ O ₃ | 36 | 35 | RSSR' | Ag | 89 | 90 |
| | Si-H | 37 | | | Au | 20 | 90-92 |
| | Si | | | | CdS | | 61 |
| RCOO-/RCOOH | α -Al ₂ O ₃ | 38,39 | | | Pd | 30 | |
| | Fe ₂ O ₃ | | 40 | | Au | 93 | |
| | Ni | | 41,42 | | | | |
| RCOO-/OOCR | Ti/TiO ₂ | 43 | | RCSSH | Au | 94 | |
| | Si(111):H | 44 | | | CdSe | | 95 |
| Ene-diol | Fe ₂ O ₃ | | 45 | RS ₂ O ₃ ⁻ Na ⁺ | Au | 96 | 98 |
| RNH ₂ | FeS ₂ | 46 | | | Cu | 97 | |
| | Mica | 47 | | RSeH | Ag | 99 | |
| | Stainless Steel 316L | 48 | | | Au | 100,101 | |
| | YBa ₂ Cu ₃ O _{7-δ} | 49 | | | CdS | | 60 |
| RC≡N | CdSe | | 50 | | CdSe | | 102 |
| | Ag | 51 | | RSeSeR' | Au | 101 | |
| R ₂ NnN'(BF ₄) | Au | | | | | | |
| | GaAs(100) | 52 | | R ₃ P | Au | | 103 |
| | Pd | 52 | | | FeS ₂ | 46 | |
| RSH | Si(111):H | 52 | | | CdS | | 104 |
| | Ag | 26 | 53,54 | | CdSe | | 104 |
| | Ag ₂ Se | 55 | | | CdTe | | 104 |
| | AgS | | 56 | R ₃ P=O | Co | | 105,106 |
| | Au | 26 | 57 | | CdS | | 104 |
| | AmAg | | 58 | | CdSe | | 104 |
| | AuCu | | 58 | | CdTe | | 104 |
| | Au ₂ Pd _{1.4} | | 58 | RPO ₃ ²⁻ /RP(O)(OH) ₂ | Al | 107 | |
| | CdTe | | 59 | | Al-OH | 108 | |
| | CdSe | | 60 | | Ca ₁₀ (PO ₄) ₆ (OH) ₂ | 109 | |
| | CdS | | 61,62 | | GaAs | 110 | |
| | Cu | 26 | 58 | | GaN | 110 | |
| | FePt | | 63-66 | | Indium tin oxide | 111 | |
| | GaAs | 67 | | | (ITO) | | |
| | Ge | 68 | | | Mica | 112 | |
| | Hg | 69-71 | | | TiO ₂ | 113,114 | |
| | HgTe | | 72 | | ZnO ₂ | 114,115 | |
| | InP | 73 | | RPO ₄ ³⁻ | CdSe | | 116-118 |
| | Ir | | 74 | | CdTe | | 118,119 |
| | Ni | 75 | | | Al ₂ O ₃ | 120 | |
| | PbS | | 76-78 | | Nb ₂ O ₅ | 120 | |
| | Pd | 30 | 74,79 | | Ta ₂ O ₅ | 121 | |
| RSn | PdAg | | 58 | RNuC | Pt | 123 | 124 |
| | Pt | 32 | 80 | | Si | 37 | |
| | Ru | | 81 | | Si(111):H | 125 | |
| | Stainless Steel 316L | 48 | | RSiX ₃ X = H, Cl, OCH ₂ CH ₃ | HfO ₂ | 126 | |
| | YBa ₂ Cu ₃ O _{7-δ} | 82 | | | ITO | 127 | |
| | Zn | 83 | | | PtO | 128 | |
| | ZnSe | 84 | | RSeX ₃ X = H, Cl, OCH ₂ CH ₃ | TiO ₂ | 113,126,129 | |
| | ZnS | | 85 | | ZrO ₂ | 126,129 | |
| | Au | 86 | | | | | |
| | Au | | 87 | | | | |
| RSn | Au | 88 | | | | | |



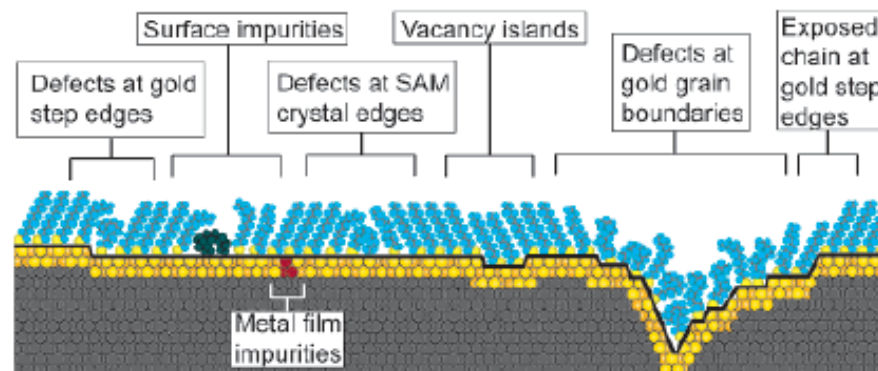
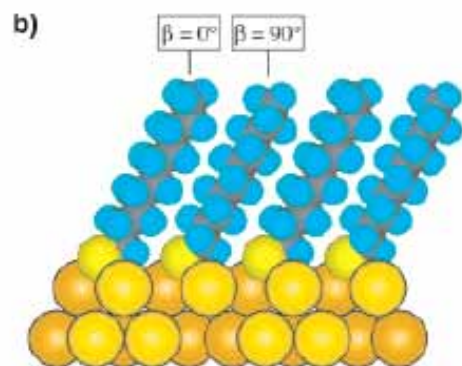
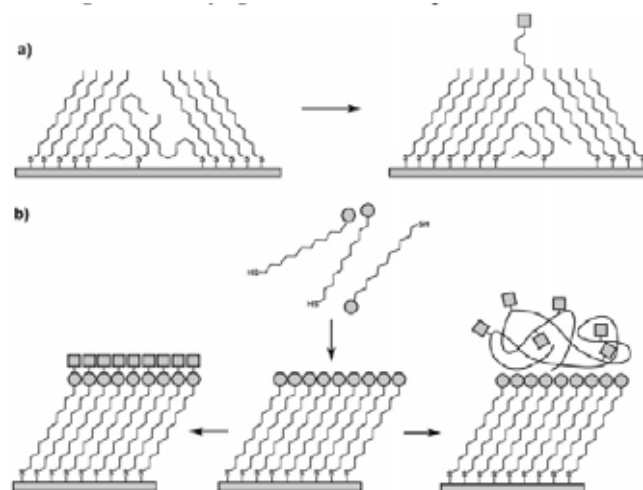
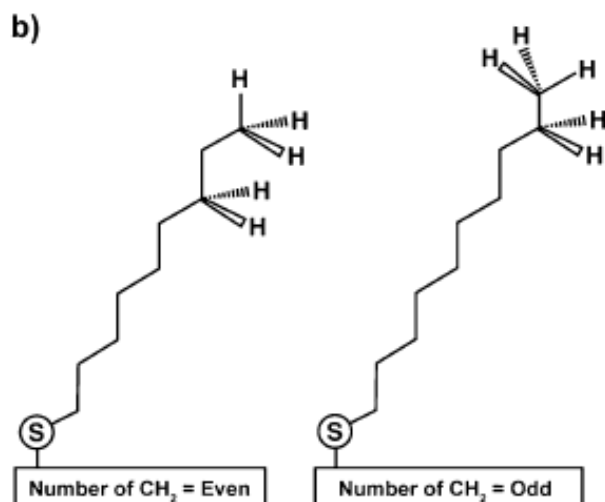


Figure 7. Schematic illustration of some of the intrinsic and extrinsic defects found in SAMs formed on polycrystalline substrates. The dark line at the metal–sulfur interface is a visual guide for the reader and indicates the changing topography of the substrate itself.



^a (a) Insertion of a functional adsorbate at a defect site in a preformed SAM. (b) Transformation of a SAM with exposed functional groups (circles) by either chemical reaction or adsorption of another material.



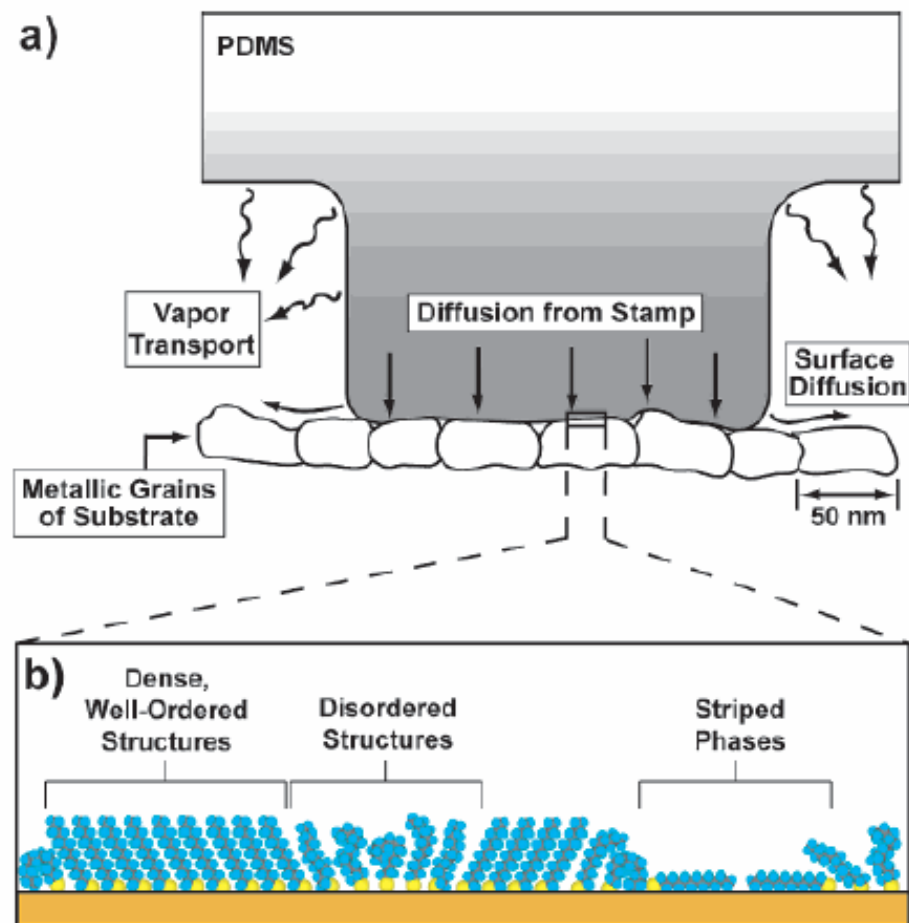


Figure 12. (a) Schematic illustration depicting the application of a PDMS stamp containing thiols to a polycrystalline metal film. The primary mechanisms of mass transport from the stamp to the surface are shown. The grayscale gradient approximates the concentration of thiols adsorbed in the stamp itself. (b) Magnified schematic view that illustrates the variety of structural arrangements found in SAMs prepared by μ CP when the stamp is wetted with a 1–10 mM solution and applied to the substrate for 1–10 s.

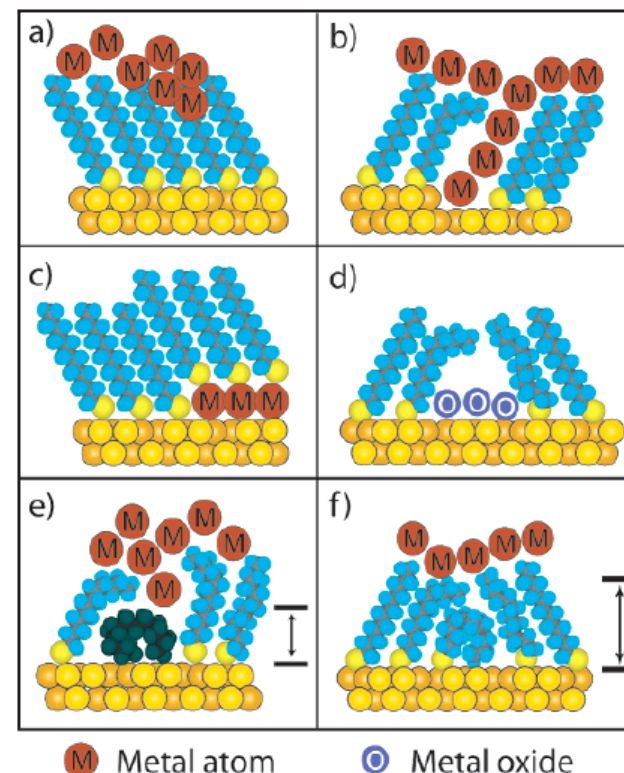


Figure 17. Schematic illustration of the types of defects in SAMs that can influence the rate of electron transfer in two-terminal (or three-terminal) devices. (a) Chemical reaction with the organic component of SAMs during evaporation of metal films. (b) Formation of metallic filaments during evaporation or operation of the device. (c) Deposition of adlayers of metal on the surface of the substrate supporting the SAM. (d) Formation of oxide impurities on the surface. (e) Organic (or organometallic) impurities in the SAM. (f) Thin regions in the SAM resulting from conformational and structural defects. In e and f the dimension normal to the surface that is denoted by the black arrows indicates the approximate shortest distance between the two metal surfaces; note that these distances are less than the nominal thickness of the ordered SAM.



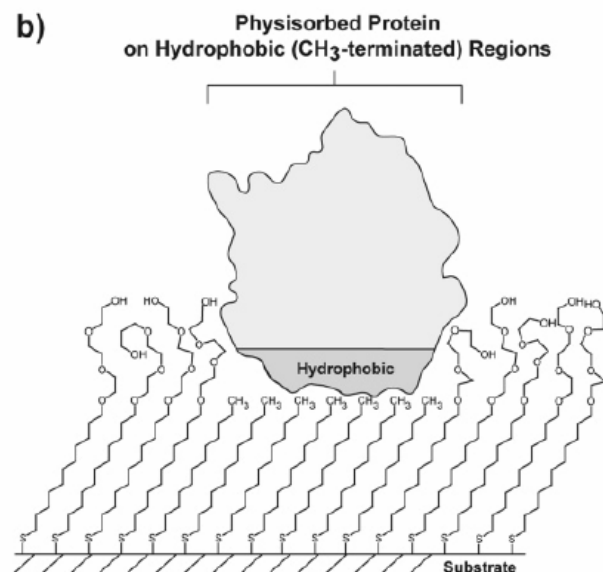
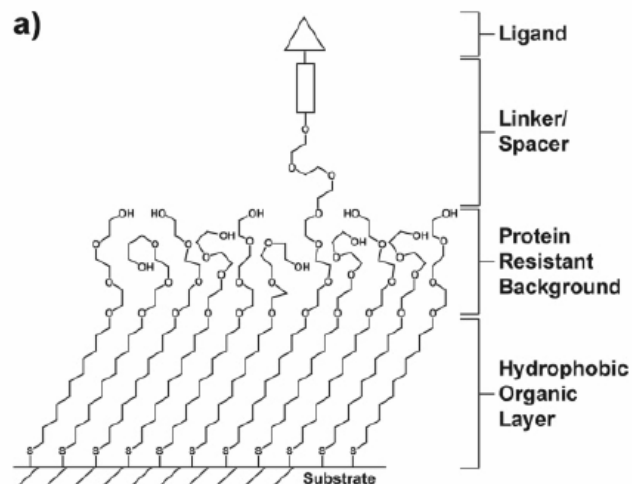


Figure 21. Schematic illustrations of (a) a mixed SAM and (b) a patterned SAM. Both types are used for applications in biology and biochemistry.

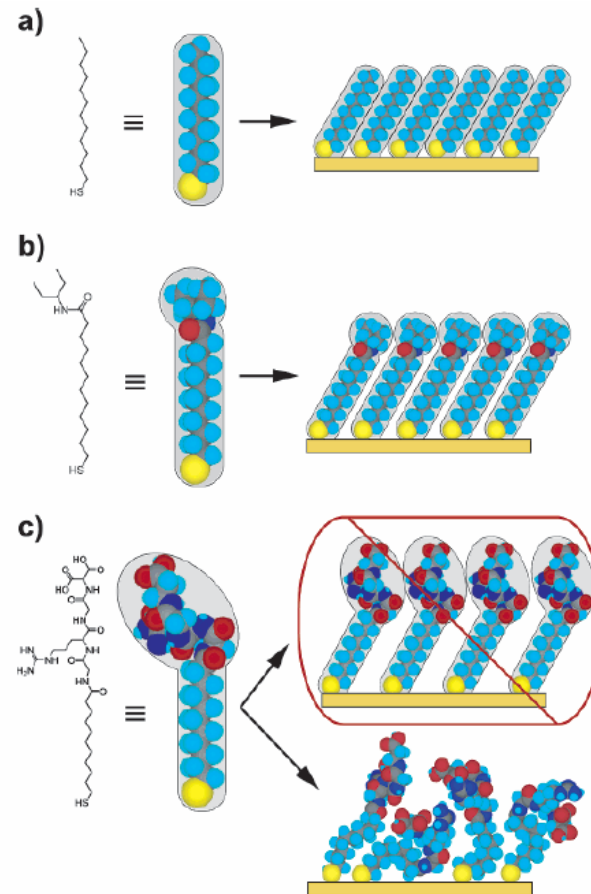


Figure 22. Schematic diagram illustrating the effects that large terminal groups have on the packing density and organization of SAMs. (a) Small terminal groups such as $-\text{CH}_3$, $-\text{CN}$, etc., do not distort the secondary organization of the organic layer and have no effect on the sulfur arrangement. (b) Slightly larger groups (like the branched amide shown here) begin to distort the organization of the organic layer, but the strongly favorable energetics of metal-sulfur binding drive a highly dense arrangement of adsorbates. (c) Large terminal groups (peptides, proteins, antibodies) sterically are unable to adopt a secondary organization similar to that for alkanethiols with small terminal groups. The resulting structures probably are more disordered and less dense than those formed with the types of molecules in a and b.



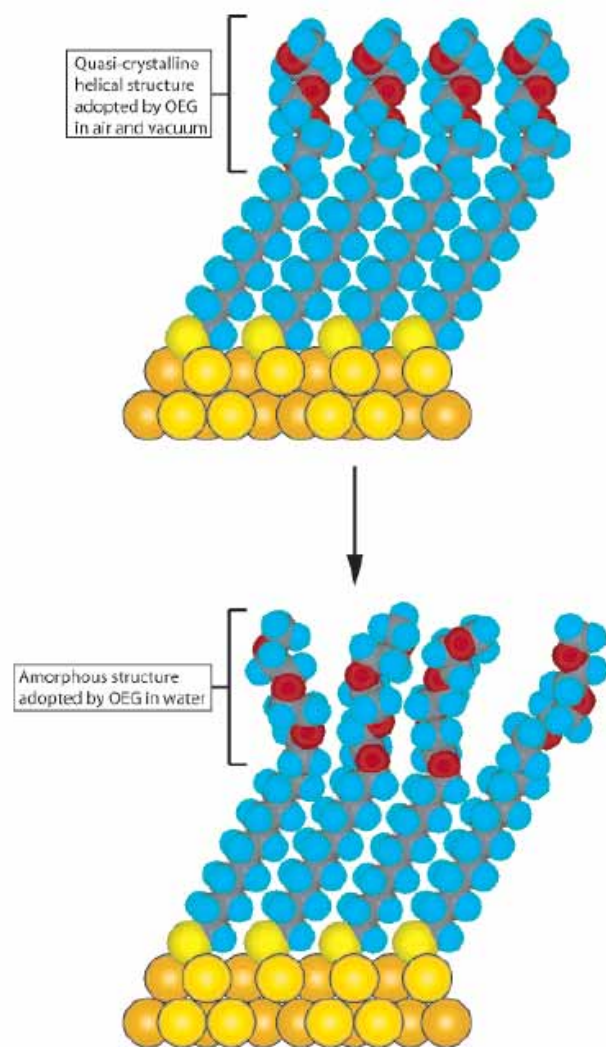
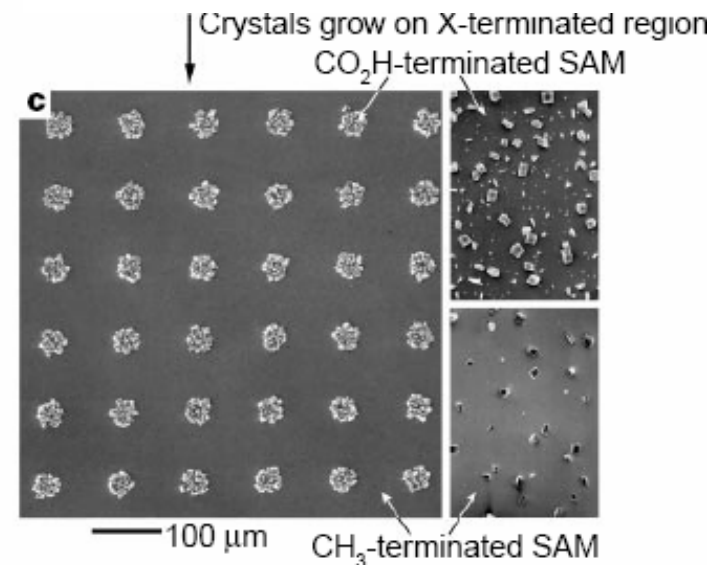
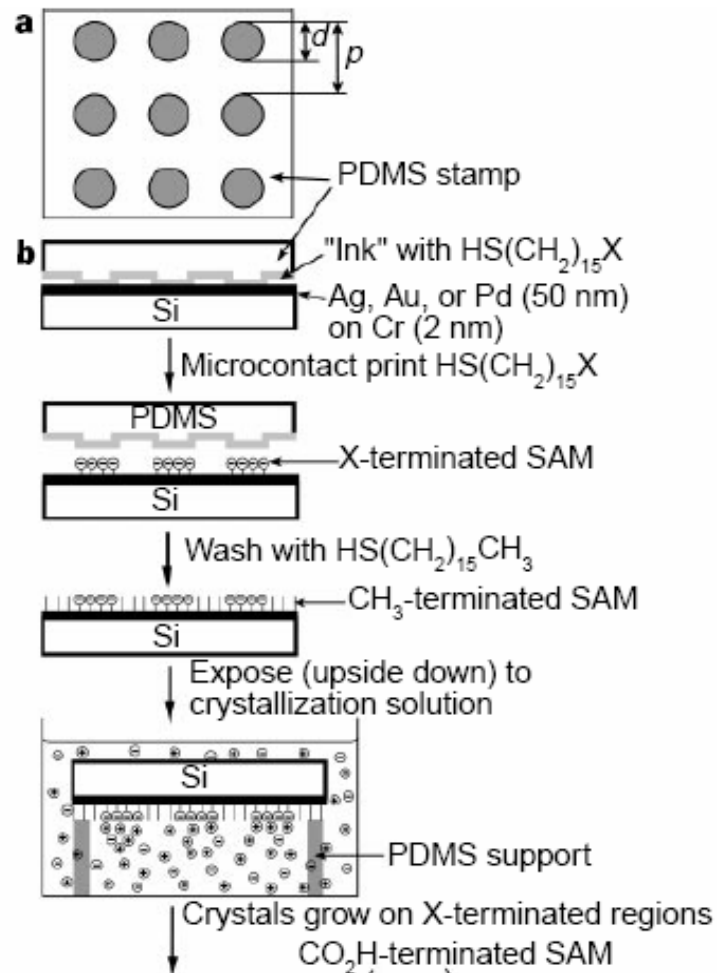


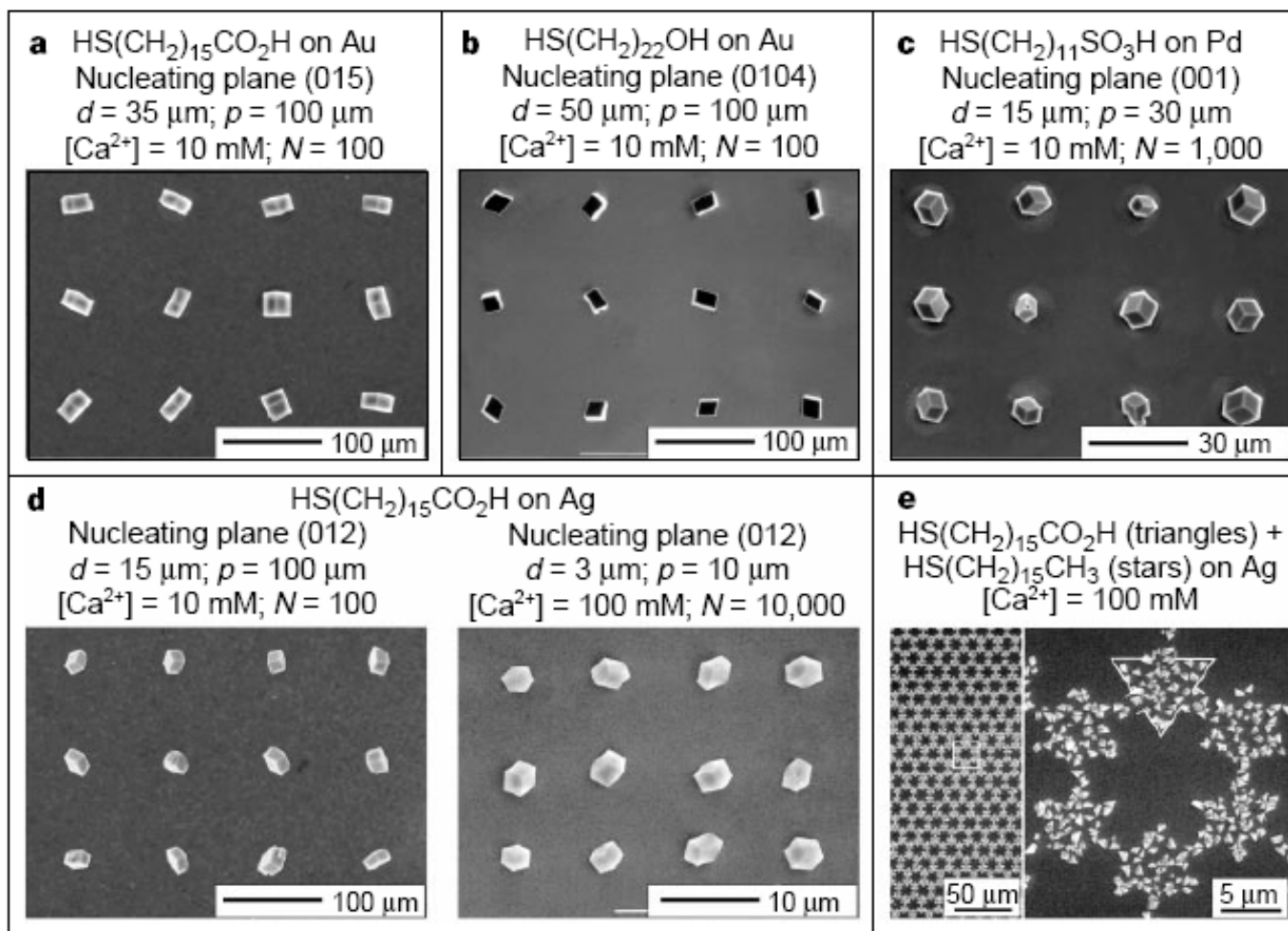
Figure 23. Schematic illustration of the order–disorder transition evidenced by SAMs of alkanethiolates terminated with triethylene glycol. The EG_3 group loses conformational ordering upon solvation in water.



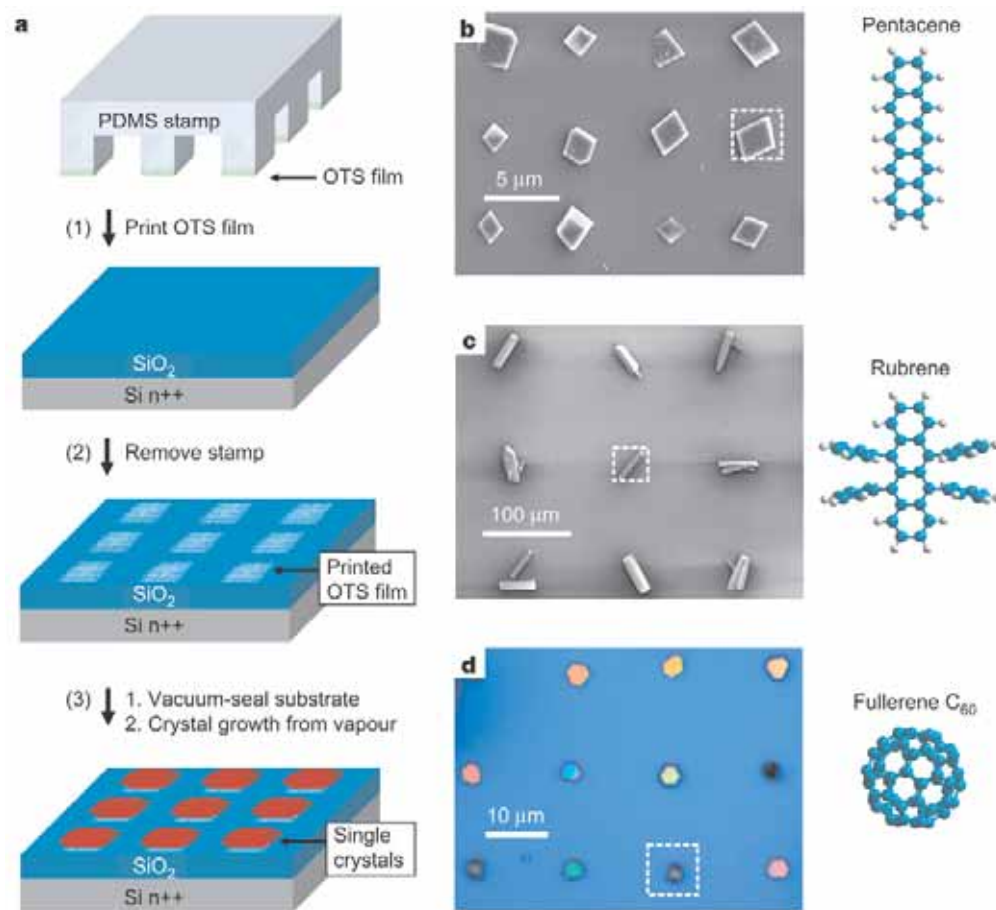
Control of crystal nucleation by patterned self-assembled monolayers

NATURE | VOL 398 | 8 APRIL 1999

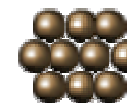




Patterning of organic single crystals



Nature 444, 913-917(14 December 2006)



Large On-Off Ratios and Negative Differential Resistance in a Molecular Electronic Device

J. Chen,¹ M. A. Reed,^{1*} A. M. Rawlett,² J. M. Tour^{2*}

19 NOVEMBER 1999 VOL 286 SCIENCE

Fig. 1. Schematics of device fabrication. (A) Cross section of a silicon wafer with a nanopore etched through a suspended silicon nitride membrane. (B) Au-SAM-Au junction in the pore area. (C) Blowup of (B) with 1c sandwiched in the junction. (D) Scanning electron micrograph (SEM) of pyramid Si structure after unisotropic Si etching [that is, the bottom view of (A)]. (E) SEM of an etched nanopore through the silicon nitride membrane. (F) The active molecular compound 1c and its precursors the free thiol 1b and the thiol-protected system 1a.

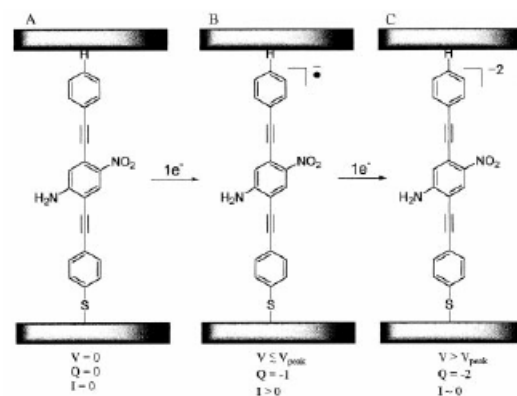
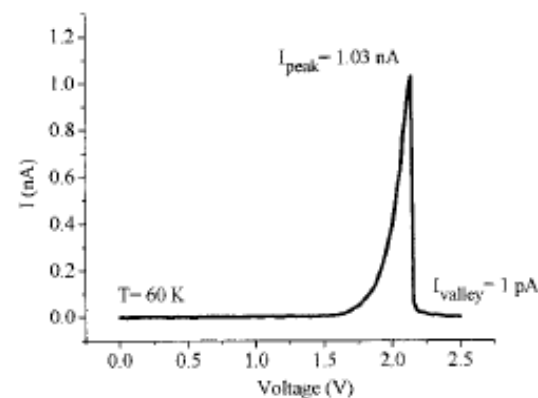
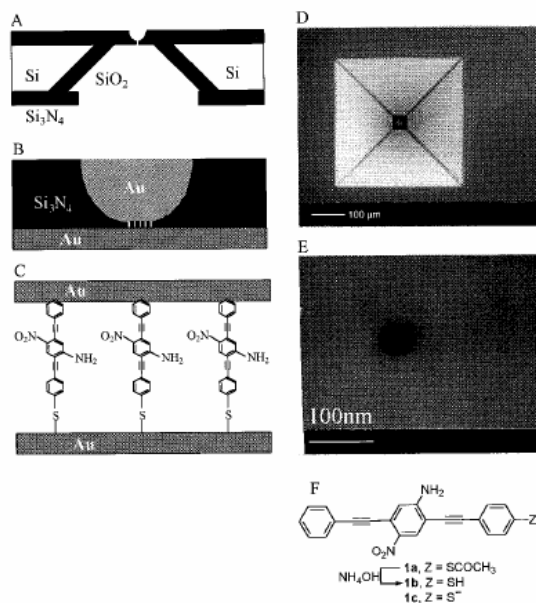


Fig. 4. Potential mechanism for the NDR effect. As voltage is applied, the molecules in the SAM (A) undergo a one-electron reduction to form the radical anion (B) that provides a conductive state. Further increase of the voltage causes another one-electron reduction to form the dianion insulating state (C). Q is the charge.



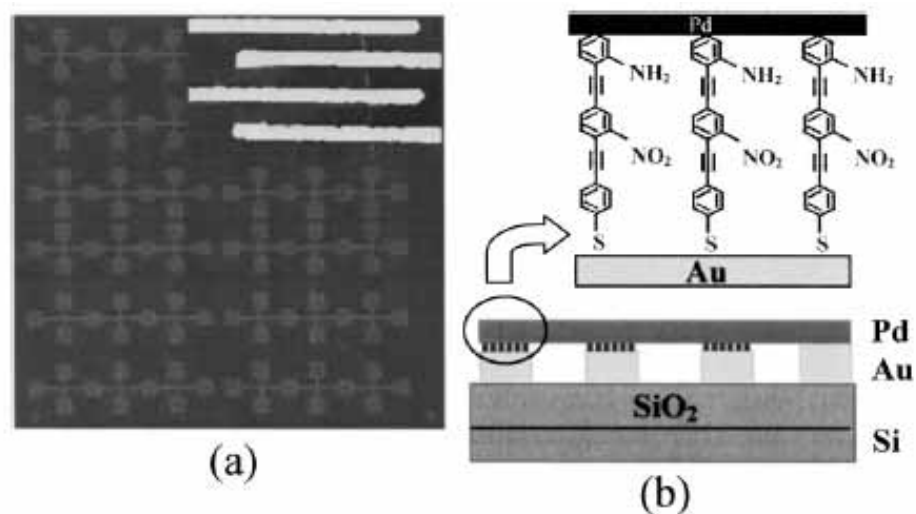


FIG. 1. (a) Optical micrograph of the nanoelectrode array. Inset: AFM image of four Au nanoelectrodes with a Pd nanowire lying across. (b) Schematic diagram of the Pd/molecular wires/Au junctions on a Si/SiO₂ substrate.

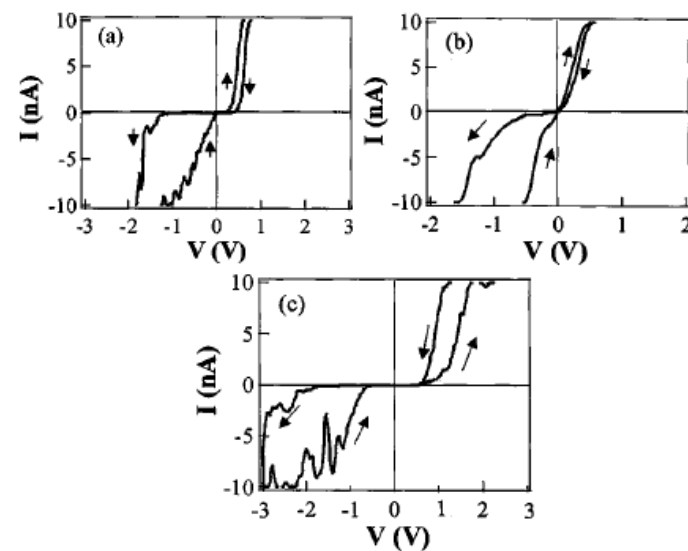
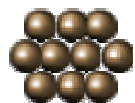
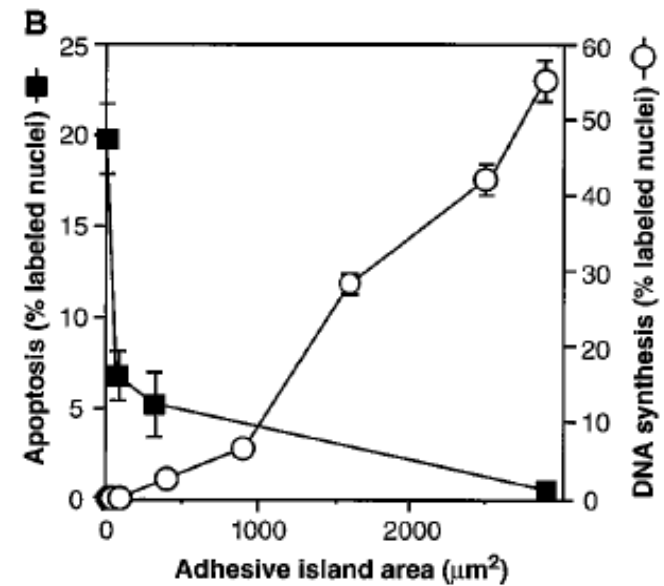
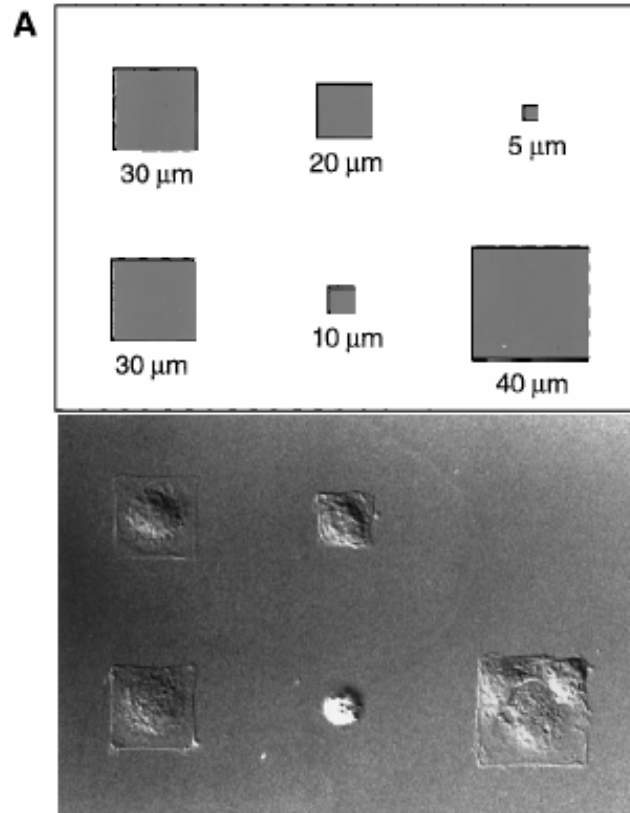


FIG. 3. Typical I - V curves of molecular devices. (a), (b), and (c) correspond to molecules a, b, and c shown in Fig. 2, respectively.



Geometric Control of Cell Life and Death

• SCIENCE • VOL. 276 • 30 MAY 1997



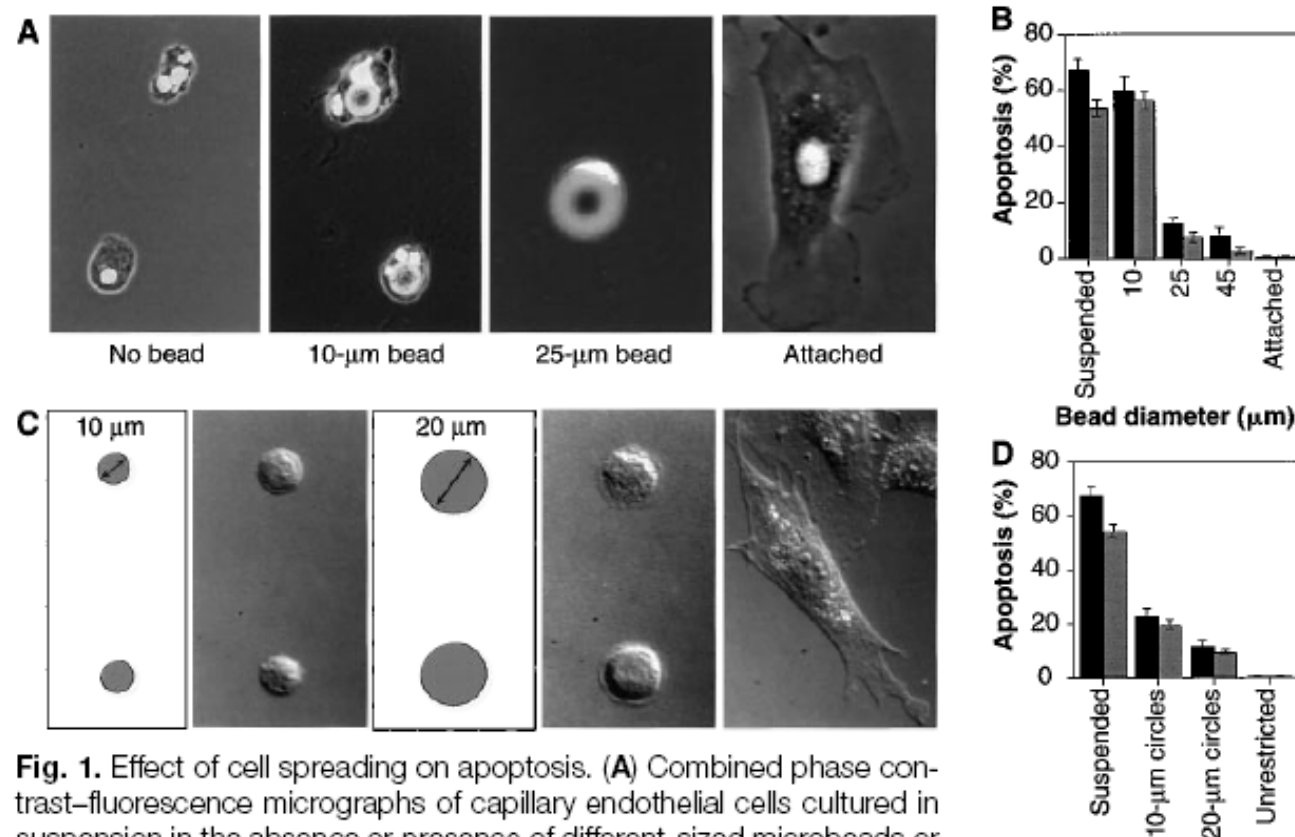


Fig. 1. Effect of cell spreading on apoptosis. **(A)** Combined phase contrast–fluorescence micrographs of capillary endothelial cells cultured in suspension in the absence or presence of different-sized microbeads or attached to a planar culture dish coated with FN for 24 hours (28). In the highly spread cell on the 25- μm bead, only the flattened 4',6'-diamidino-2-phenylindole (DAPI)–stained nucleus is clearly visible. **(B)** Apoptosis in cells attached to different-sized beads, in suspension, or attached to a dish. The apoptotic index was quantitated by measuring the percentage of cells exhibiting positive TUNEL staining (black bars) (Boehringer Mannheim), which detects DNA fragmentation; similar results were obtained by analyzing changes in nuclear condensation and fragmentation in cells stained with DAPI at 24 hours (gray bars). Apoptotic indices were determined only within single cells bound to single beads. Error bars indicate SEM. **(C)** Differential interference-contrast micrographs of cells plated on substrates micropatterned with 10- or 20- μm -diameter circles coated with FN (left), by a microcontact printing method (29) or on a similarly coated unpatterned substrate (right). **(D)** Apoptotic index of cells attached to different-sized adhesive islands coated with a constant density of FN for 24 hours; similar results were obtained with human and bovine capillary endothelial cells (28). Bars same as in (B).



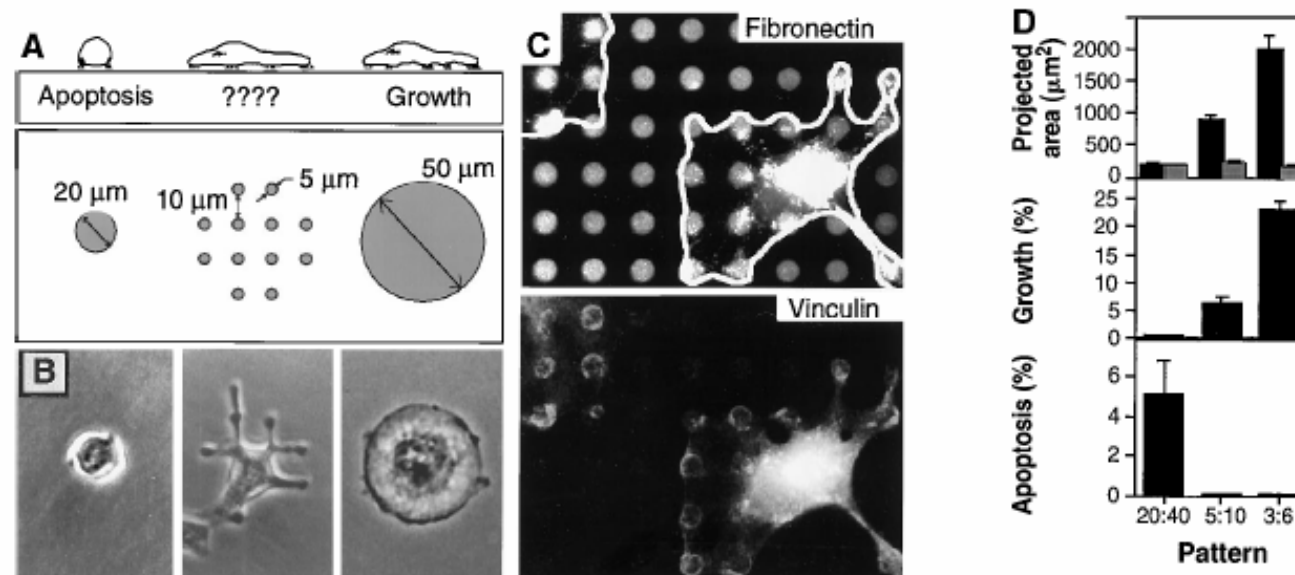


Fig. 3. Cell-ECM contact area versus cell spreading as a regulator of cell fate. **(A)** Diagram of substrates used to vary cell shape independently of the cell-ECM contact area. Substrates were patterned with small, closely spaced circular islands (center) so that cell spreading could be promoted as in cells on larger, single round islands, but the ECM contact area would be low as in cells on the small islands. **(B)** Phase-contrast micrographs of cells spread on single 20- or 50- μm -diameter circles or multiple 5- μm circles patterned as shown in (A). **(C)** Immunofluorescence micrographs of cells on a micropatterned substrate stained for FN (top) and vinculin (bottom). White outline indicates cell borders; note circular rings of vinculin staining, which coincide precisely with edges of the FN-coated adhesive islands. **(D)** Plots of projected cell area (black bars) and total ECM contact area (gray bars) per cell (top), growth index (middle), and apoptotic index (bottom) when cells were cultured on single 20- μm circles or on multiple circles 5 or 3 μm in diameter separated by 40, 10, and 6 μm , respectively.



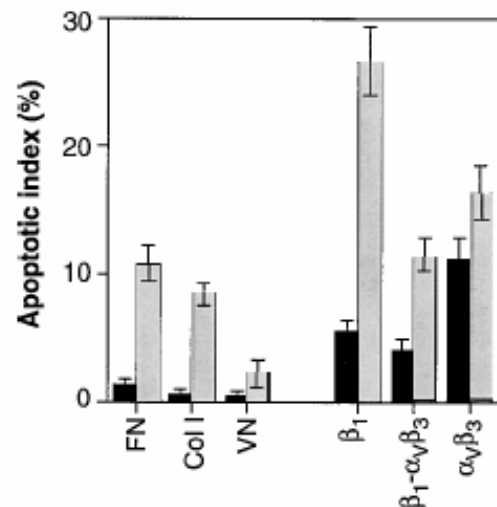
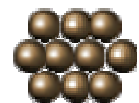


Fig. 4. Role of different integrin ligands in cell shape-regulated apoptosis. Apoptotic indices (percentage positive TUNEL staining) for cells cultured for 24 hours on unpatterned substrates (black bars) or on 20- μ m circles (gray bars) coated with FN, type I collagen (Col I), vitronectin (VN), anti- β_1 , anti- $\alpha_v\beta_3$, or antibodies to both integrin β_1 and integrin $\alpha_v\beta_3$ (29).

hexadecanethiol [$\text{HS}(\text{CH}_2)_{15}\text{CH}_3$] was printed onto gold-coated substrates with a flexible stamp containing a relief of the desired pattern. The substrate was immersed immediately in 2 mM tri(ethylene glycol)-terminated alkanethiol [$\text{HS}(\text{CH}_2)_{11}(\text{OCH}_2\text{CH}_2)_3\text{OH}$ in ethanol], which coated the remaining bare regions of gold. When these substrates were immersed in a solution of FN, vitronectin, or type I collagen (50 $\mu\text{g/ml}$ in phos-



Electrochemical Desorption of Self-Assembled Monolayers Noninvasively Releases Patterned Cells from Geometrical Confinements

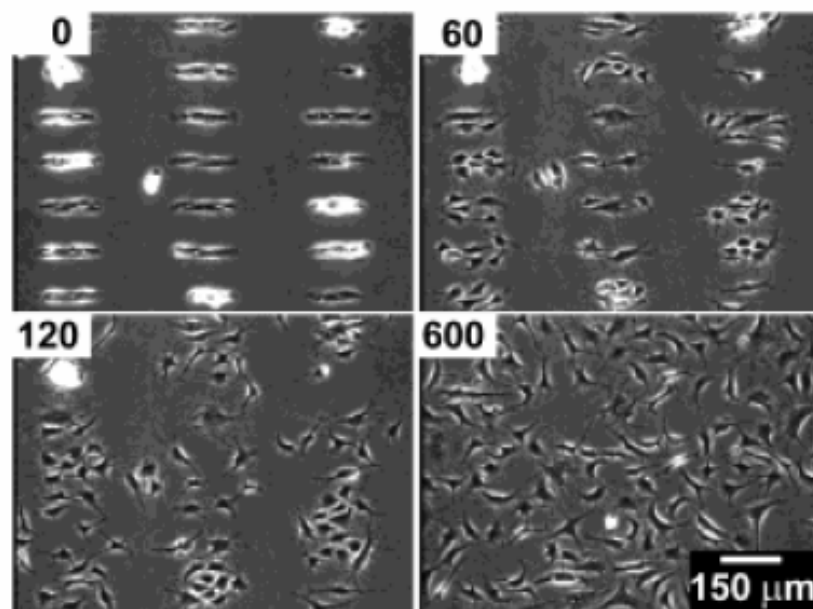


Figure 1. BCE cells were allowed to attach to a surface patterned with $C_{11}EG_3$ and C_{18} . Application of a cathodic voltage pulse (-1.2 V for 30 s in this case) released the cells from the microislands. The numbers indicate the time elapsed (in minutes) after the voltage pulse.



Directing cell migration with asymmetric micropatterns <http://www.pnas.org/cgi/reprint/102/4/>

PNAS | January 25, 2005 | vol. 102 | no. 4 | 975

Xingyu Jiang*, Derek A. Bruzewicz*, Amy P. Wong*, Matthieu Piel†, and George M. Whitesides**

*Department of Chemistry and Chemical Biology, Harvard University, 12 Oxford Street, Cambridge, MA 02138; and †Department of Molecular and Cell Biology, Harvard University, 16 Divinity Avenue, Cambridge, MA 02138

Contributed by George M. Whitesides, December 2, 2004

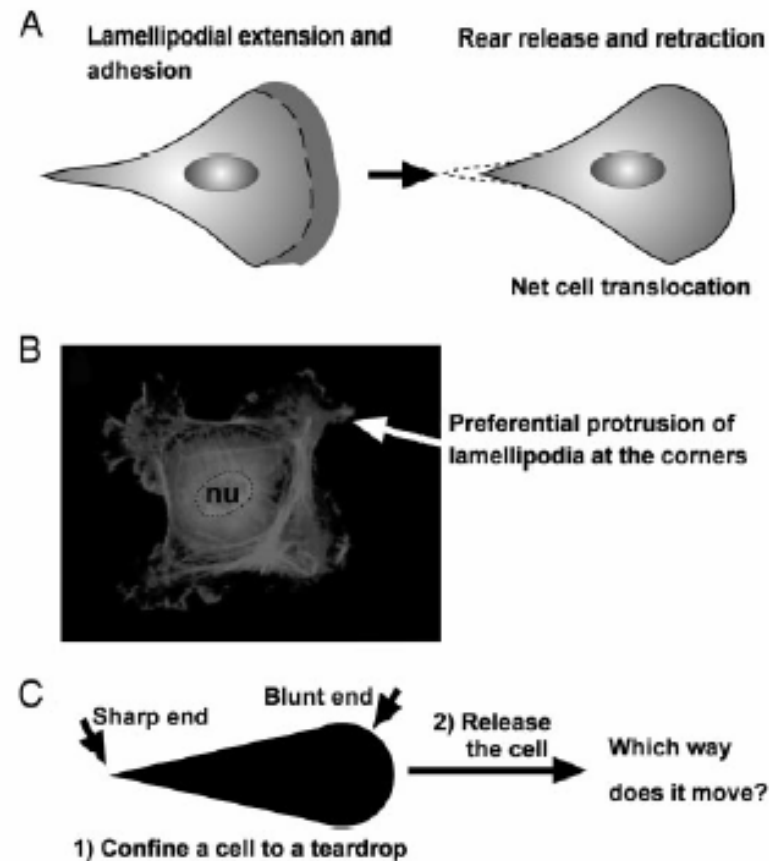


Fig. 1. A problem on cell motility. (A) A cartoon illustration of the migration of a typical mammalian cell on a flat surface. This teardrop shape is found in many types of cells. (B) Cells confined to squares preferentially extend their lamellipodia from the corners. nu, nucleus. (C) If a cell is confined to a shape of teardrop, will the cell preferentially extend its lamellipodia from the sharp end or from the blunt end? If released from confinement, in which direction will it likely move?

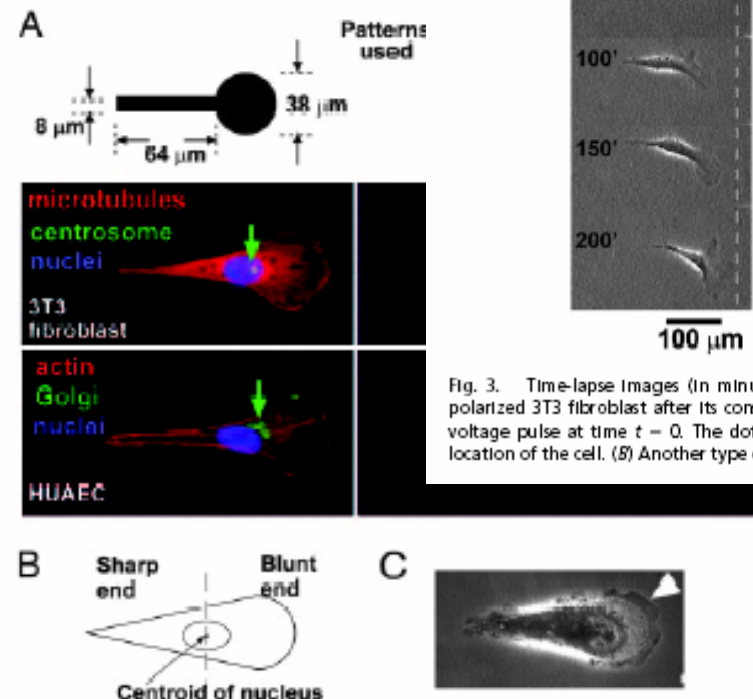


Fig. 2. Asymmetric patterns polarize immobilized cells. (A) The Golgi and the centrosome are located closer to the half of a cell with the blunt end. We used phalloidin, antigolgin, DAPI, antitubulin, and antipericentrin to identify actin (red), the Golgi (green), the nucleus (blue), microtubules (red), and the centrosome (green), respectively. The green arrows indicate the location of centrosomes in 3T3 cells and Golgi in human umbilical artery endothelial cells (HUAE). (B) We divided the cell into a half with the sharp end and a half with the blunt end by a vertical line drawn at the centroid of the nucleus; >80% ($n = 30$) of the centrosomes and Golgi were localized in the region of the wide end. (C) The lamellipodia of immobilized 3T3 cells tended to extend more from the blunt end as well (arrowhead). The dotted line indicates the edges of the adhesive pattern.

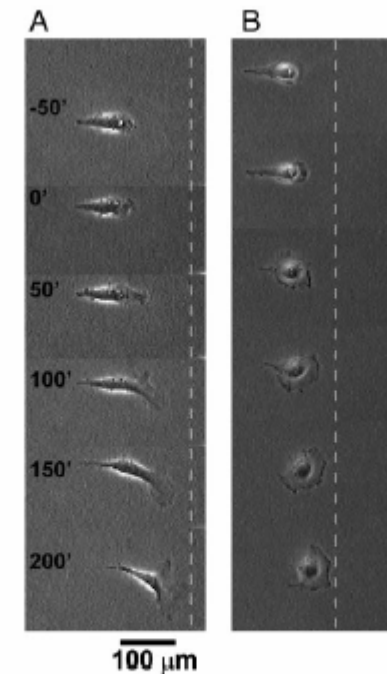


Fig. 3. Time-lapse images (in minutes) show the motility of an initially polarized 3T3 fibroblast after its constraint is released. (A) We applied the voltage pulse at time $t = 0$. The dotted line serves as a reference for the location of the cell. (B) Another type of cell, COS-7, shows similar behavior.



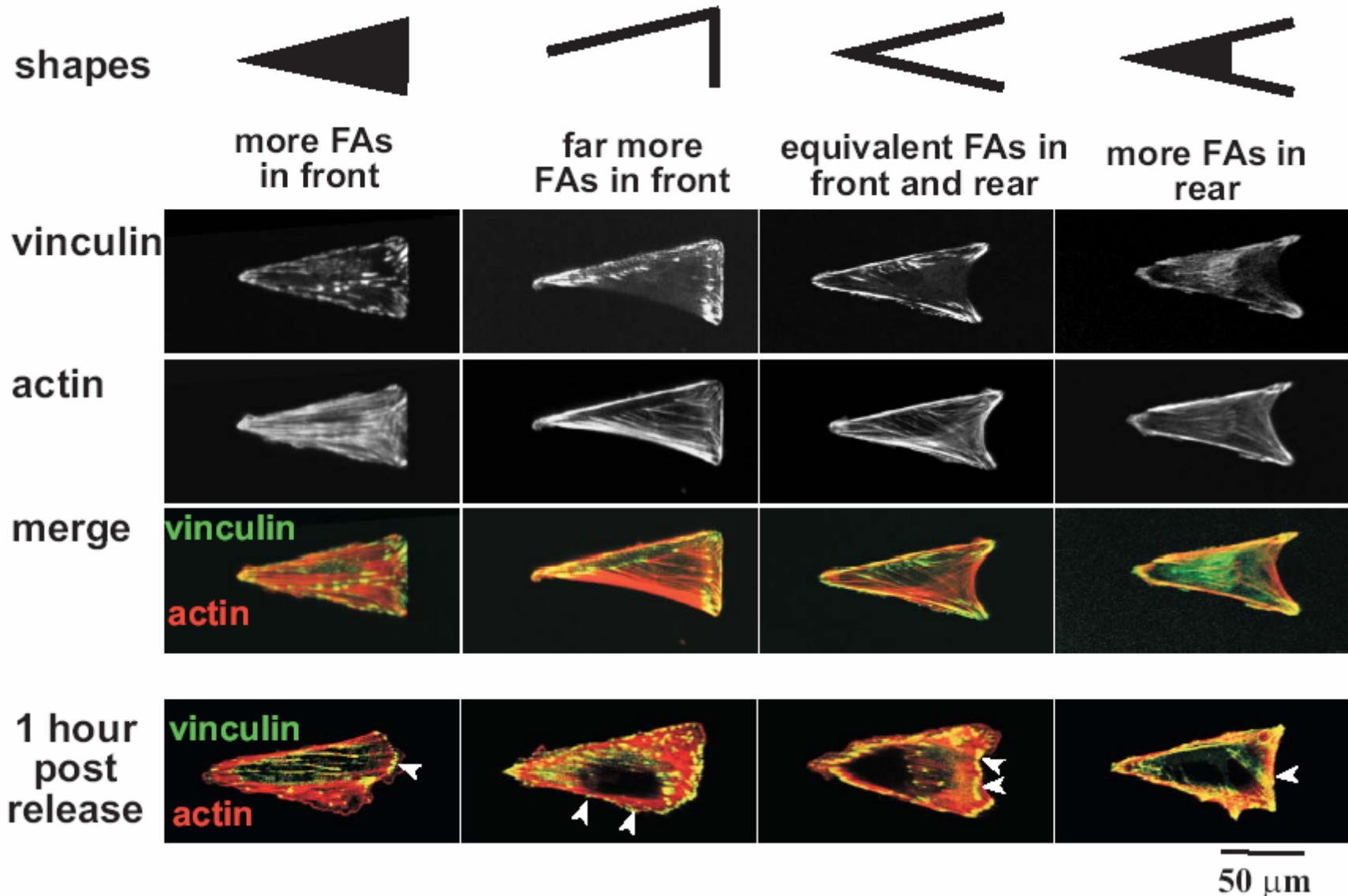


Fig. 11. A series of patterns that confine cells to approximately the same projected geometry (visualized by the actin cytoskeleton) but distribute the focal adhesions (FAs; visualized by immunostaining for vinculin) differently. The bottom row shows that new focal adhesions formed 1 h after release in areas that were inert to attachment of cells prior to release (arrowheads).

Soft-Lithography

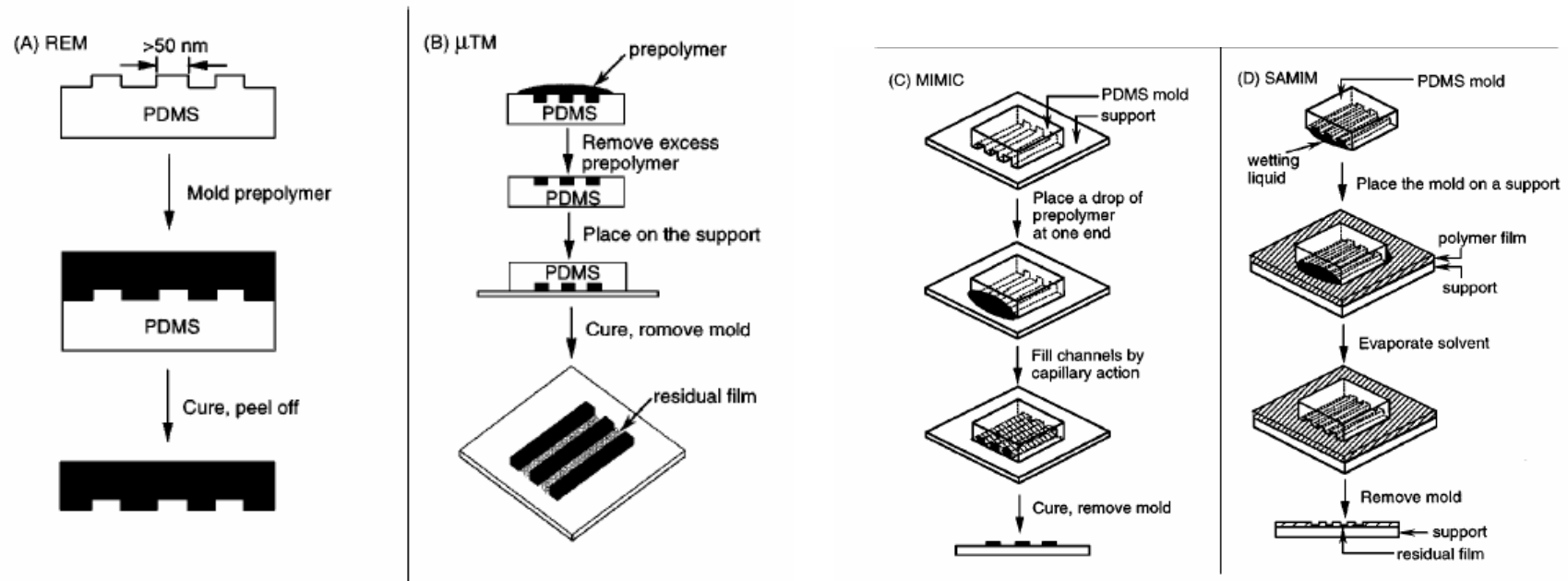
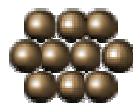
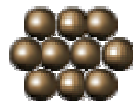
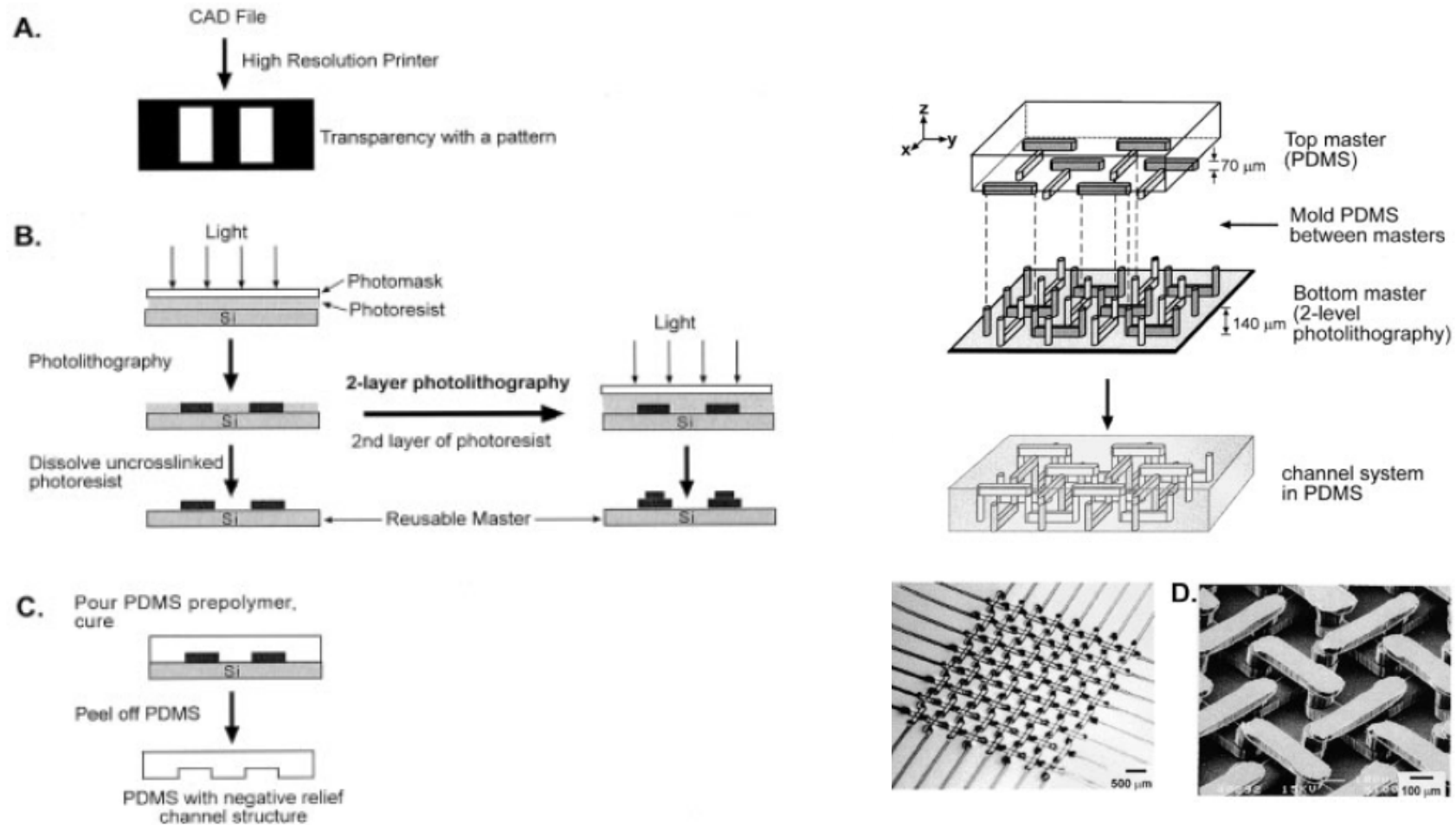


Figure 5 Schematic illustration of procedures for (a) replica molding (REM), (b) microtransfer molding (μ TM), (c) micromolding in capillaries (MIMIC), and (d) solvent-assisted micromolding (SAMIM).

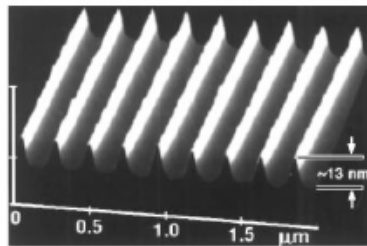


Electrophoresis 2002, 23, 3461–3473

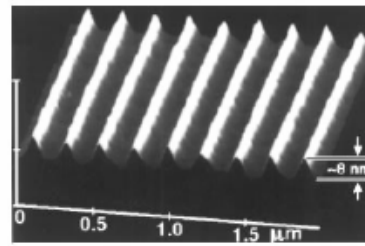


Replication Result

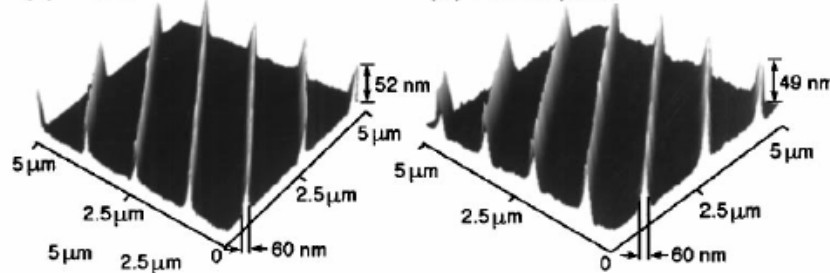
(a) Master I



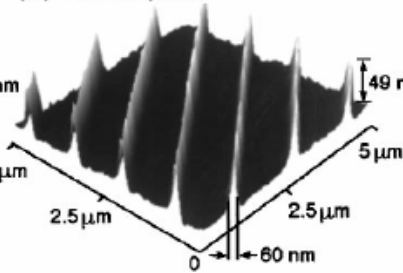
(b) PU Replica



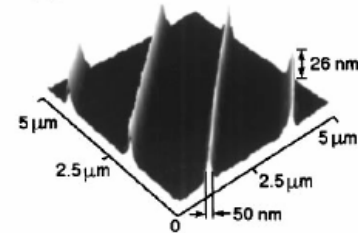
(c) Master II



(d) PU Replica



(e) Master III



(f) PU Replica

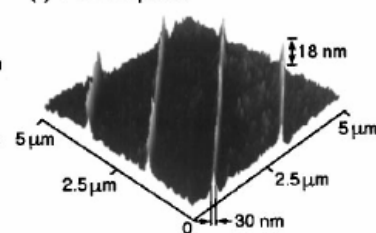
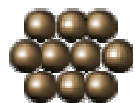
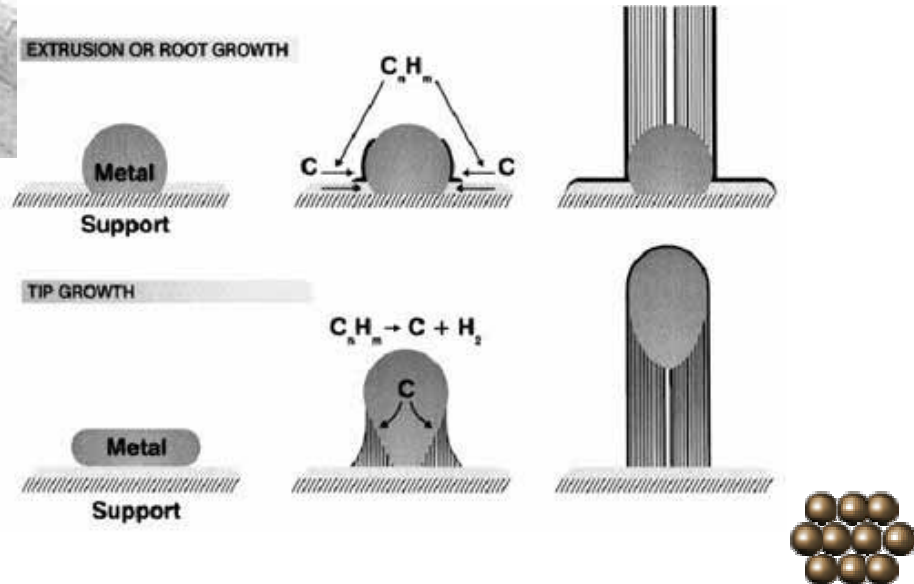
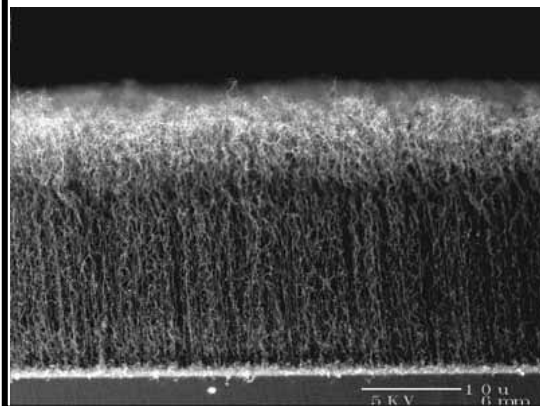
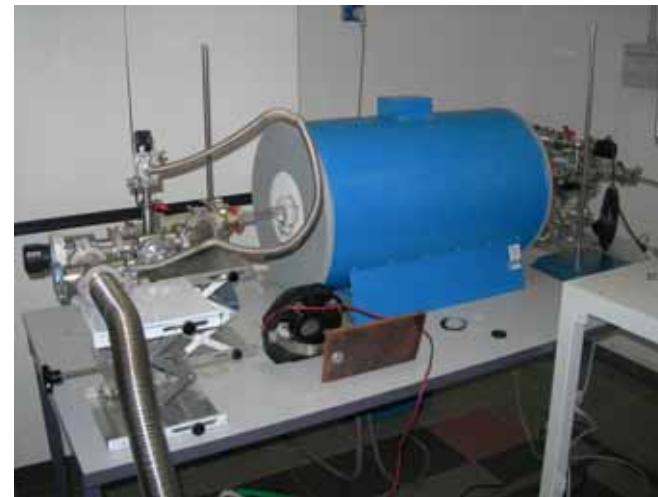
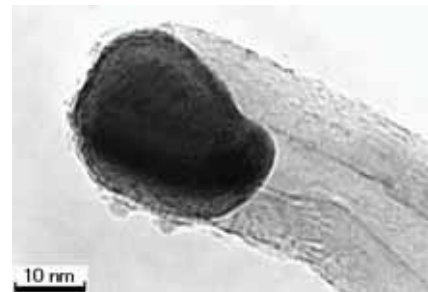
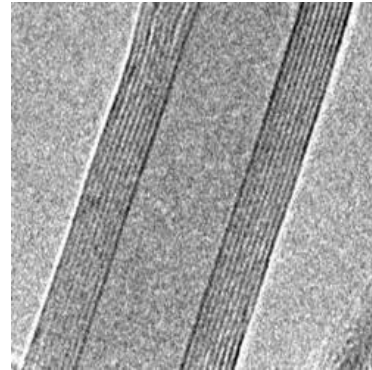
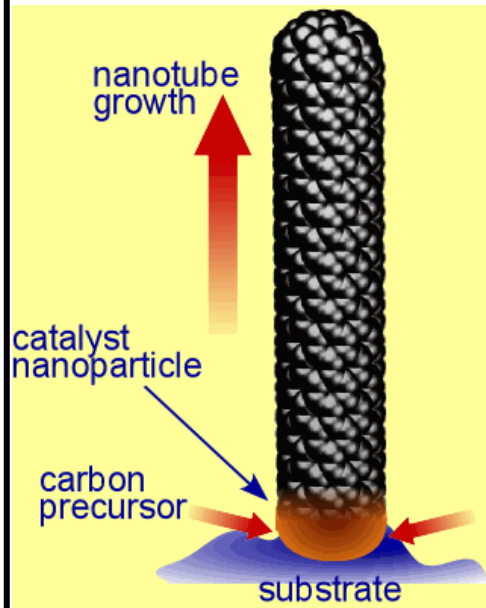


Figure 6 (a,b) Atomic force microscopy (AFM) images of Cr structures on a master, and a PU replica prepared from a PDMS mold cast from this master (153). (c,d) AFM images of Au structures on another master, and a PU replica produced from a PDMS mold cast from this master. (e,f) AFM images of Au structures on a third master, and a PU replica fabricated from a PDMS mold (cast from this master) while this mold was mechanically deformed by bending in a manner that generated narrower lines.



CVD Carbon Nanotube



LP CVD

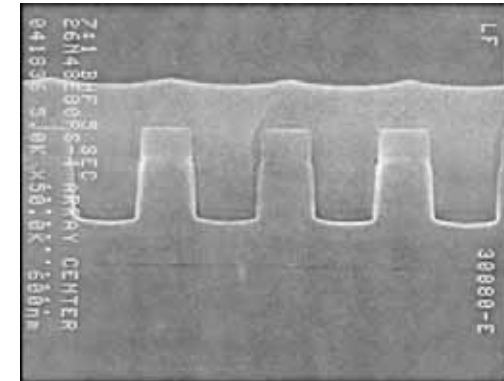
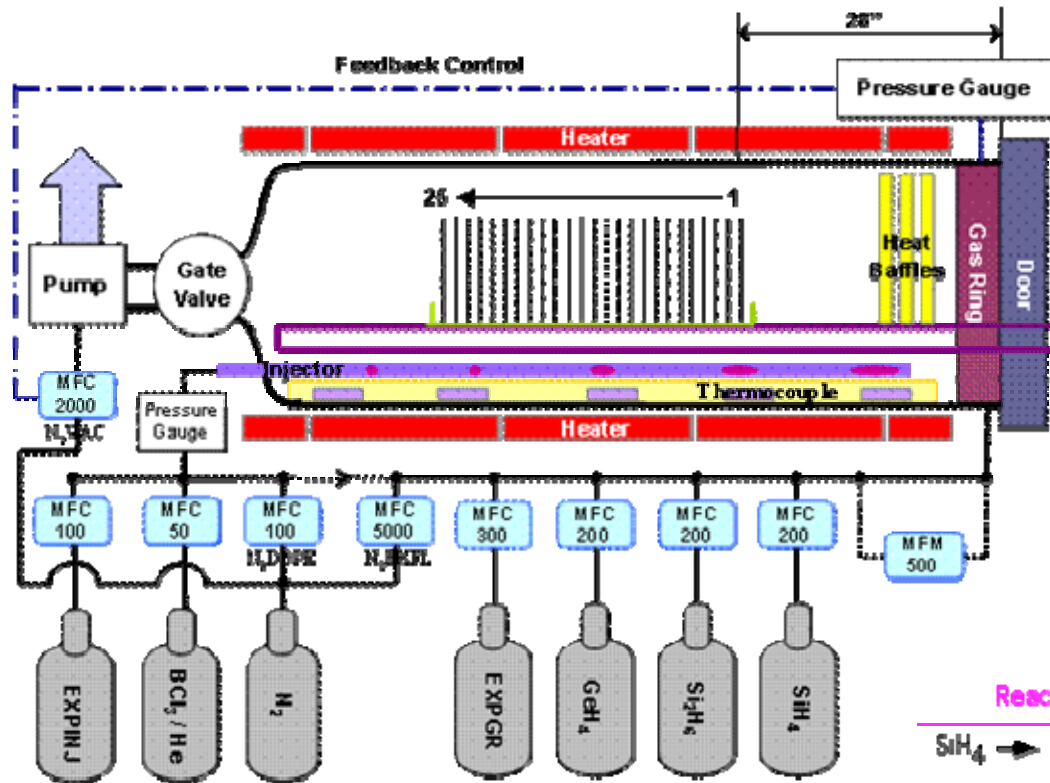
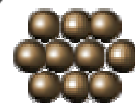


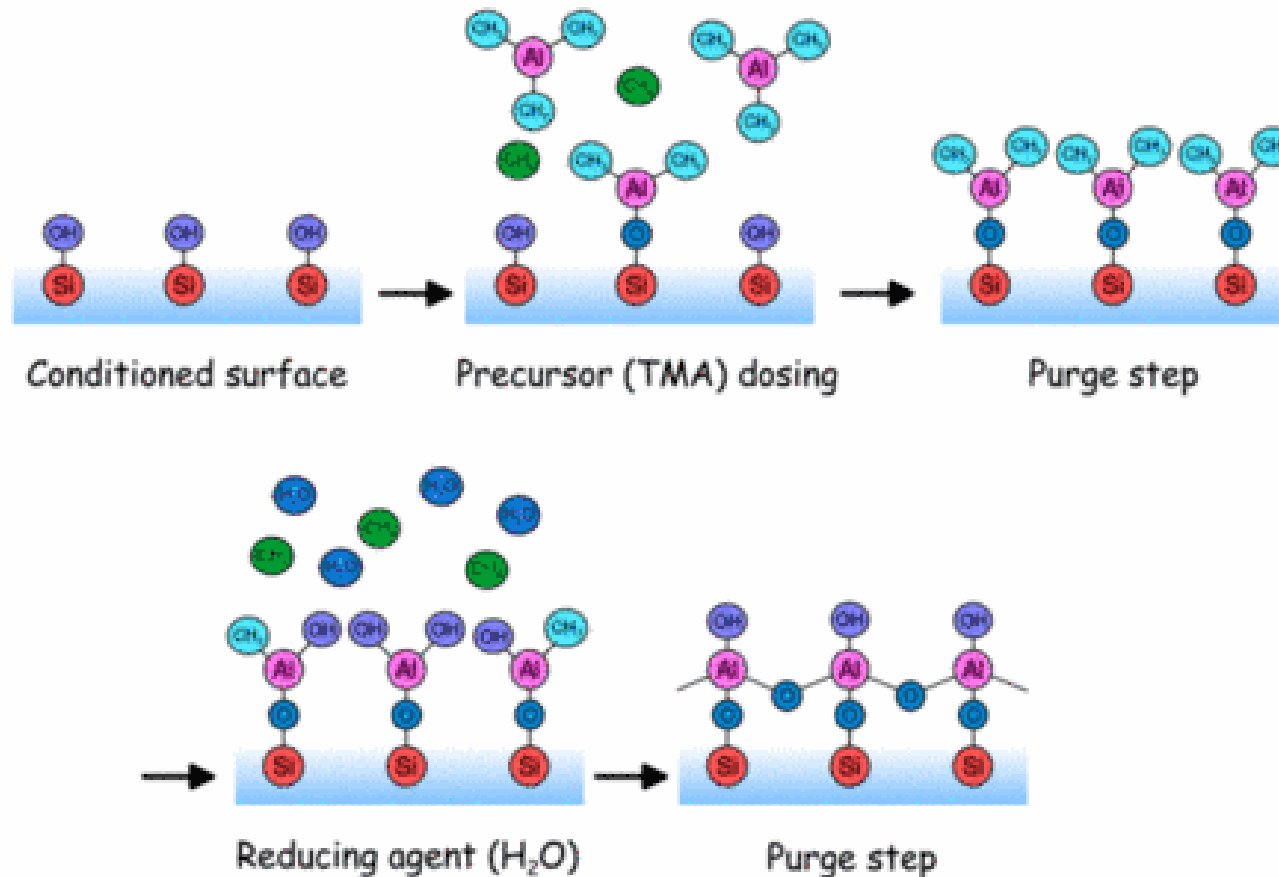
Figure 17

SEM cross-section micrograph illustrating gap filling and local planarization of a shallow-trench isolation structure, achieved using HDP CVD of silicon oxide.

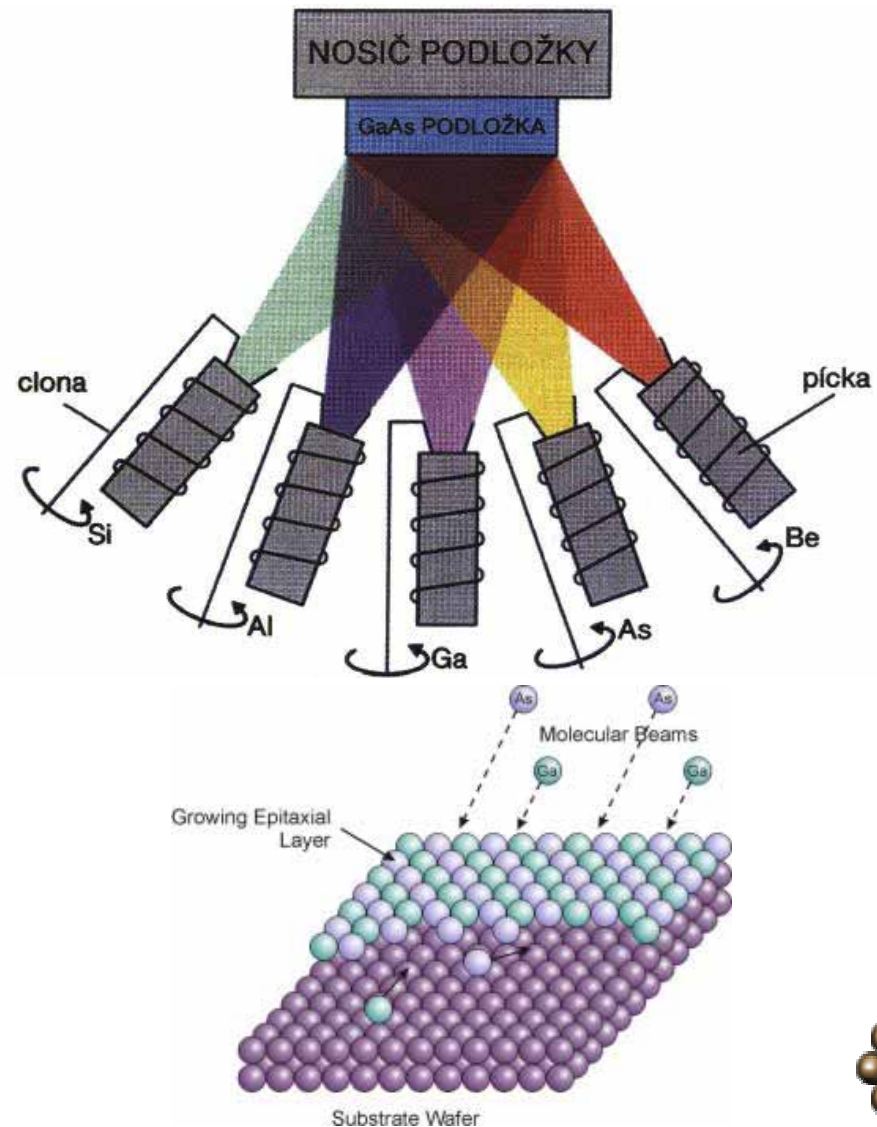
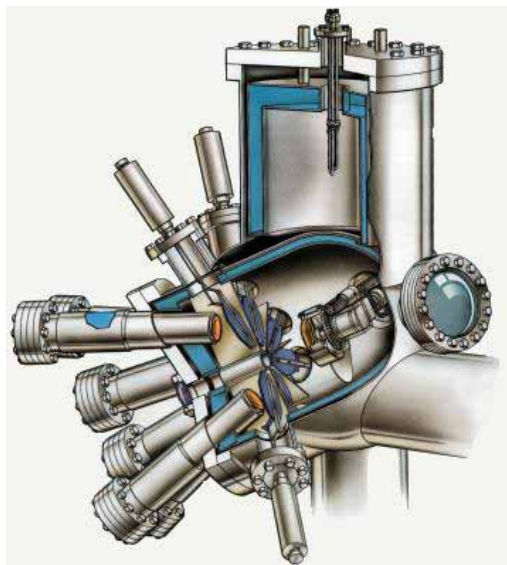
| Reaction | ΔH (KJ/mole) | conformality |
|---|----------------------|-------------------|
| $\text{SiH}_4 \rightarrow \text{Si} + 2\text{H}_2$ | -34 | spectacular |
| $\text{WF}_6 + 3\text{H}_2 \rightarrow \text{W} + 6\text{HF}$ | -111 | spectacular |
| $\text{TEOS} \rightarrow \text{SiO}_2 + 2\text{C}_2\text{H}_4 + 2\text{CH}_3\text{CH}_2\text{OH}$ | (small) | excellent |
| $3\text{SiH}_4 + 4\text{NH}_3 \rightarrow \text{Si}_3\text{N}_4 + 2\text{H}_2$ | -374 | good to excellent |
| $\text{SiH}_4 + 2\text{O}_2 \rightarrow \text{SiO}_2 + 2\text{H}_2\text{O}$ | -1364 | mediocre |



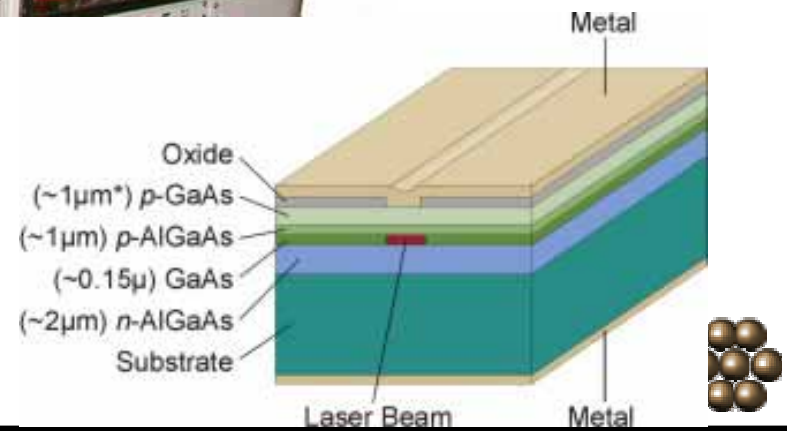
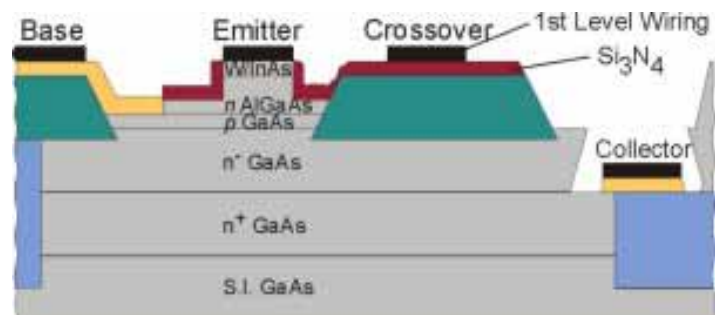
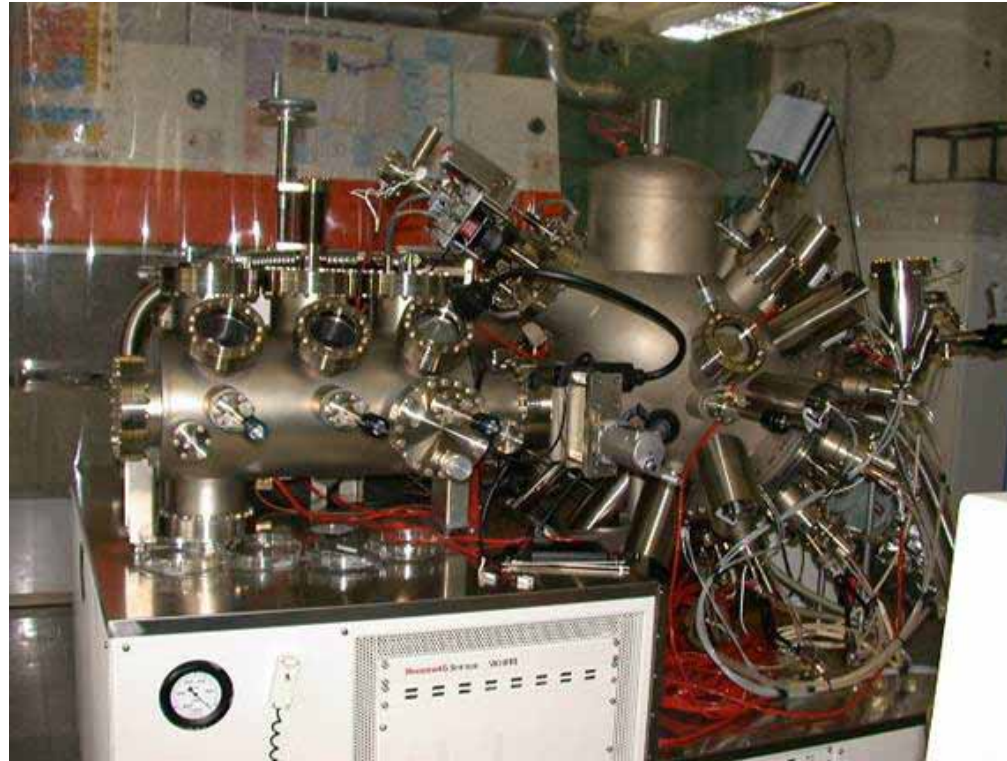
Atomic Layer Deposition



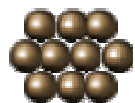
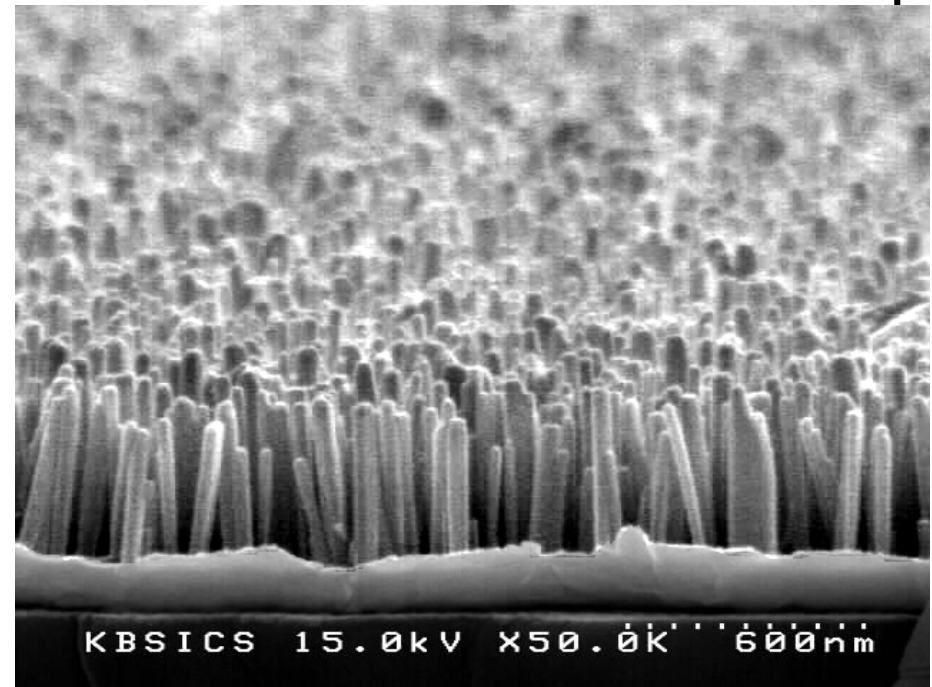
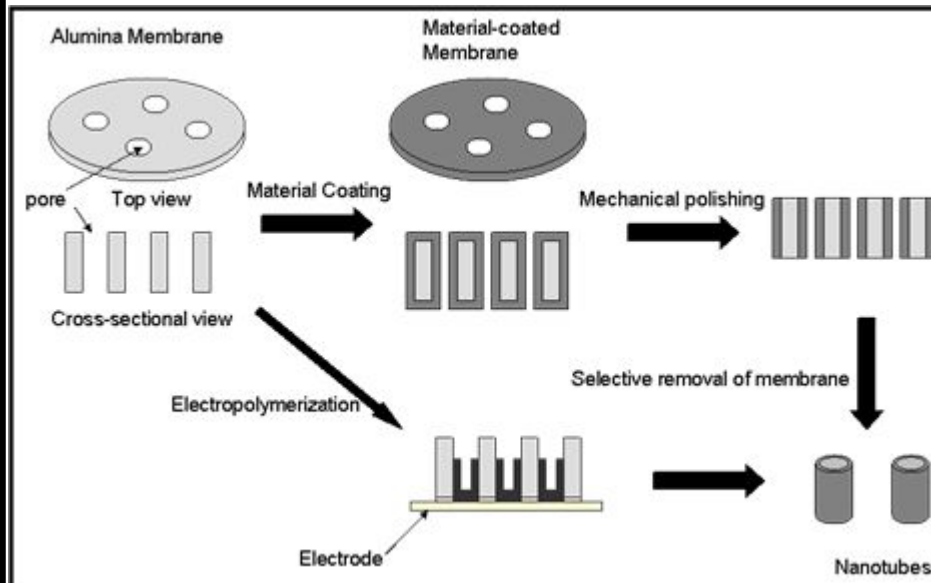
Molecular Beam Epitaxy (MBE)



MBE



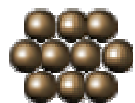
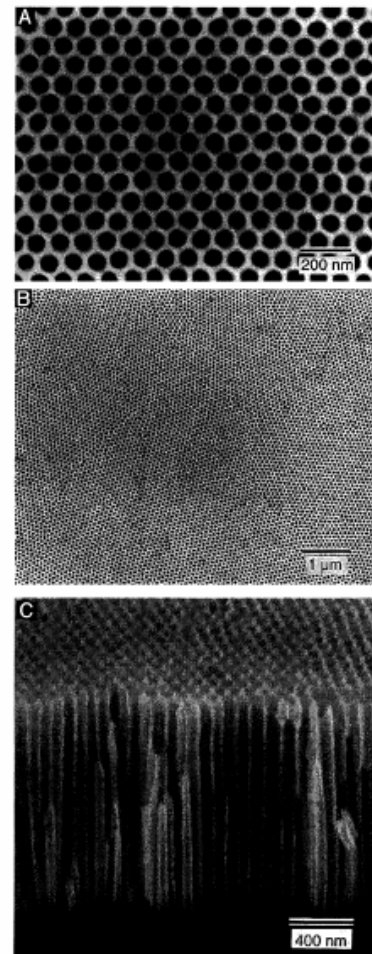
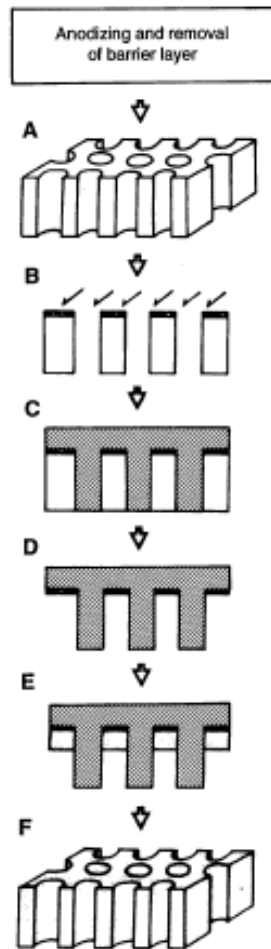
Template Synthesis



Ordered Metal Nanohole Arrays Made by a Two-Step Replication of Honeycomb Structures of Anodic Alumina

SCIENCE • VOL. 268 • 9 JUNE 1995

Hideki Masuda* and Kenji Fukuda



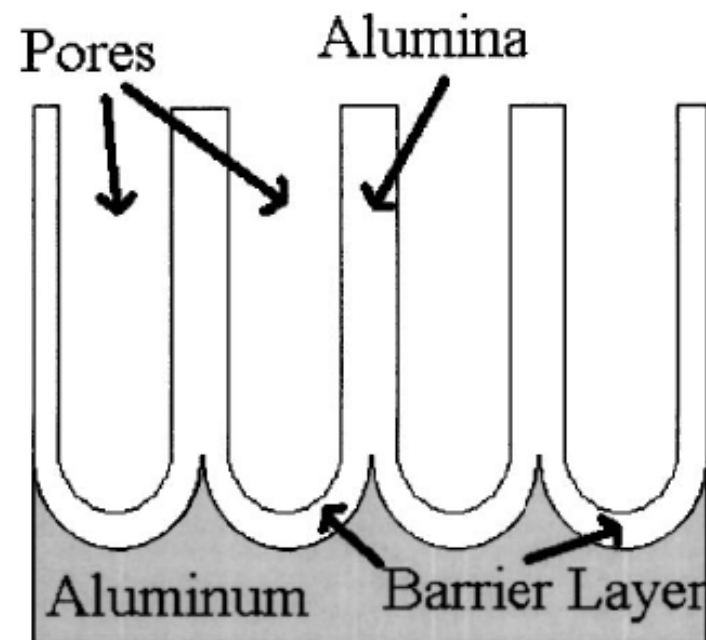
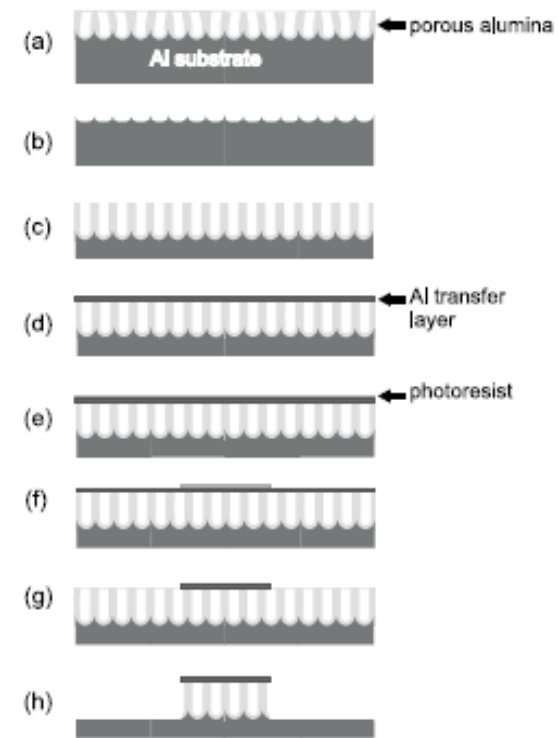
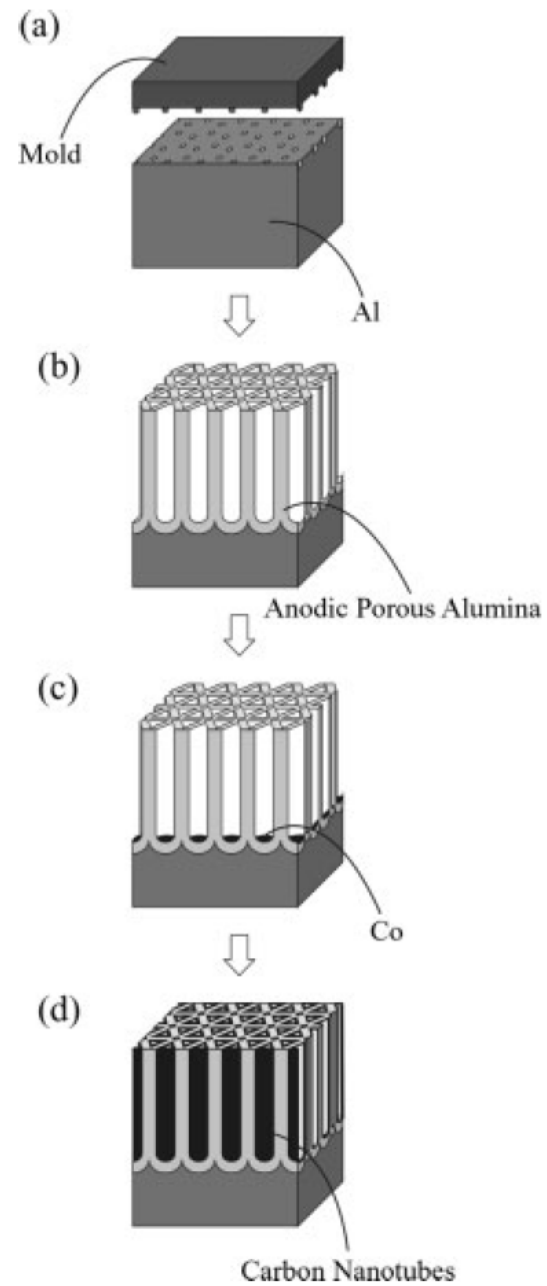
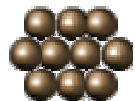
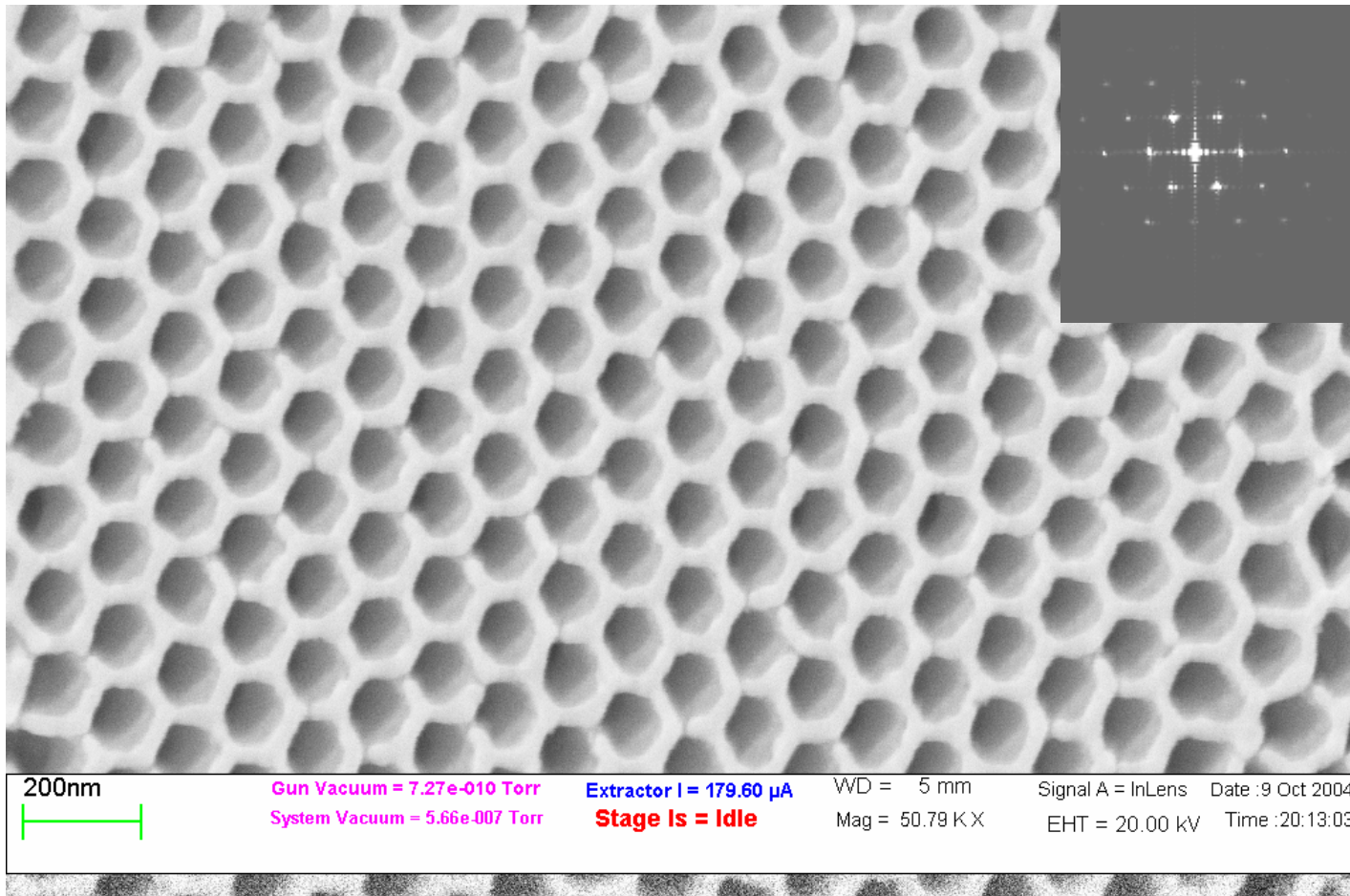


FIG. 1. Diagram of the typical porous alumina structure when fabricated using bulk aluminum.

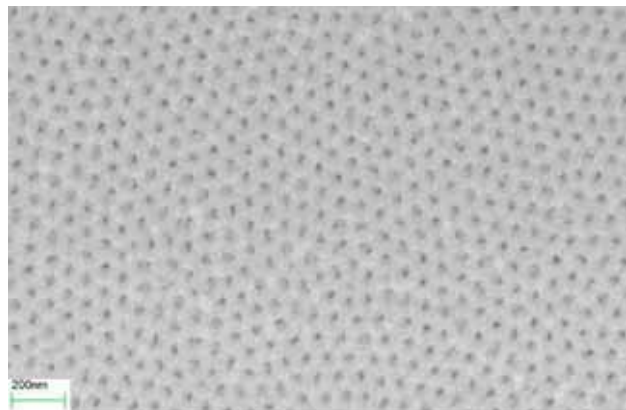




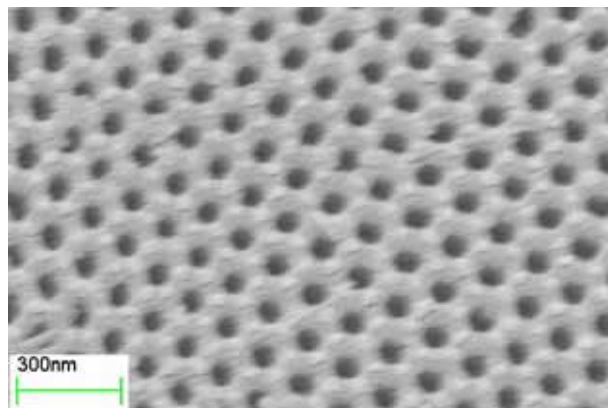
Project IV: Growth of 1D Nanofibers Using AAO Templates



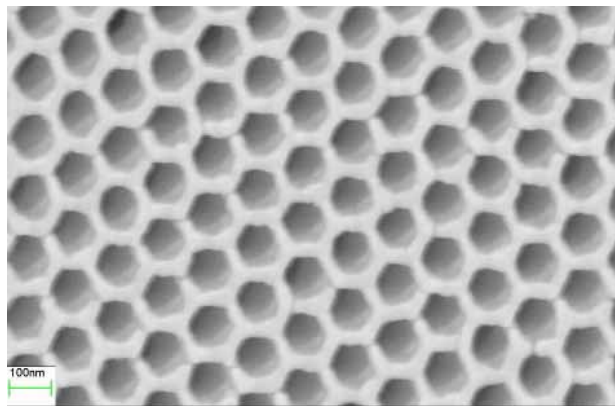
AAO Templates



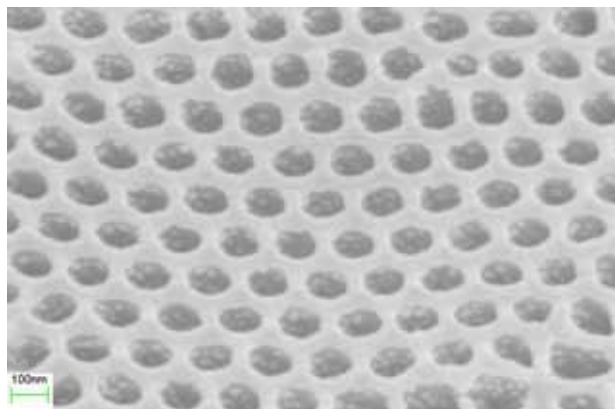
30 V



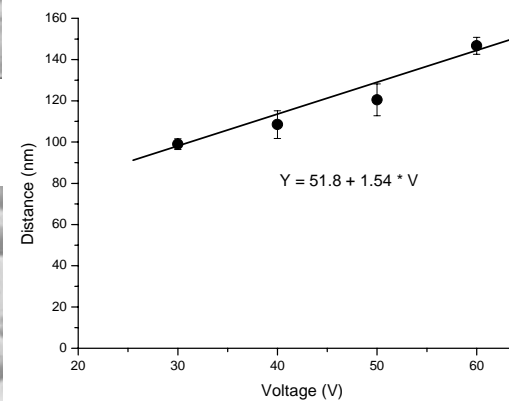
50 V



40 V



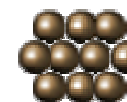
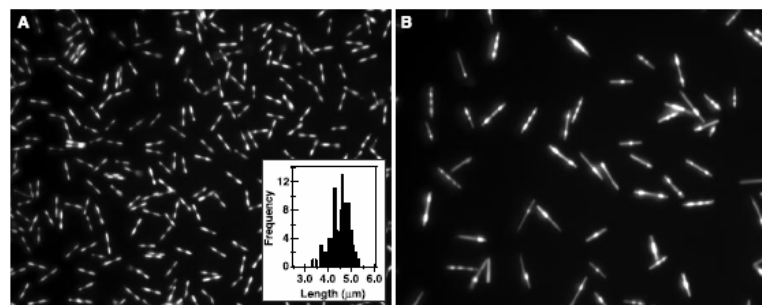
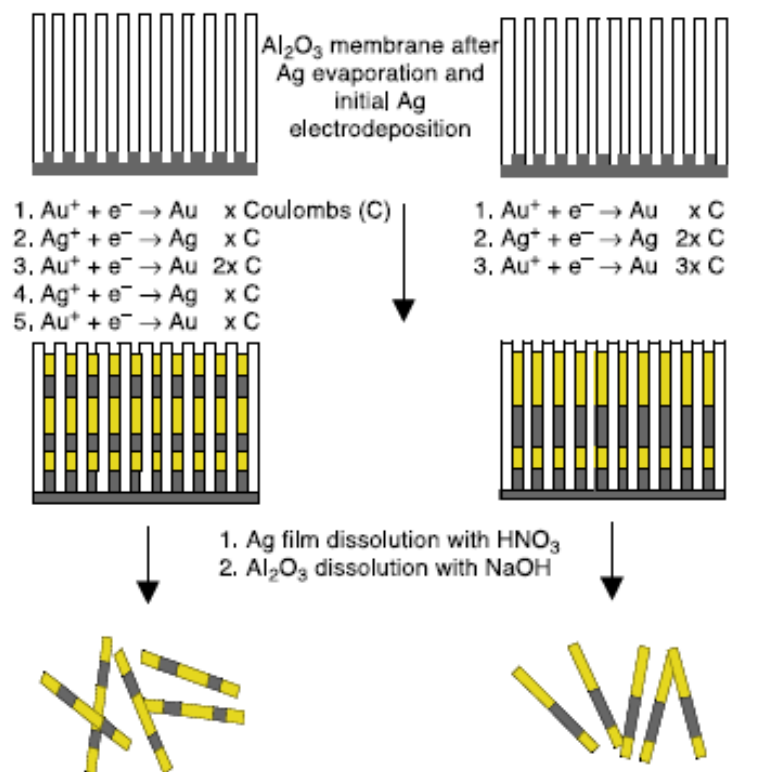
60 V



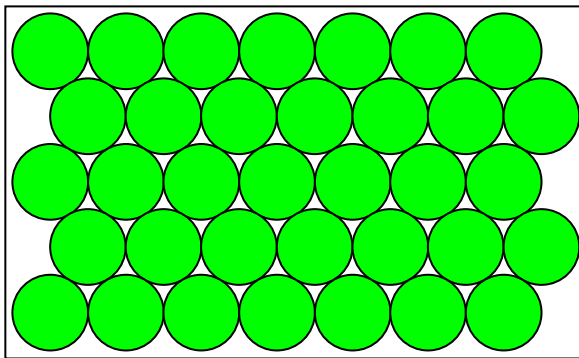
Submicrometer Metallic Barcodes

Sheila R. Nicewarner-Peña,¹ R. Griffith Freeman,²
 Brian D. Reiss,¹ Lin He,² David J. Peña,¹ Ian D. Walton,²
 Remy Cromer,² Christine D. Keating,^{1*} Michael J. Natan^{2*}

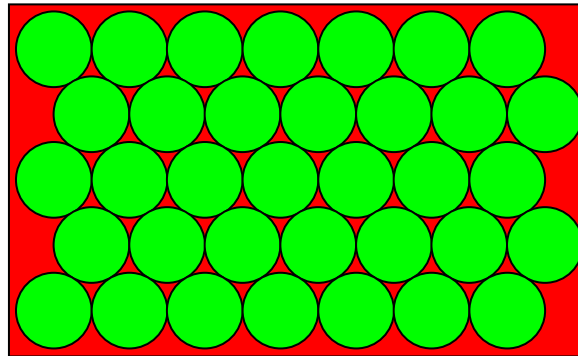
SCIENCE VOL 294 5 OCTOBER 2001



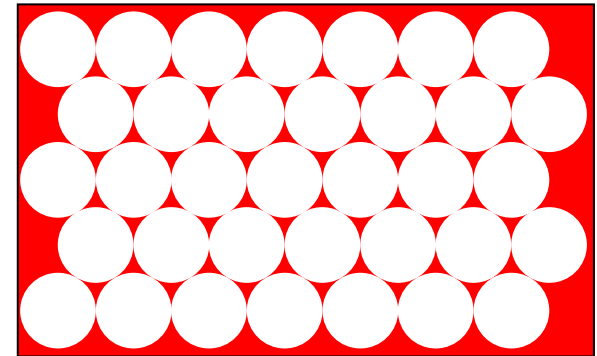
Nanosphere Lithography



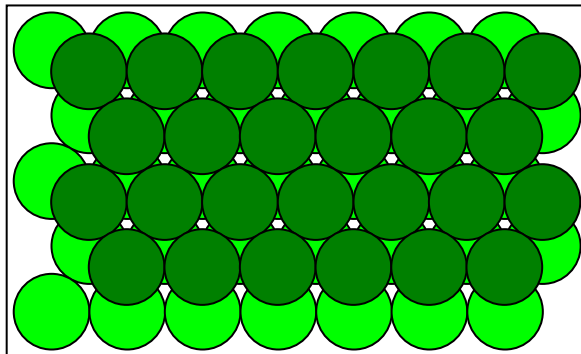
Single layer →



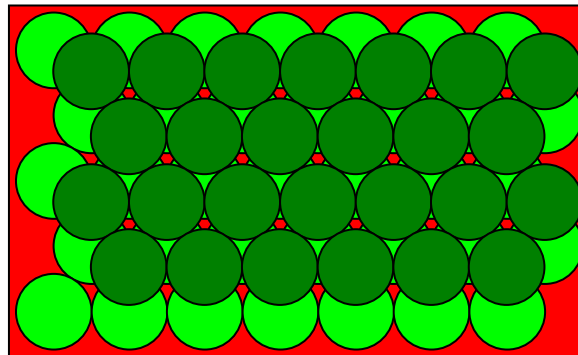
Metal deposition →



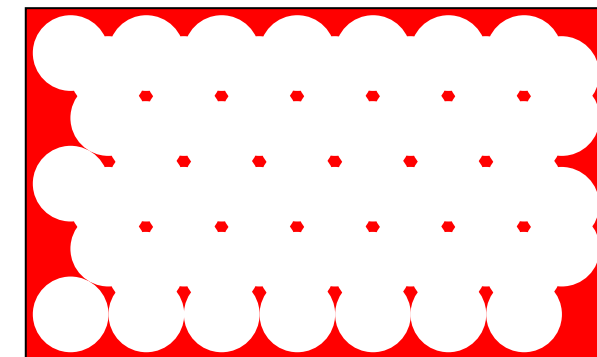
Lift-off



Double layer



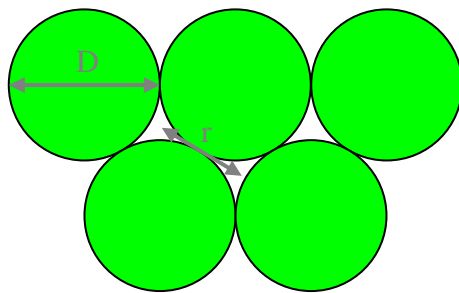
Metal deposition



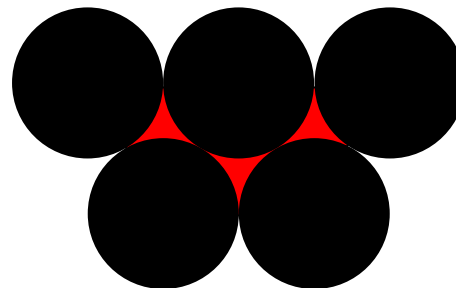
Lift-off



Array Dimension

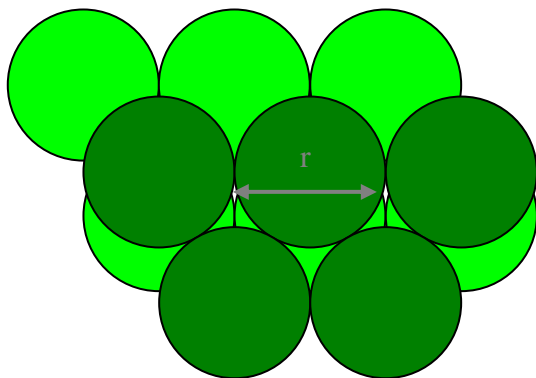


$$r = \frac{1}{\sqrt{3}} D$$

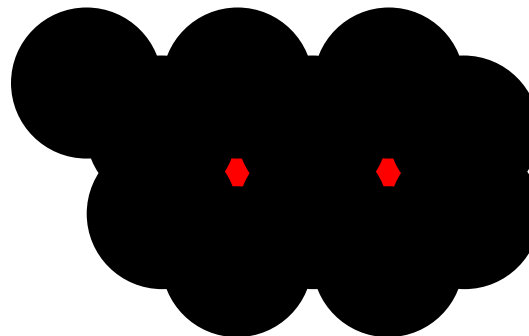


$$a = \frac{3}{2} \left(\sqrt{3} - 1 - \frac{1}{\sqrt{3}} \right) D$$

$$\sim 1/4 D$$

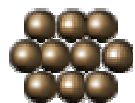


$$r = D$$



$$a = \left(\sqrt{3} - 1 - \frac{1}{\sqrt{3}} \right) D$$

$$\sim 1/7 D$$



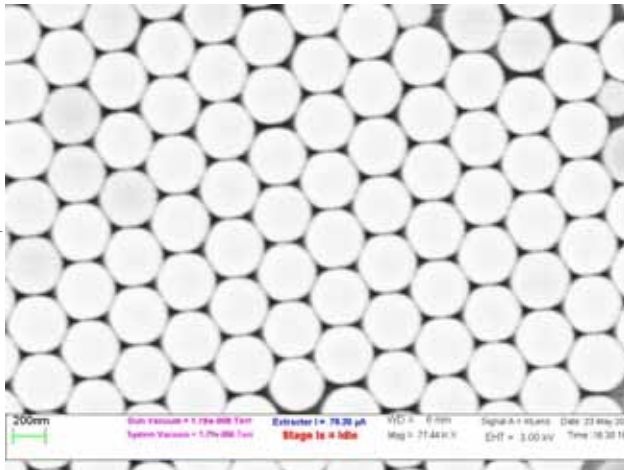
Optical Image of PS Template

800 nm PS

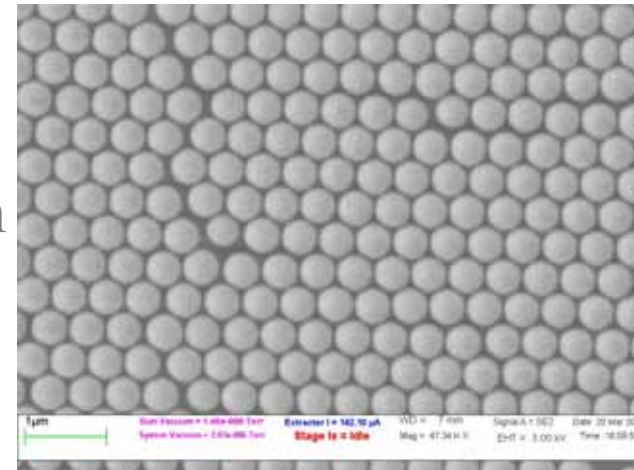


Nanosphere Lithography

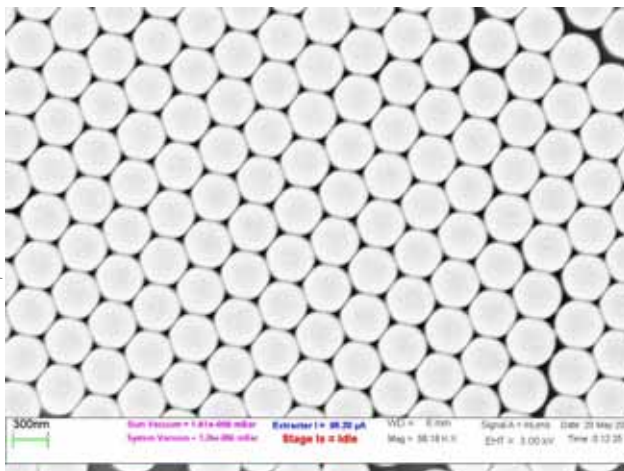
350 nm



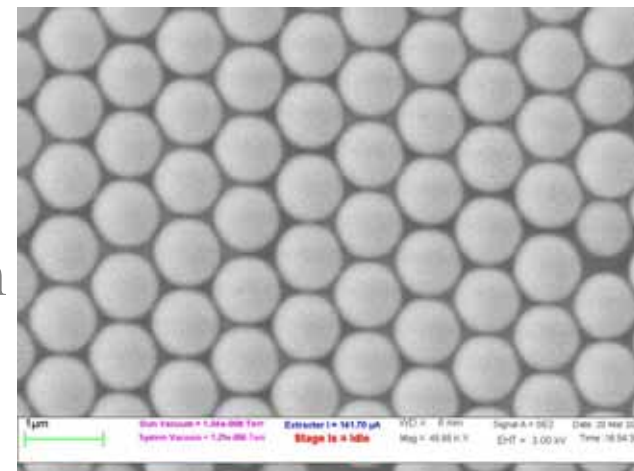
550 nm



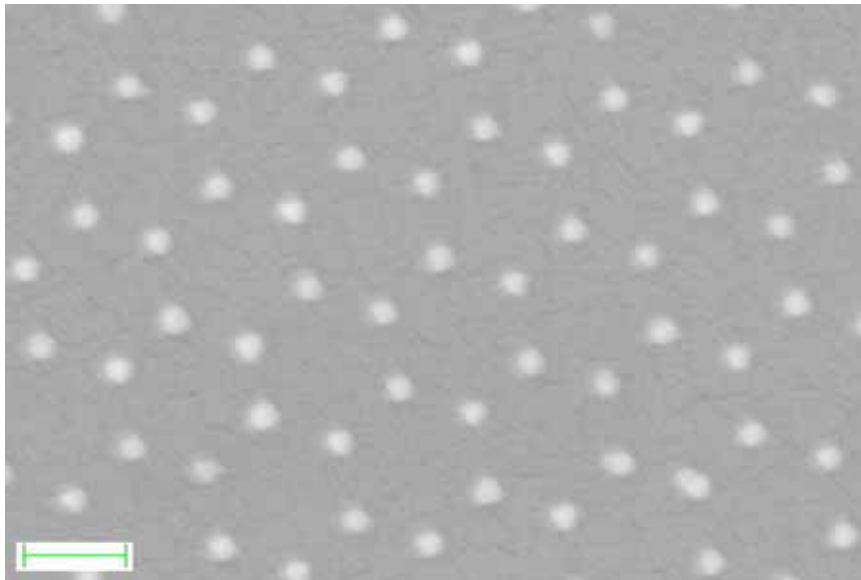
400 nm



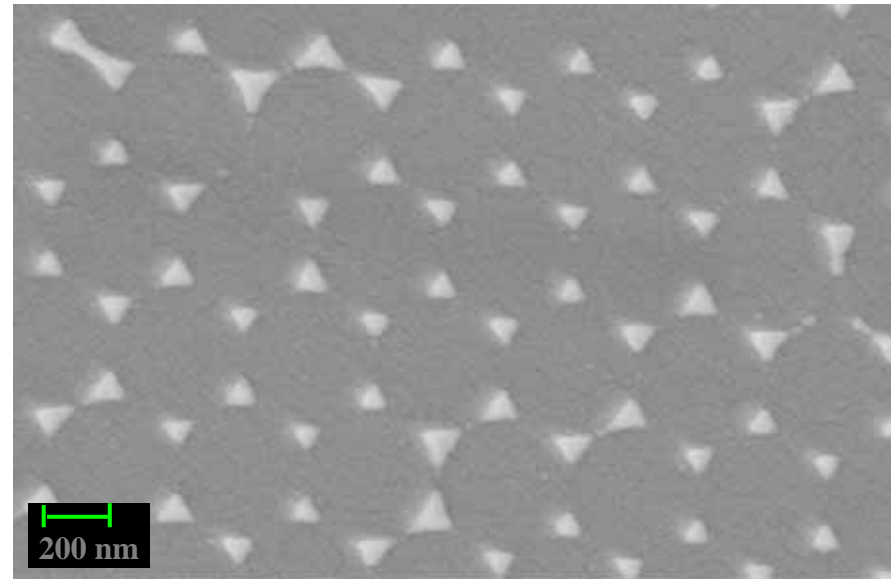
880 nm



Single Layer Templates



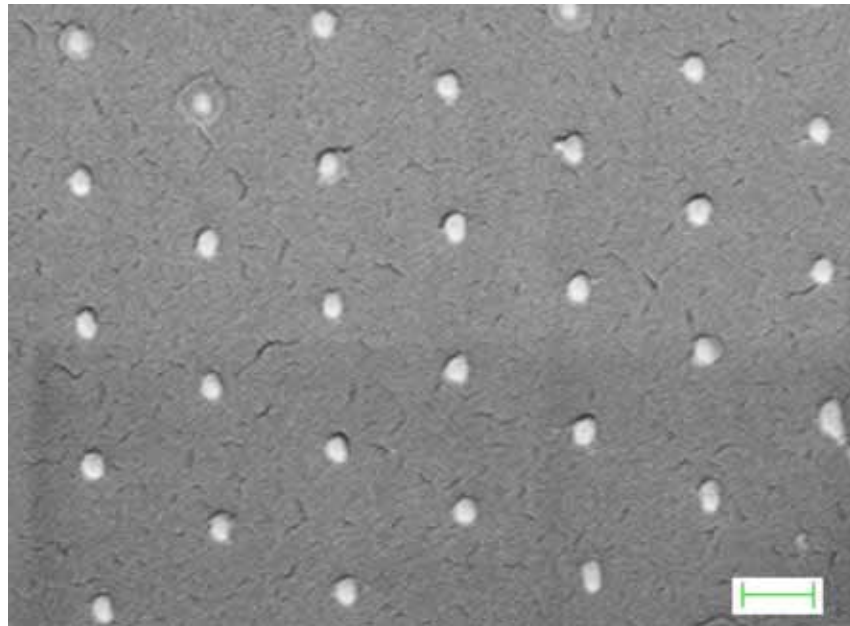
280 nm



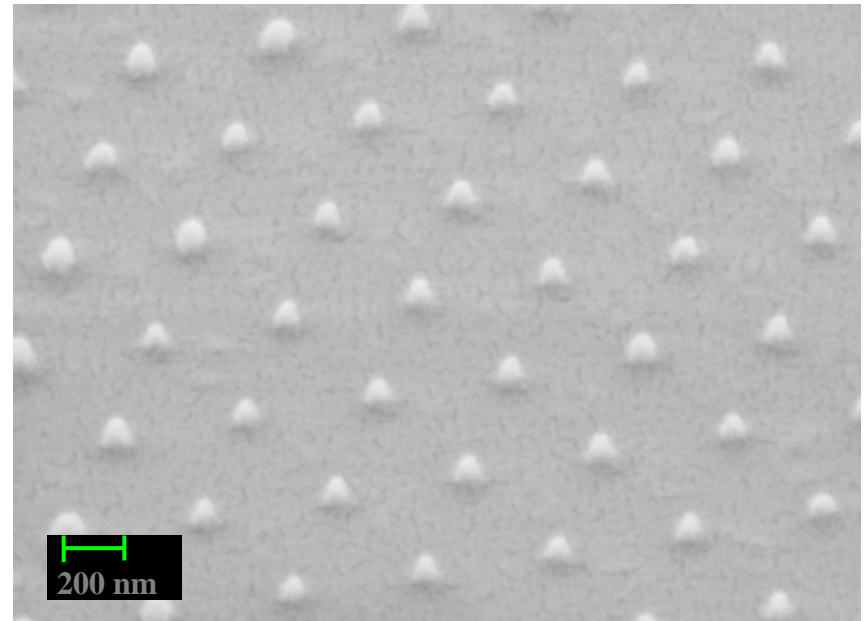
550 nm



Double Layer Templates



400 nm

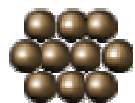
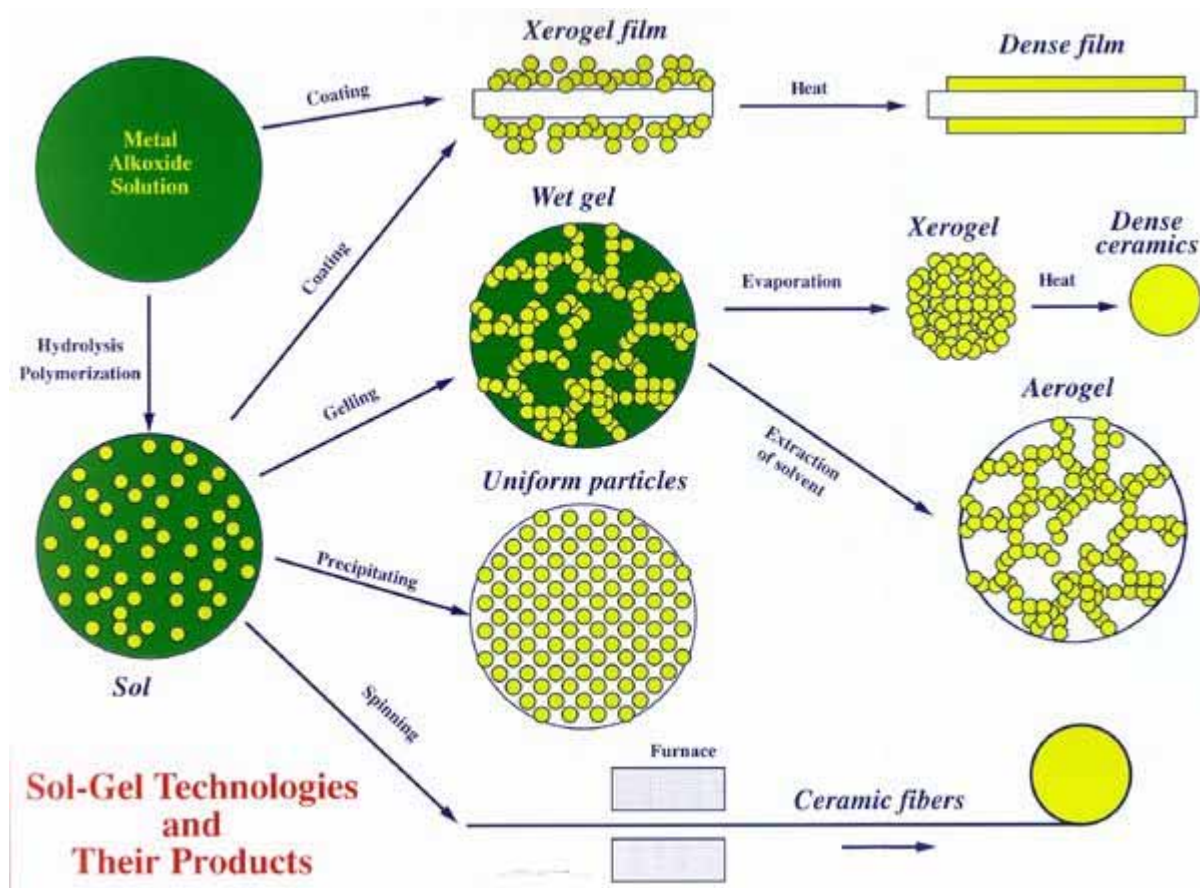


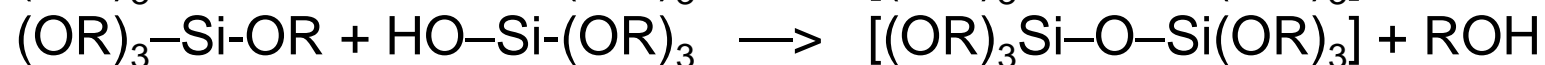
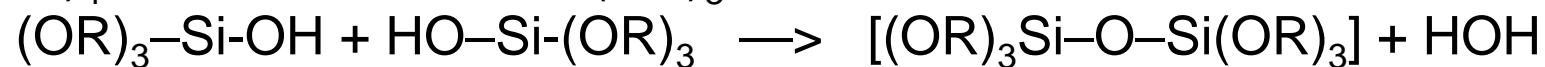
550 nm


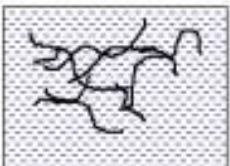






Sol-Gel

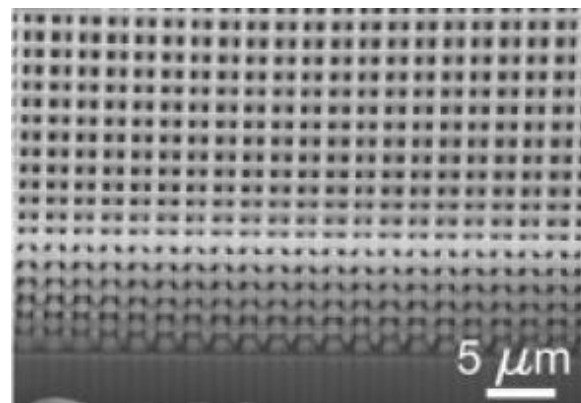
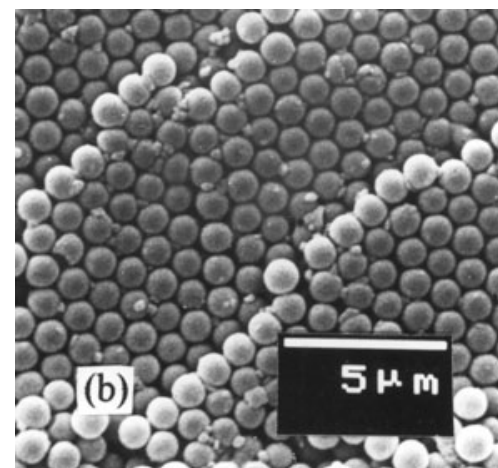
Sol: a colloidal suspension of solid particles within a liquid
Gel: a solid that contains liquids within its pore structures



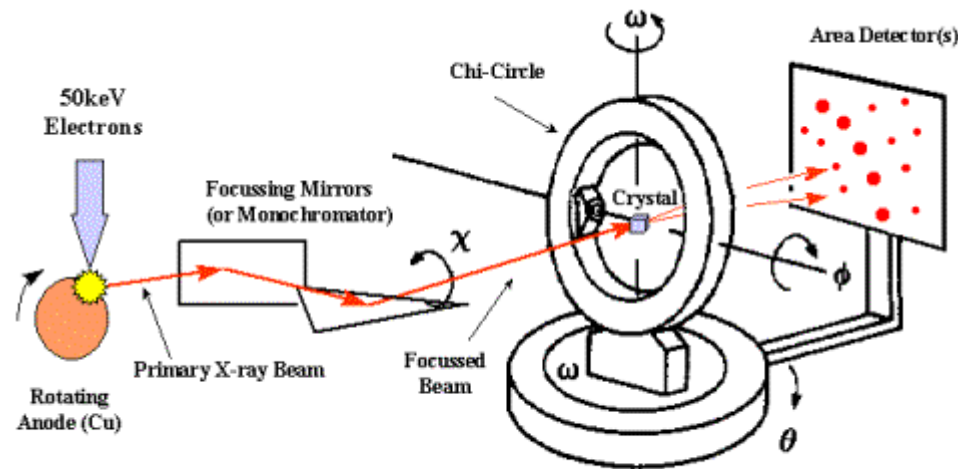


| | Sol | Gel formation | Gel |
|----------------|---|---|--|
| acid solution |  |  |  |
| basic solution |  |  |  |

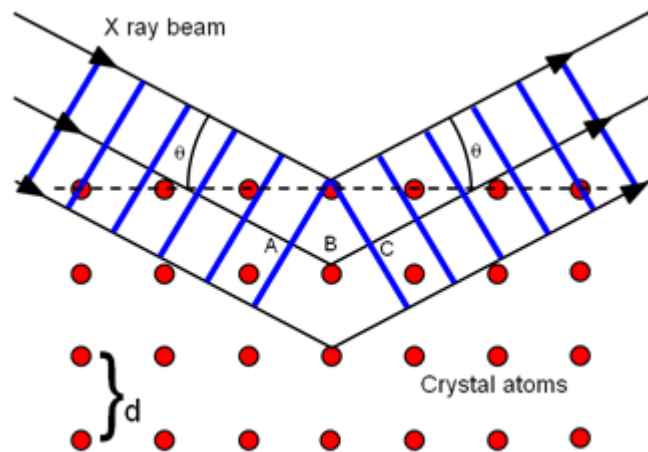
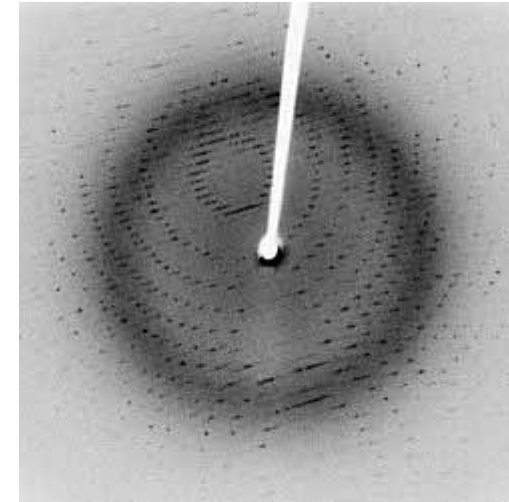
Sol: Dispersion of metal organical Polymers
(Size 1 - 100 nm)



X-ray Diffraction



4-Circle Goniometer (Eulerian or Kappa Geometry)



BRAGG LAW

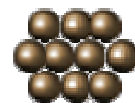
$$2d(\sin\theta) = \lambda_0$$

where:

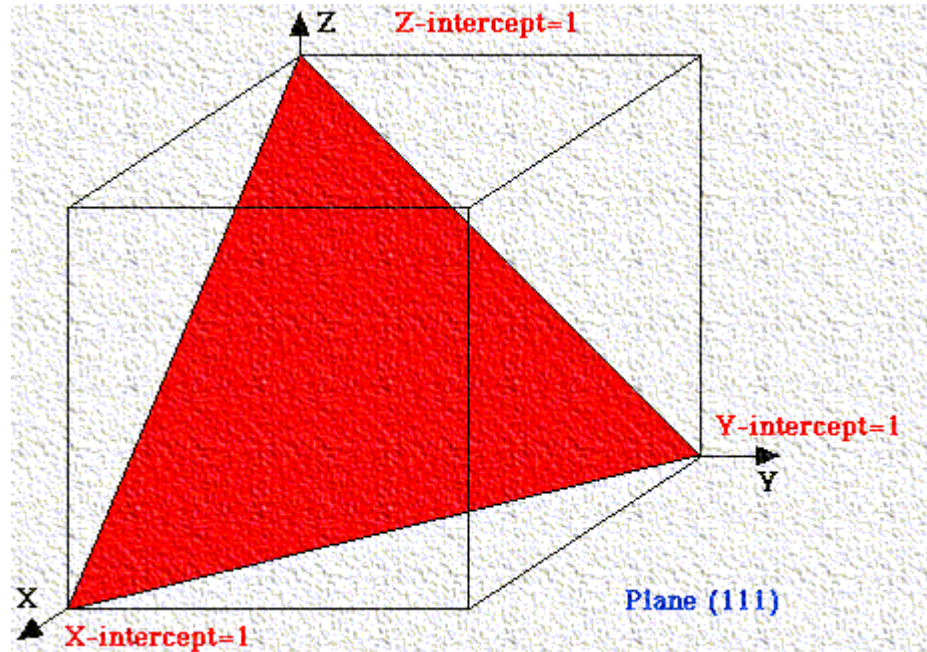
d = lattice interplanar spacing of the crystal

θ = x-ray incidence angle (Bragg angle)

λ = wavelength of the characteristic x-rays

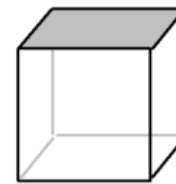


Miller Index

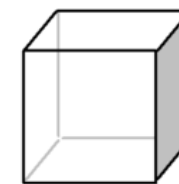


$$l\mathbf{b}_1 + m\mathbf{b}_2 + n\mathbf{b}_3.$$

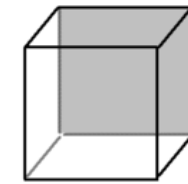
$$(hkl) = h\vec{a}^* + k\vec{b}^* + l\vec{c}^* = \frac{2}{3a^2}(2h+k)\vec{a} + \frac{2}{3a^2}(h+2k)\vec{b} + \frac{1}{c^2}(l)\vec{c}.$$



(001)



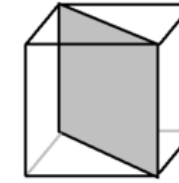
(100)



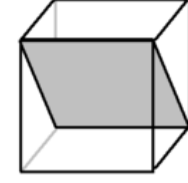
(010)



(101)



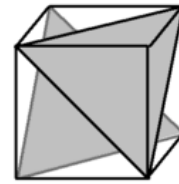
(110)



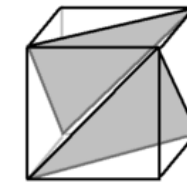
(011)



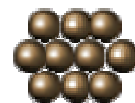
(111)



(1 $\bar{1}$ 1)



($\bar{1}$ 11)



Scherrer Equation

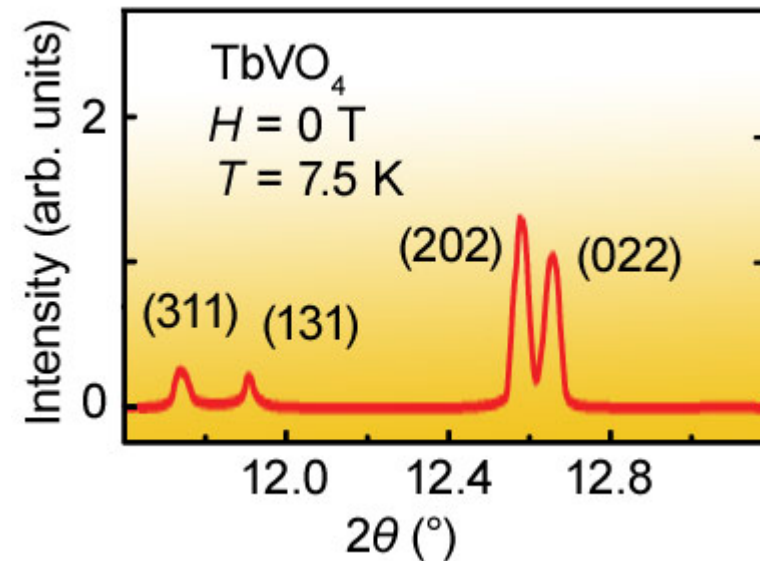
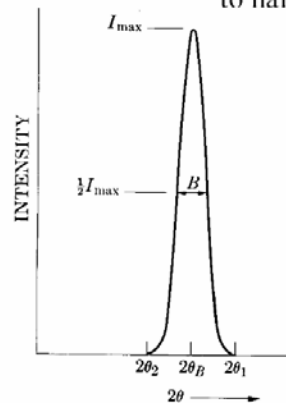
$$\beta_{hkl} = \frac{K\lambda}{L_{hkl} \cos \theta_{hkl}}$$

Scherrer formula:

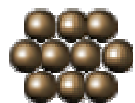
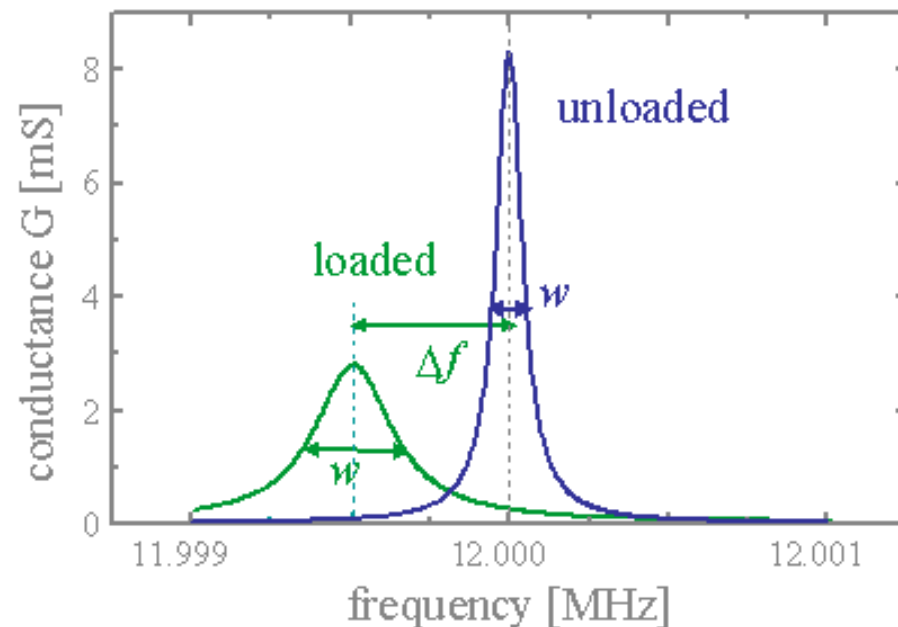
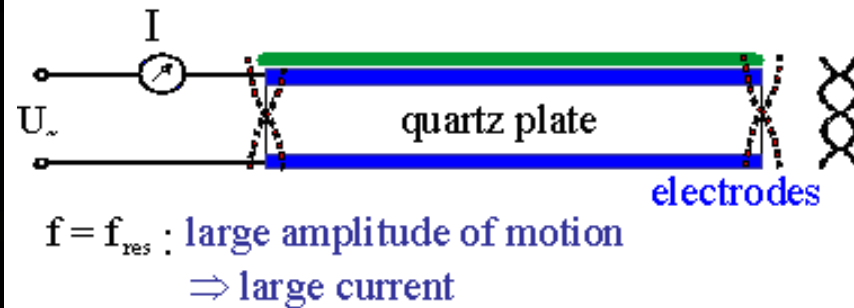
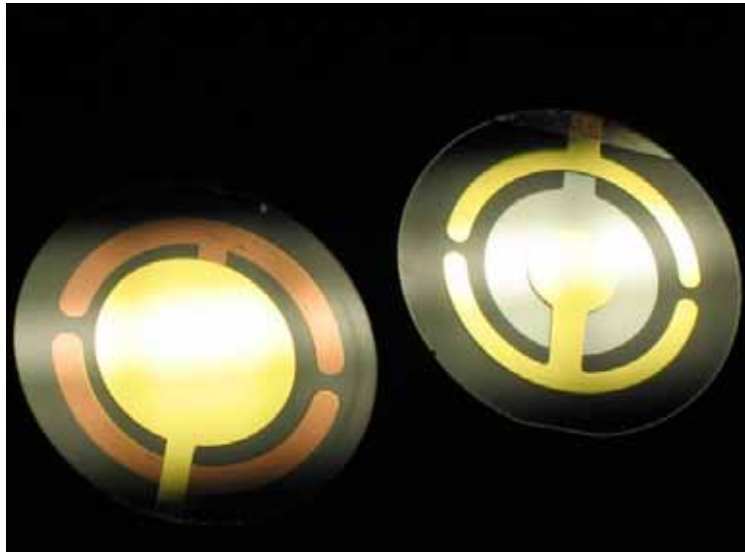
$$t = \frac{0.9\lambda}{B \cos \theta}$$

t : particle size

B (width): in radians, at an intensity equal to half the maximum intensity.



Quartz Crystal Microbalance (QCM)



Dynamic Light Scattering

$$g^2(q; \tau) = \frac{\langle I(t)I(t + \tau) \rangle}{\langle I(t) \rangle^2}$$

$$D = \frac{k_B T}{6\pi \eta r}$$

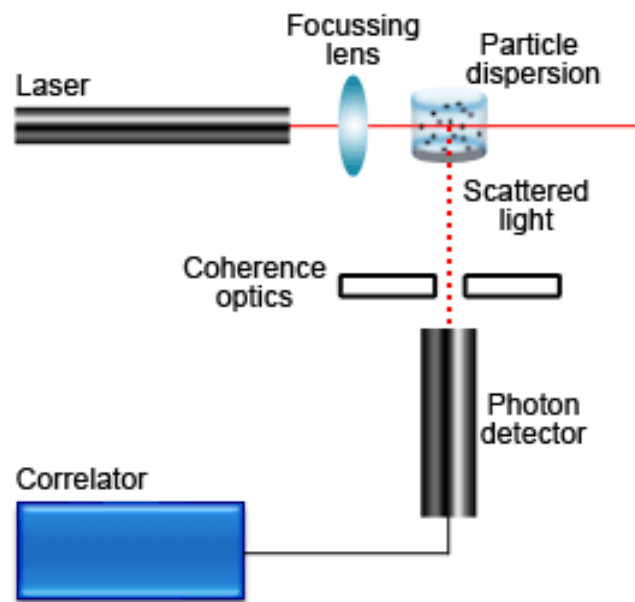
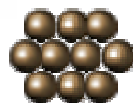
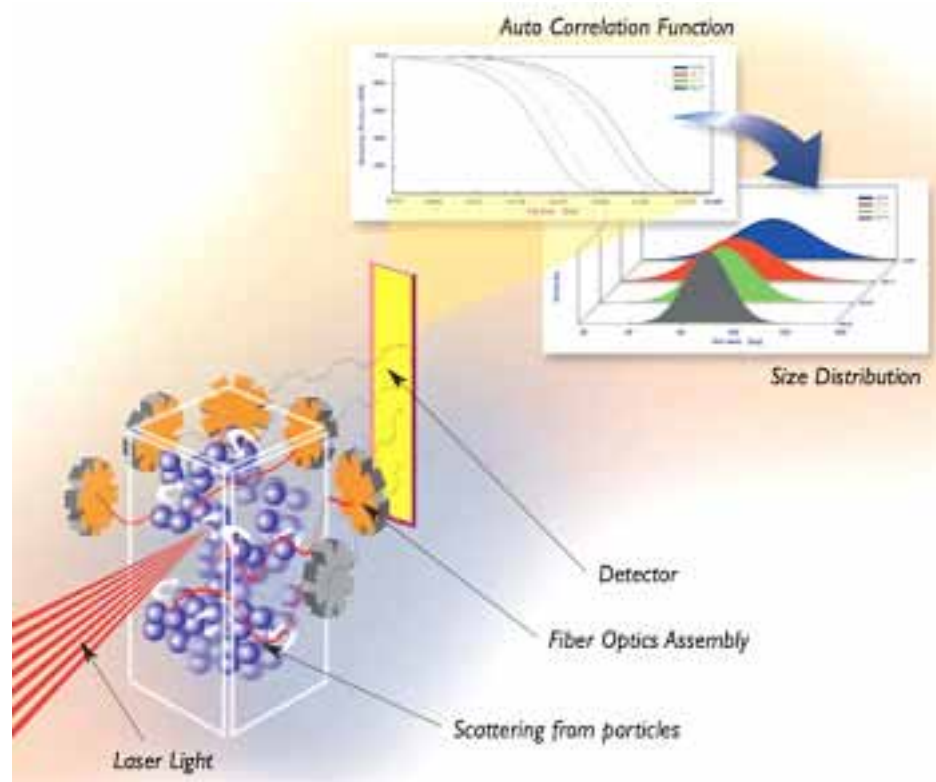


Figure 1: Schematic diagram of a conventional, 90° dynamic light scattering instrument.



Nanomaterials

- Metals and Alloys
 - Fe, Al, Au
- Semiconductors
 - Band gap, CdS, TiO₂, ZnO
- Ceramic
 - Al₂O₃, Si₃N₄, MgO, , SiO₂, ZrO₂
- Carbon based
 - Diamond, graphite, nanotube, C60
- Polymers
 - Soft mater, block co-polymer
- Biological
 - Photonic, hydrophobic, adhesive,
- Composites



Surfaces

- Collective surface area of nanocube 1 nm
- Porous materials
 - Micropore (<2 nm)
 - Mesopore (2 nm ~ 50 nm)
 - Marcopore (> 50nm)
- Void volume
 - $V_{\text{pore}}/V_{\text{material}}$



Surface to Volume Ratio

Au: AAA

Atomic mass: 196.967

Density 19.31

Radii =0.144 nm

| | |
|---------------------------|-----------------------|
| Number of Au atoms in 1 m | $3.4 \cdot 10^9$ |
| Volume of Au atom | $4.19 \cdot 10^{-28}$ |
| Surface area Au atom | $7.22 \cdot 10^{-19}$ |
| Surface/volume ratio | $1.72 \cdot 10^9$ |



Review of Biochemistry



Periodic Table of Elements

| | I A | II A | | | | | | | III A | IV A | V A | VI A | VII A | O | | | | |
|---|-----|------|-------|------|-----|------|-------|---------|-------|------|-----|------|-------|----|----|----|----|----|
| 1 | H | | | | | | | | | | | | | | He | | | |
| 2 | Li | Be | | | | | | | B | C | N | O | F | Ne | | | | |
| 3 | Na | Mg | III B | IV B | V B | VI B | VII B | — VII — | IB | IB | Al | Si | P | S | Cl | Ar | | |
| 4 | K | Ca | Sc | Ti | V | Cr | Mn | Fe | Co | Ni | Cu | Zn | Ga | Ge | As | Se | Br | Kr |
| 5 | Rb | Sr | Y | Zr | Nb | Mo | Tc | Ru | Rh | Pd | Ag | Cd | In | Sn | Sb | Te | I | Xe |
| 6 | Cs | Ba | *La | Hf | Ta | W | Re | Os | Ir | Pt | Au | Hg | Tl | Pb | Bi | Po | At | Rn |
| 7 | Fr | Ra | +Ac | Rf | Ha | 106 | 107 | 108 | 109 | 110 | | | | | | | | |

| | | | | | | | | | | | | | |
|-----------------|-----------------|-----------------|-----------------|-----------------|-----------------|-----------------|-----------------|-----------------|-----------------|------------------|------------------|------------------|------------------|
| 58 Ce | 59 Pr | 60 Nd | 61 Pm | 62 Sm | 63 Eu | 64 Gd | 65 Tb | 66 Dy | 67 Ho | 68 Er | 69 Tm | 70 Yb | 71 Lu |
| 90 Th | 91 Pa | 92 U | 93 Np | 94 Pu | 95 Am | 96 Cm | 97 Bk | 98 Cf | 99 Es | 100 Fm | 101 Md | 102 No | 103 Lr |

+ Actinide
Series

Legend - click to find out more...

Tc - synthetic

Halogens

Inert Elements



Chemical bond

Hydrogen



Carbon



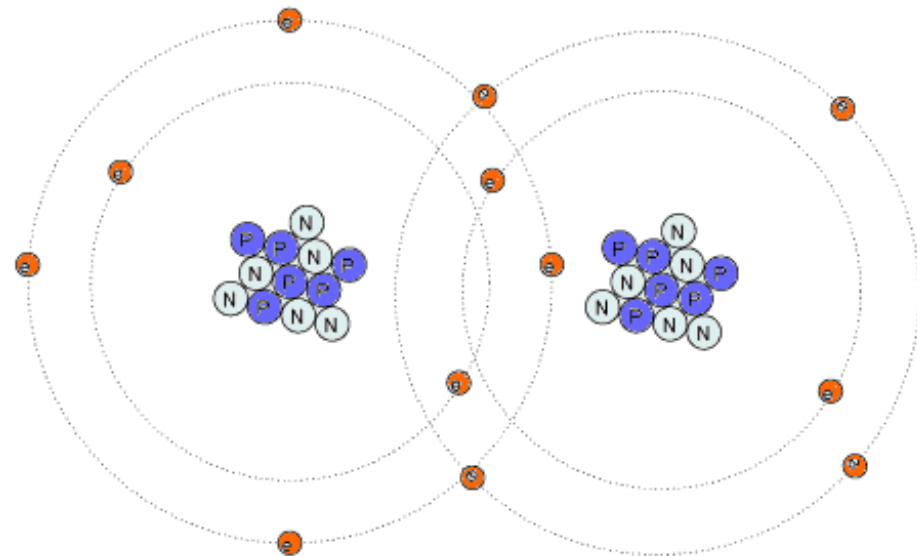
Water



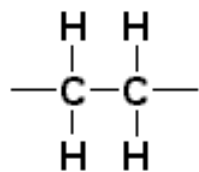
Ethylene



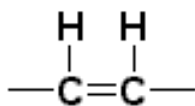
Acetylene



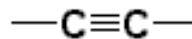
Functional Groups



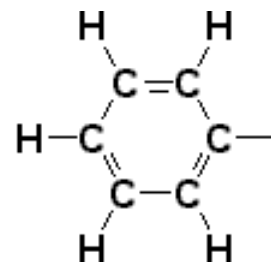
alkane



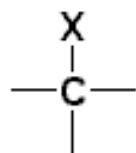
alkene



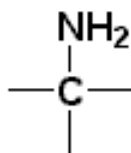
alkyne



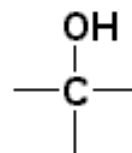
phenyl



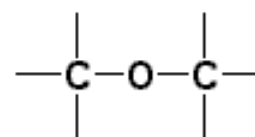
alkyl halide
(X = F, Cl, Br, I)



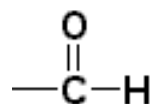
amine



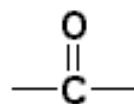
alcohol



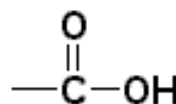
ether



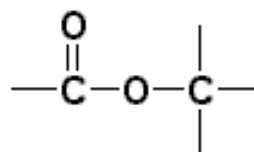
aldehyde



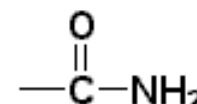
ketone



carboxylic
acid



ester



amide

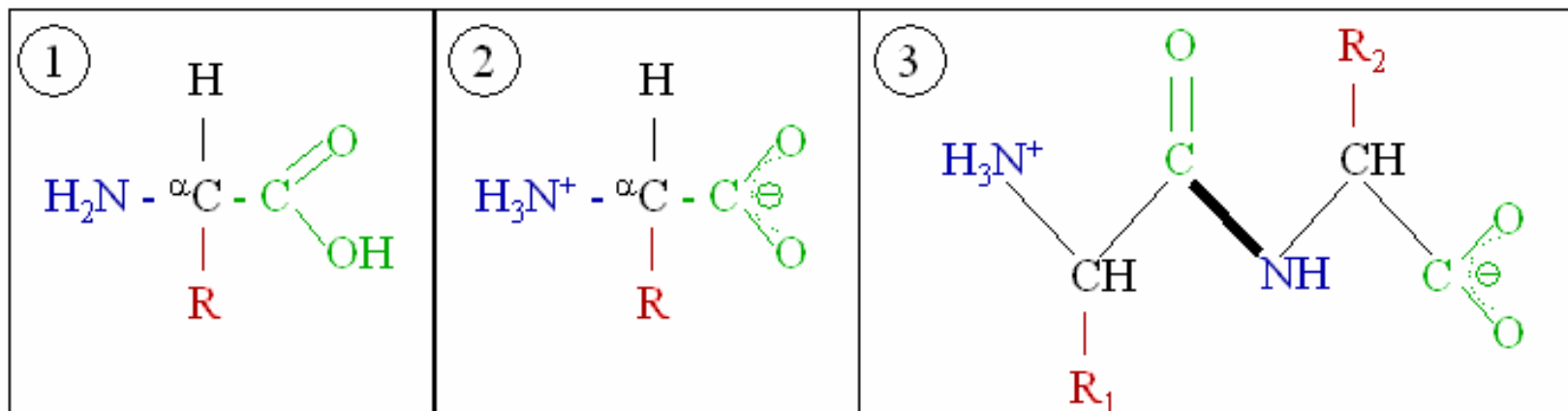
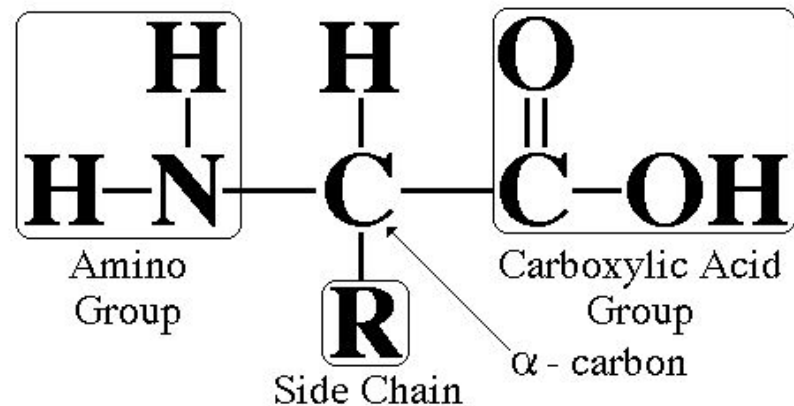


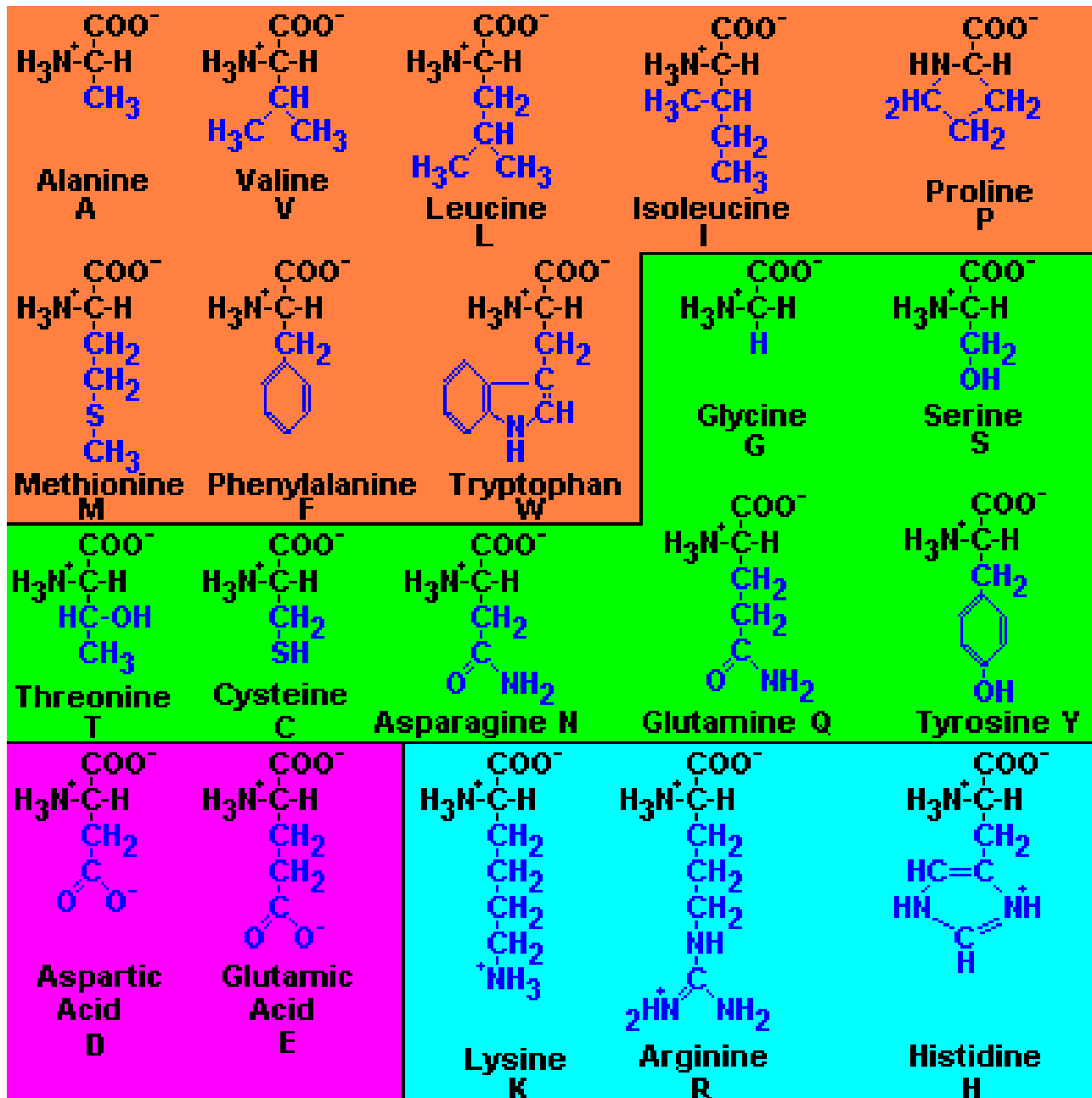
TABLE 18.1 Functional Groups of Importance in Biochemical Molecules

| Functional Group | Structure | Type of Biomolecule |
|------------------------------|--|--|
| Amino group | $-\text{NH}_3^+, -\text{NH}_2$ | Amino acids and proteins (Sections 18.3, 18.7) |
| Hydroxyl group | $-\text{OH}$ | Monosaccharides (carbohydrates) and glycerol: a component of triacylglycerols (lipids) (Sections 22.4, 24.2) |
| Carbonyl group | $\begin{array}{c} \text{O} \\ \parallel \\ -\text{C}- \end{array}$ | Monosaccharides (carbohydrates); in acetyl group (CH_3CO) used to transfer carbon atoms during catabolism (Sections 22.4, 21.4, 21.8) |
| Carboxyl group | $\begin{array}{c} \text{O} \\ \parallel \\ -\text{C}-\text{OH}, \end{array} \begin{array}{c} \text{O} \\ \parallel \\ -\text{C}-\text{O}^- \end{array}$ | Amino acids, proteins, and fatty acids (lipids) (Sections 18.3, 18.7, 24.2) |
| Amide group | $\begin{array}{c} \text{O} \\ \parallel \\ -\text{C}-\text{N}- \\ \end{array}$ | Links amino acids in proteins; formed by reaction of amino group and carboxyl group (Section 18.7) |
| Carboxylic acid ester | $\begin{array}{c} \text{O} \\ \parallel \\ -\text{C}-\text{O}-\text{R} \end{array}$ | Triacylglycerols (and other lipids); formed by reaction of carboxyl group and hydroxyl group (Section 24.2) |
| Phosphates, mono-, di-, tri- | $\begin{array}{c} \\ \\ -\text{C}-\text{O}-\text{P}(=\text{O})(\text{O}^-)-\text{O}^- \\ \end{array}$ $\begin{array}{c} \\ \\ -\text{C}-\text{O}-\text{P}(=\text{O})(\text{O}^-)-\text{O}-\text{P}(=\text{O})(\text{O}^-)-\text{O}^- \\ \quad \end{array}$ $\begin{array}{c} \\ \\ -\text{C}-\text{O}-\text{P}(=\text{O})(\text{O}^-)-\text{O}-\text{P}(=\text{O})(\text{O}^-)-\text{O}-\text{P}(=\text{O})(\text{O}^-)-\text{O}^- \\ \quad \quad \end{array}$ | ATP and many metabolism intermediates (Sections 17.8, 21.5, and throughout metabolism sections) |
| Hemiacetal group | $\begin{array}{c} \\ -\text{C}-\text{OH} \\ \\ \text{OR} \end{array}$ | Cyclic forms of monosaccharides; formed by a reaction of carbonyl group with hydroxyl group (Sections 16.7, 22.4) |
| Acetal group | $\begin{array}{c} \\ -\text{C}-\text{OR} \\ \\ \text{OR} \end{array}$ | Connects monosaccharides in disaccharides and larger carbohydrates; formed by reaction of carbonyl group with hydroxyl group (Sections 16.7, 22.7, 22.9) |

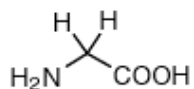
Amino Acid

Amino Acid Structure

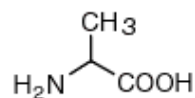




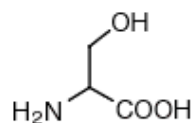
Small



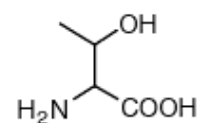
Glycine (Gly, G)
MW: 57.05



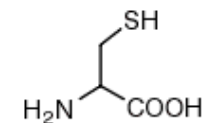
Alanine (Ala, A)
MW: 71.09



Serine (Ser, S)
MW: 87.08, pK_a ~ 16

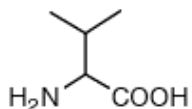


Threonine (Thr, T)
MW: 101.11, pK_a ~ 16

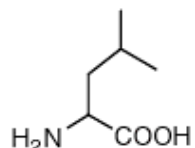


Cysteine (Cys, C)
MW: 103.15, pK_a = 8.35

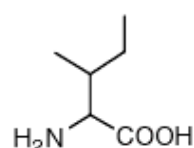
Hydrophobic



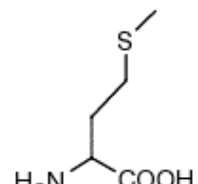
Valine (Val, V)
MW: 99.14



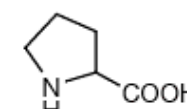
Leucine (Leu, L)
MW: 113.16



Isoleucine (Ile, I)
MW: 113.16

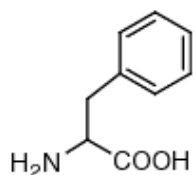


Methionine (Met, M)
MW: 131.19

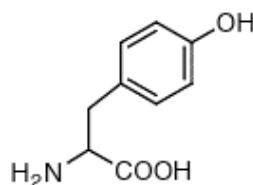


Proline (Pro, P)
MW: 97.12

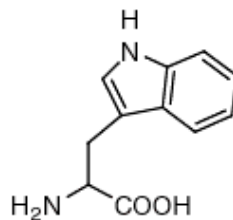
Aromatic



Phenylalanine (Phe, F)
MW: 147.18

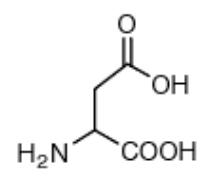


Tyrosine (Tyr, Y)
MW: 163.18

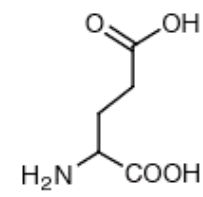


Tryptophan (Trp, W)
MW: 186.21

Acidic

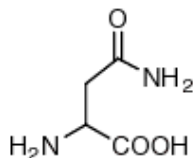


Aspartic Acid (Asp, D)
MW: 115.09, pK_a = 3.9

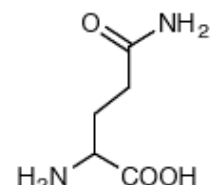


Glutamic Acid (Glu, E)
MW: 129.12, pK_a = 4.07

Amide

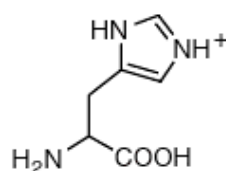


Asparagine (Asn, N)
MW: 114.11

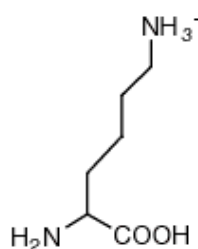


Glutamine (Gln, Q)
MW: 128.14

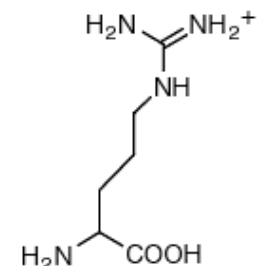
Basic



Histidine (His, H)
MW: 137.14, pK_a = 6.04



Lysine (Lys, K)
MW: 128.17, pK_a = 10.79



Arginine (Arg, R)
MW: 156.19, pK_a = 12.48

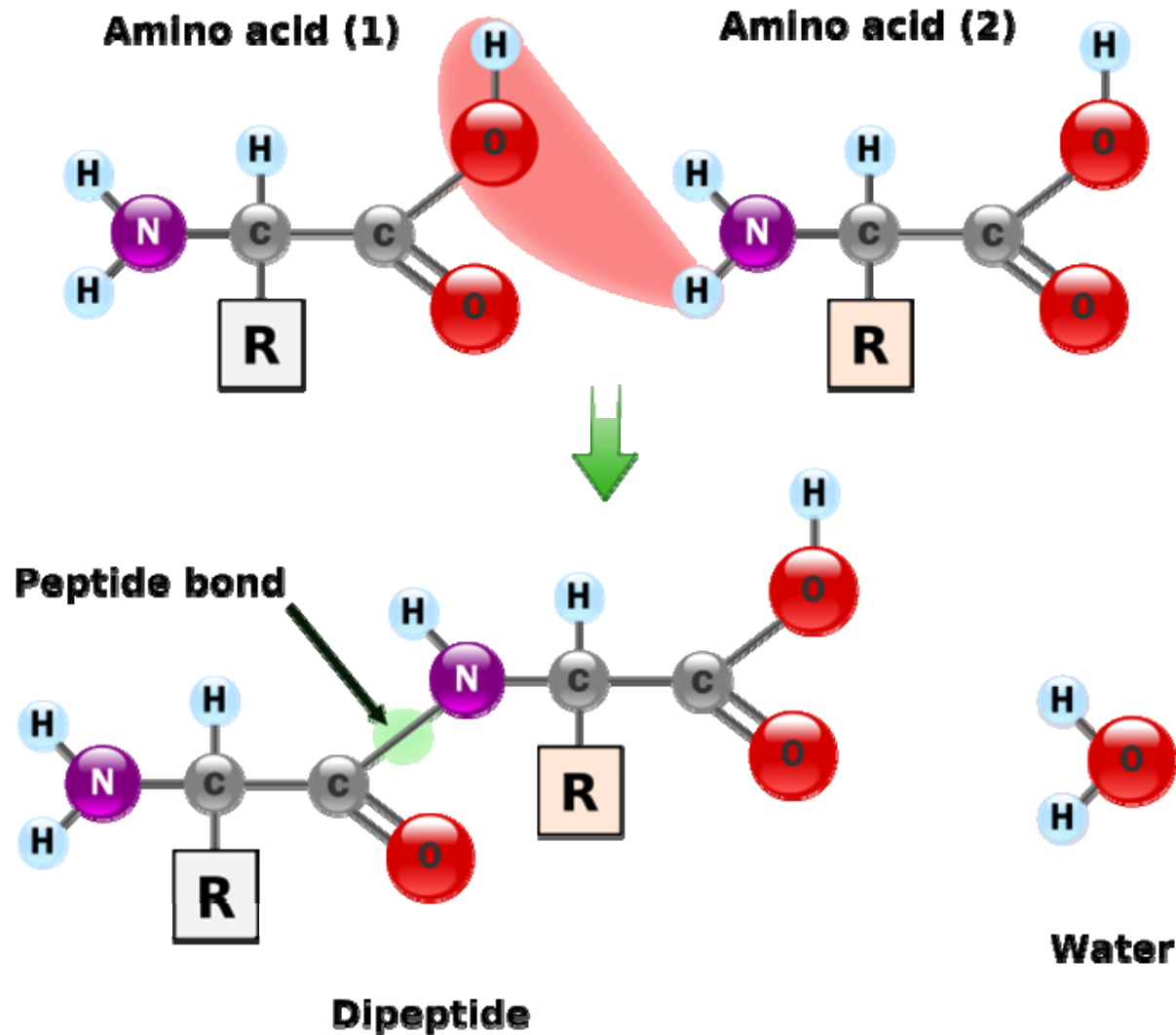


Protein Structure and Function

- Proteins are **polymers** of amino acids.
- Each amino acids in a protein contains a amino group, -NH₂, a carboxyl group, -COOH, and an R group, all bonded to the central carbon atom. The R group may be a hydrocarbon or they may contain functional group.
- All amino acids present in a proteins are ***α-amino acids*** in which the amino group is bonded to the carbon next to the carboxyl group.
- Two or more amino acids can join together by forming amide bond, which is known as a ***peptide bond*** when they occur in proteins.

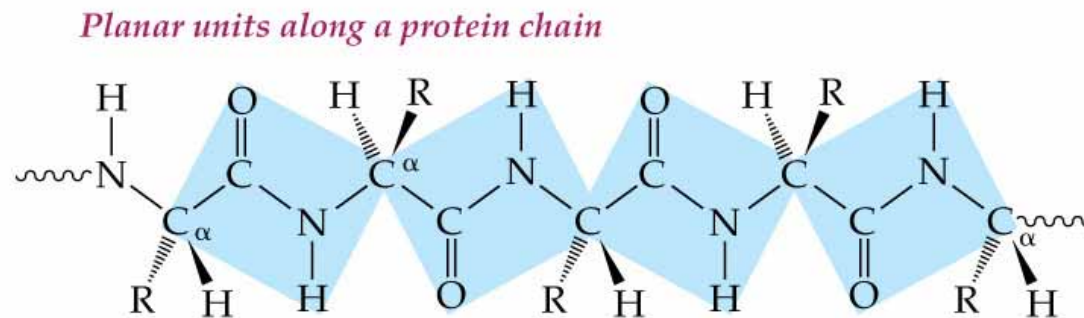


Peptide bond

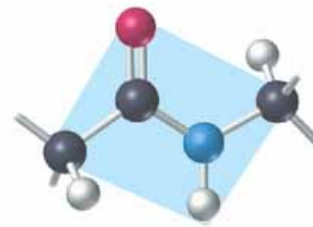


Primary Protein Structure

- Primary structure of a proteins is the sequence of amino acids connected by **peptide bonds**. Along the backbone of the proteins is a chain of alternating peptide bonds and α -carbons and the amino acid side chains are connected to these



One planar unit



- By convention, peptides and proteins are always written with the amino terminal amino acid (N-terminal) on the left and carboxyl-terminal amino acid (C-terminal) on the right.

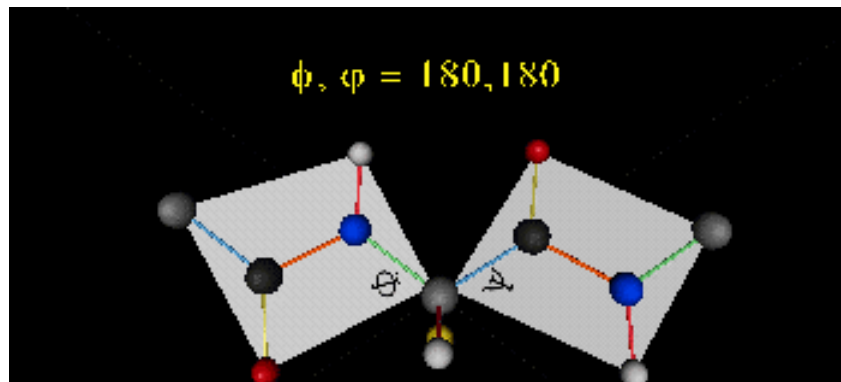
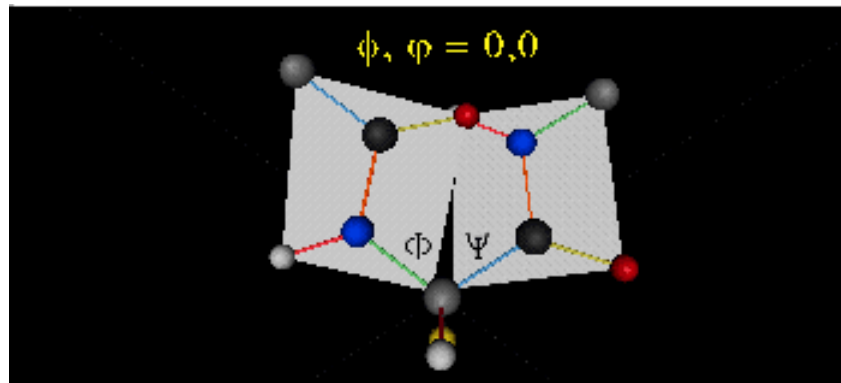
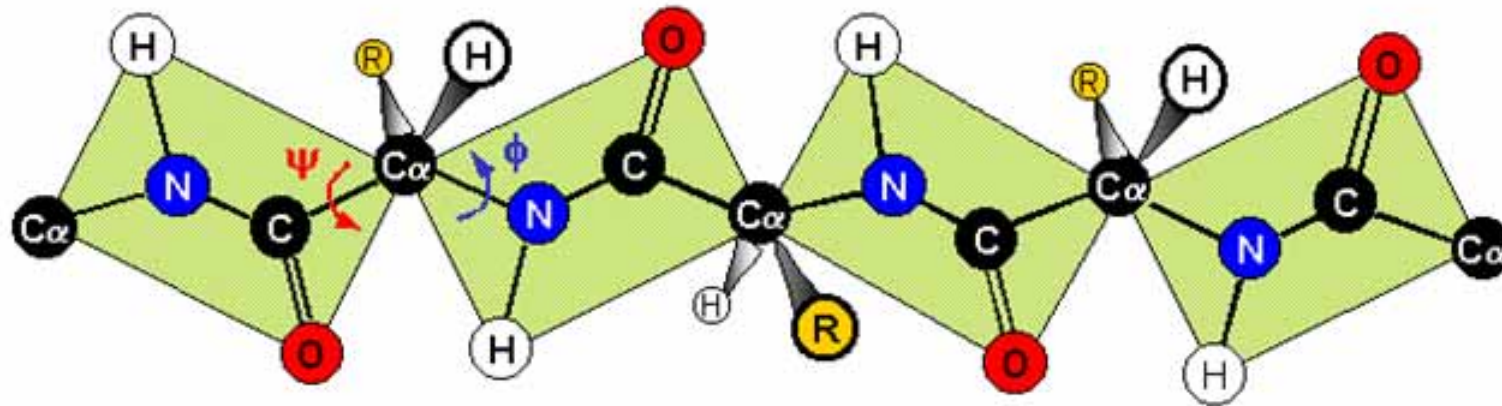


Secondary Protein Structure

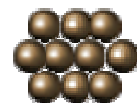
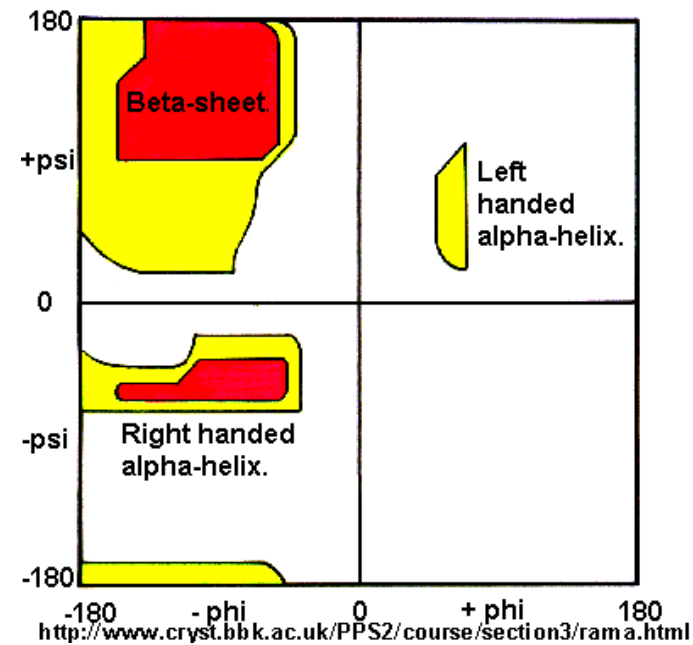
- Secondary structure of a protein is the arrangement of polypeptide backbone of the protein in space. The secondary structure includes two kinds of repeating pattern known as the *α -helix* and *β -sheet*.
- Hydrogen bonding between backbone atoms are responsible for both of these secondary structures.



FULLY EXTENDED POLYPEPTIDE CHAIN

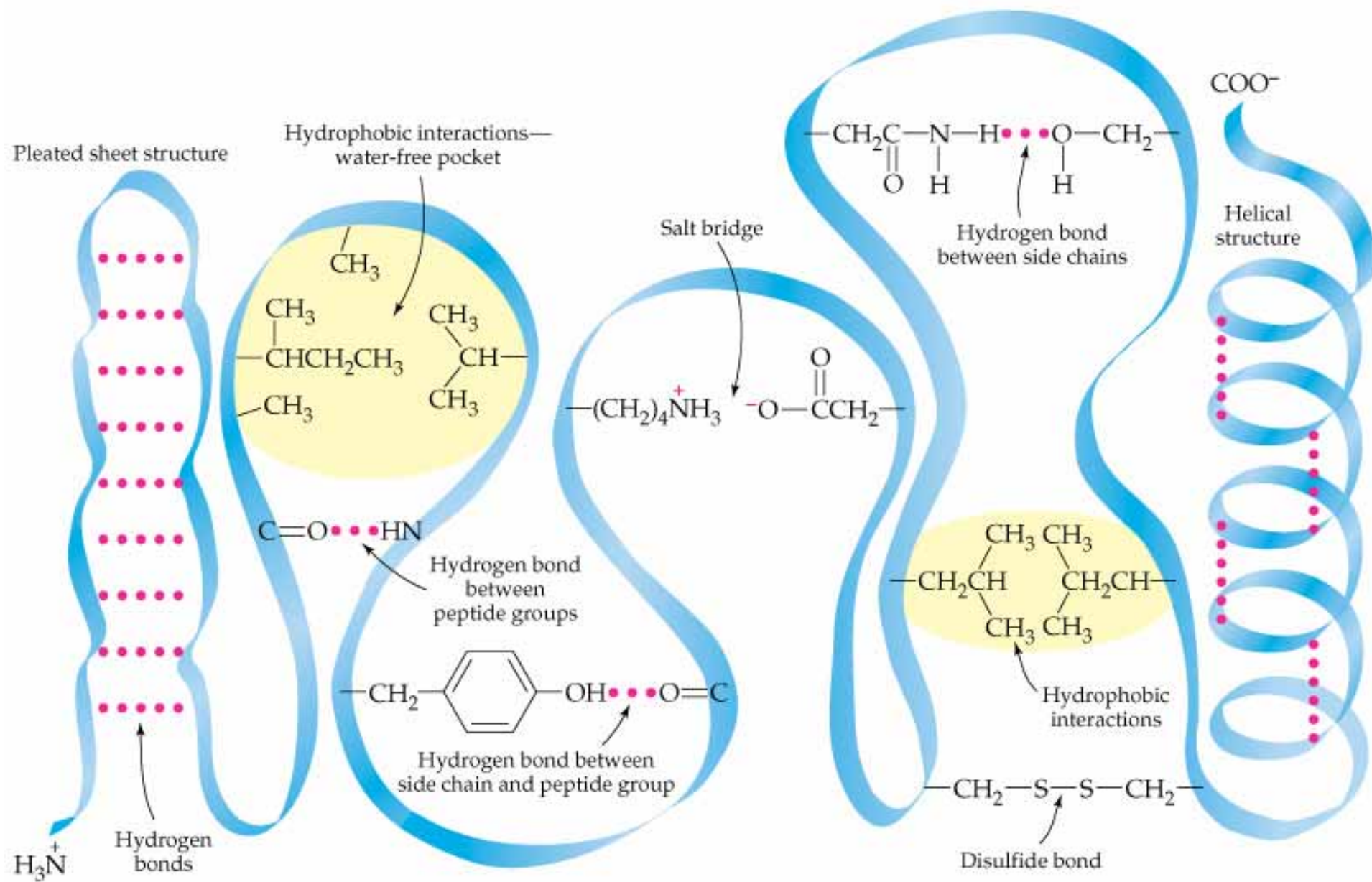


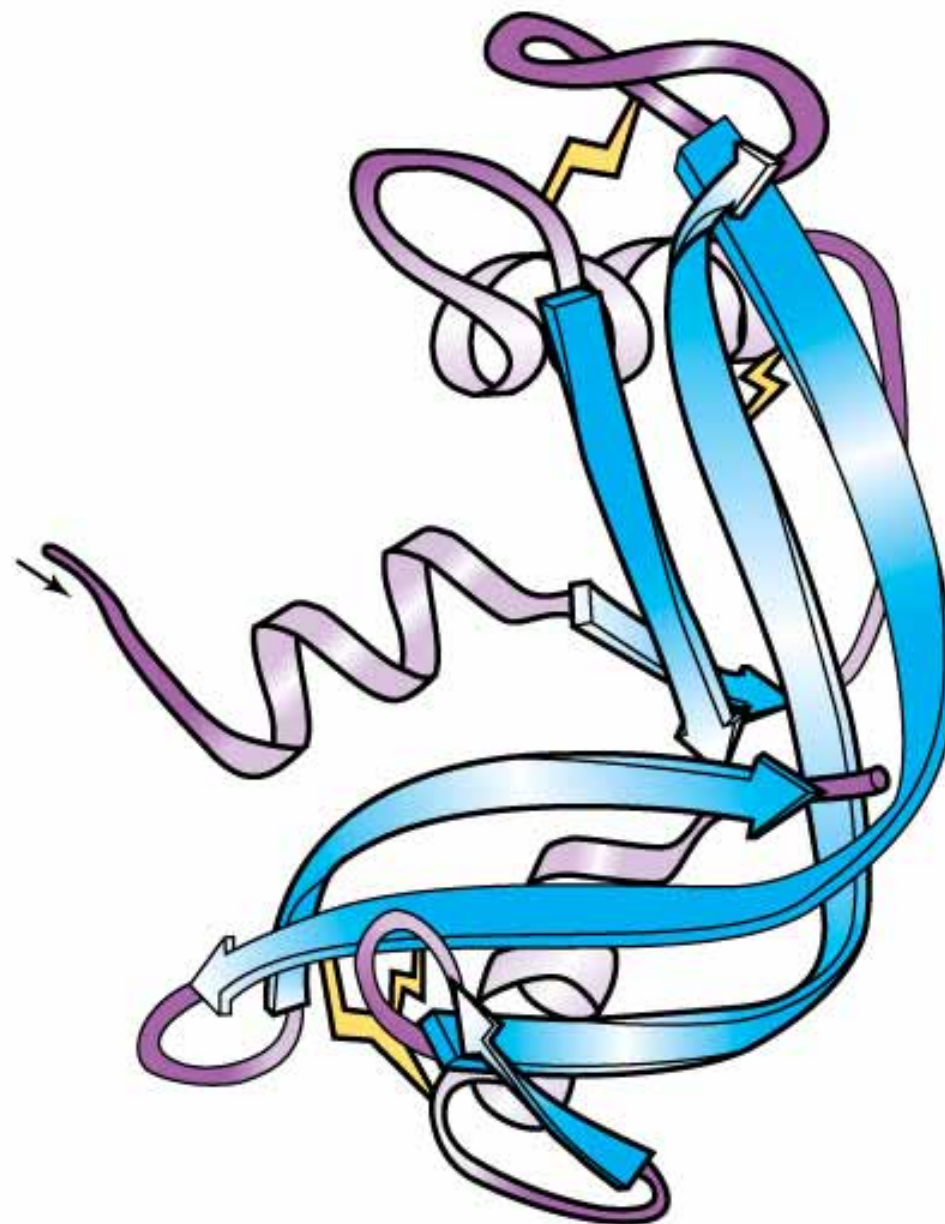
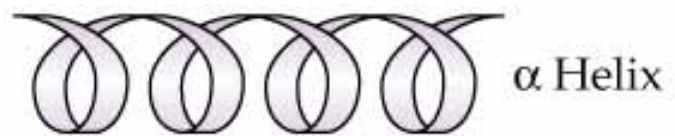
The Ramachandran Plot.



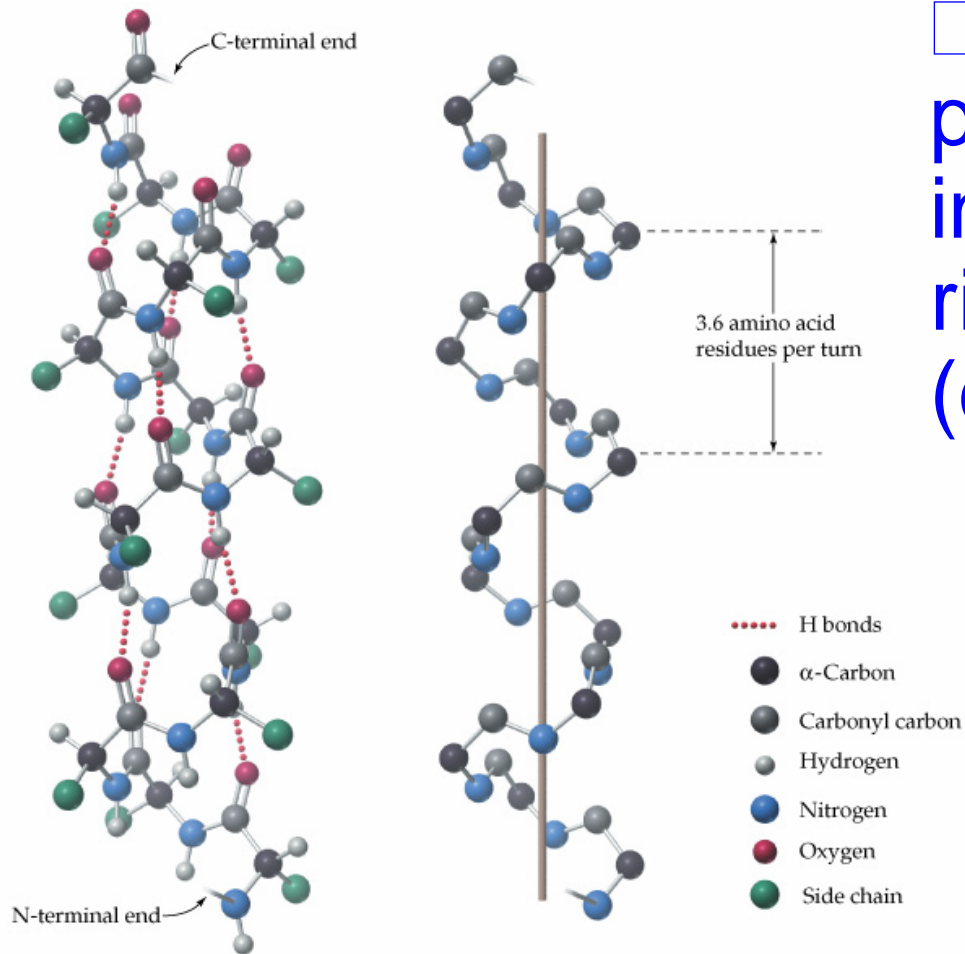
- Protein shape determining interactions are summarized below:
- **Hydrogen bond** between neighboring backbone segments.
- Hydrogen bonds of side chains with each other or with backbone atoms.
- **Ionic attractions** between side chain groups or salt bridge.
- **Hydrophobic** interactions between side chain groups.
- Covalent **sulfur-sulfur** bonds.



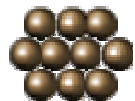




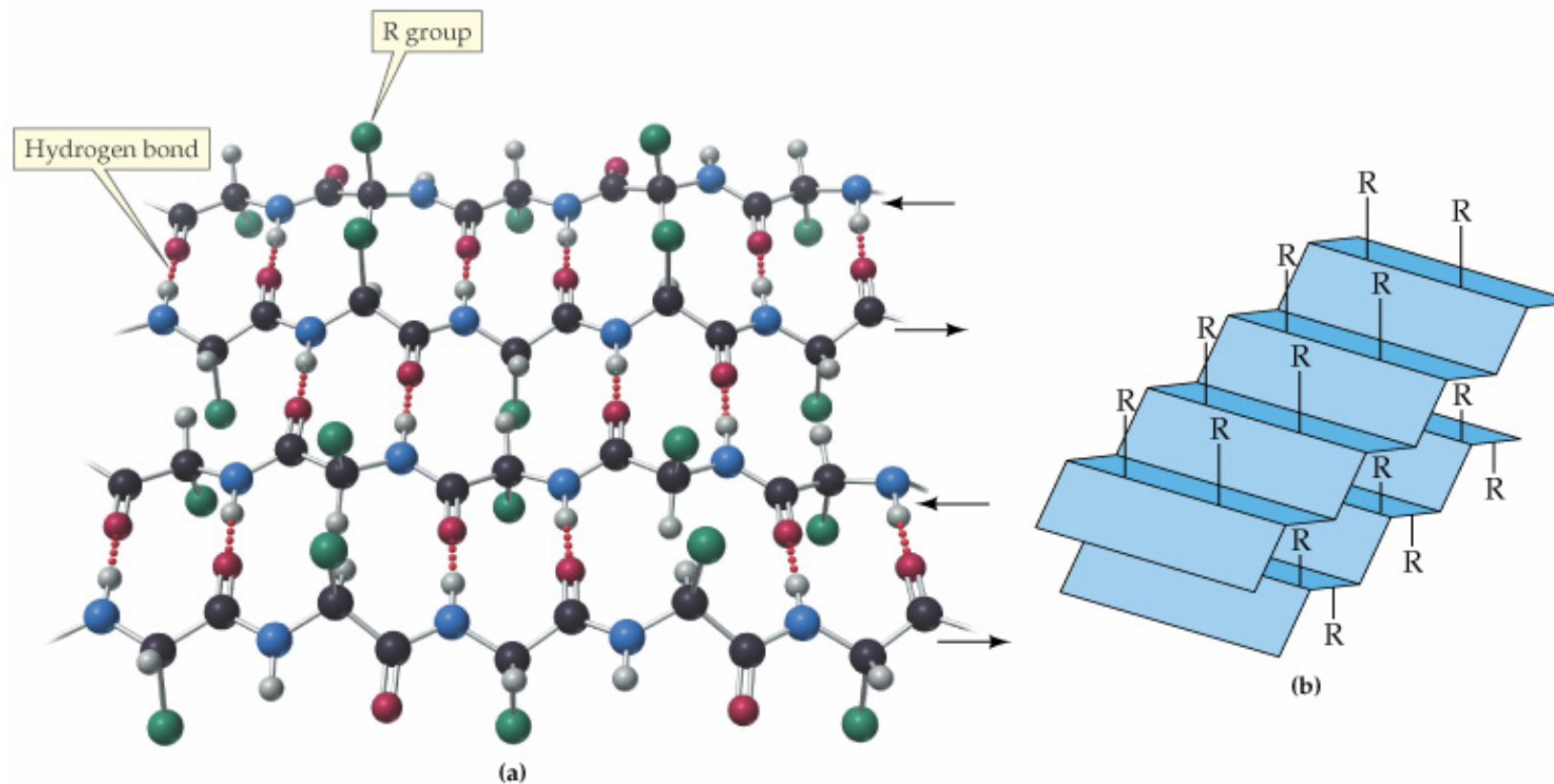
Ribonuclease



□ **α -Helix:** A single protein chain coiled in a spiral with a right-handed (clockwise) twist.

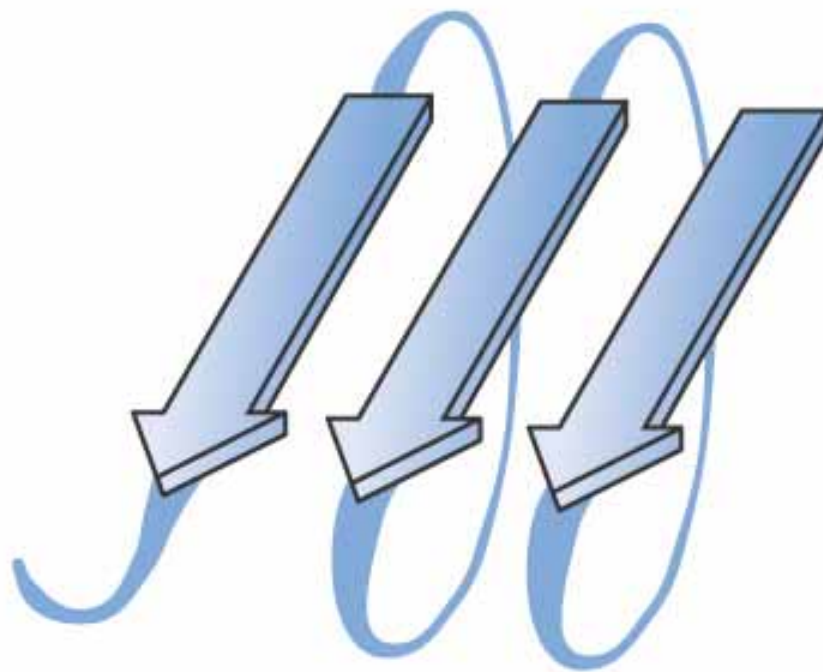


□ **β -Sheet:** The polypeptide chain is held in place by hydrogen bonds between pairs of peptide units along neighboring backbone segments.





α helix



β sheet

Shape-Determining Interactions in Proteins

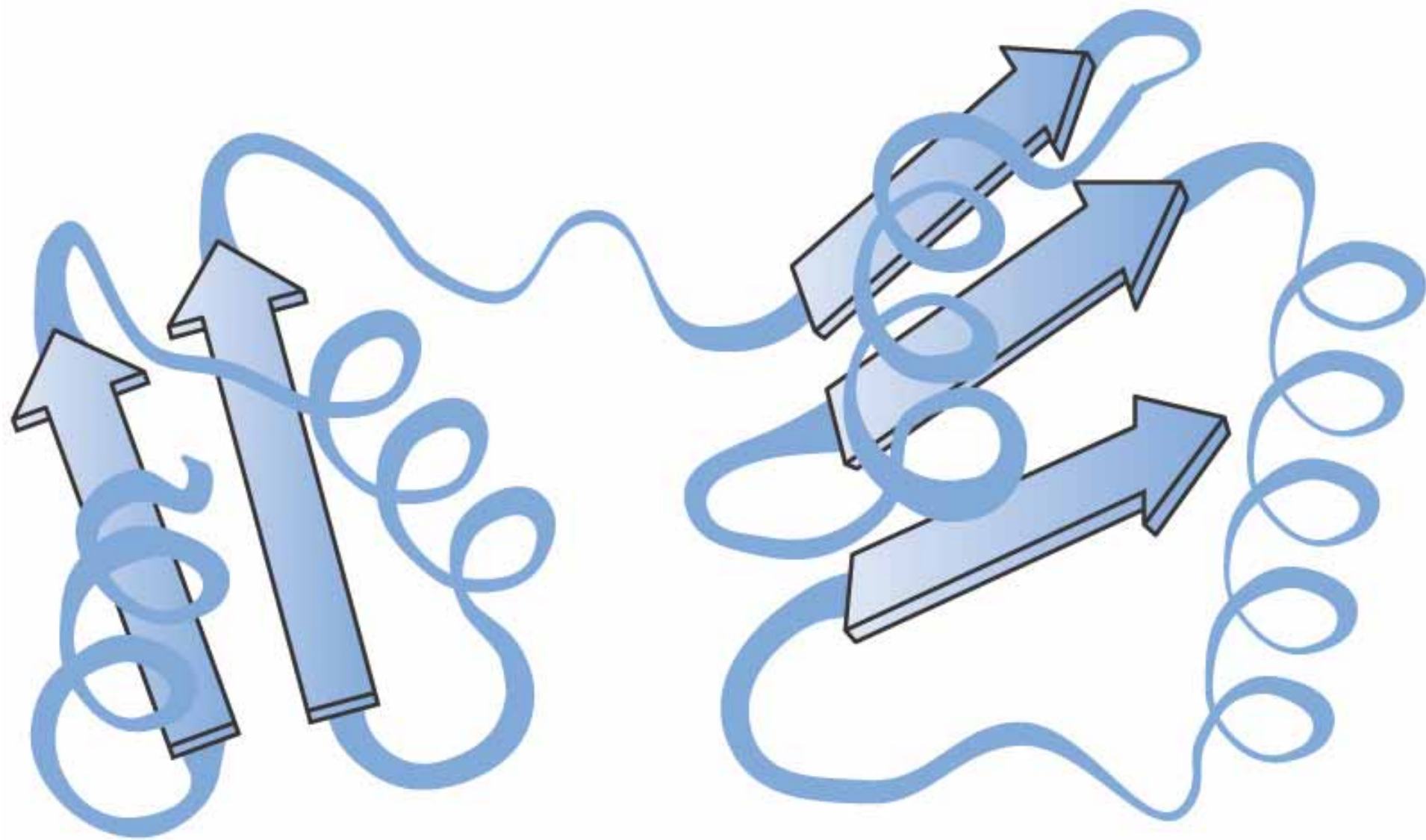
- The essential structure-function relationship for each protein depends on the polypeptide chain being held in its necessary shape by the interactions of atoms in the side chains.



Tertiary Protein Structure

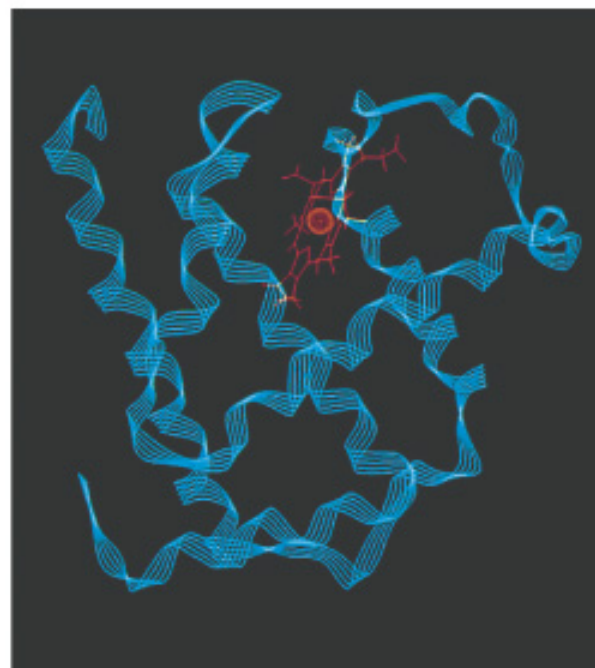
- ***Tertiary Structure of a proteins*** The overall three dimensional shape that results from the folding of a protein chain. Tertiary structure depends mainly on attractions of amino acid side chains that are far apart along the same backbone. Non-covalent interactions and disulfide covalent bonds govern tertiary structure.
- A protein with the shape in which it exist naturally in living organisms is known as a *native protein*.



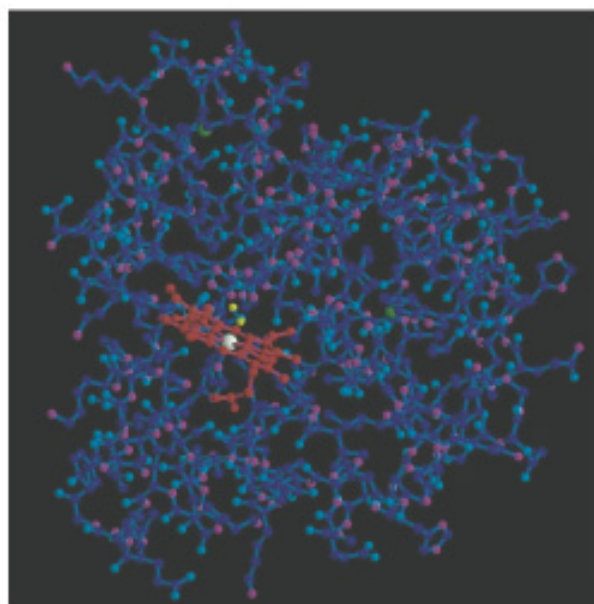




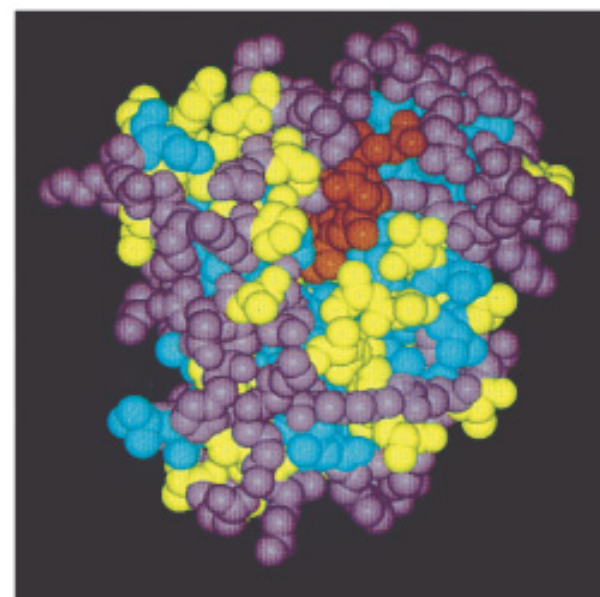
(a)



(b)



(c)

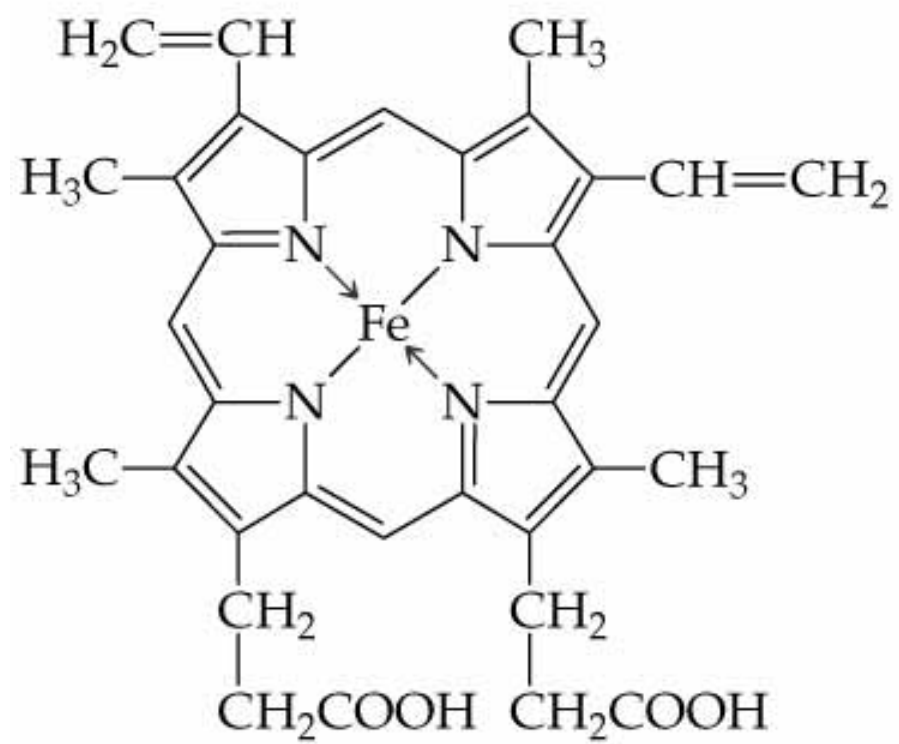


(d)

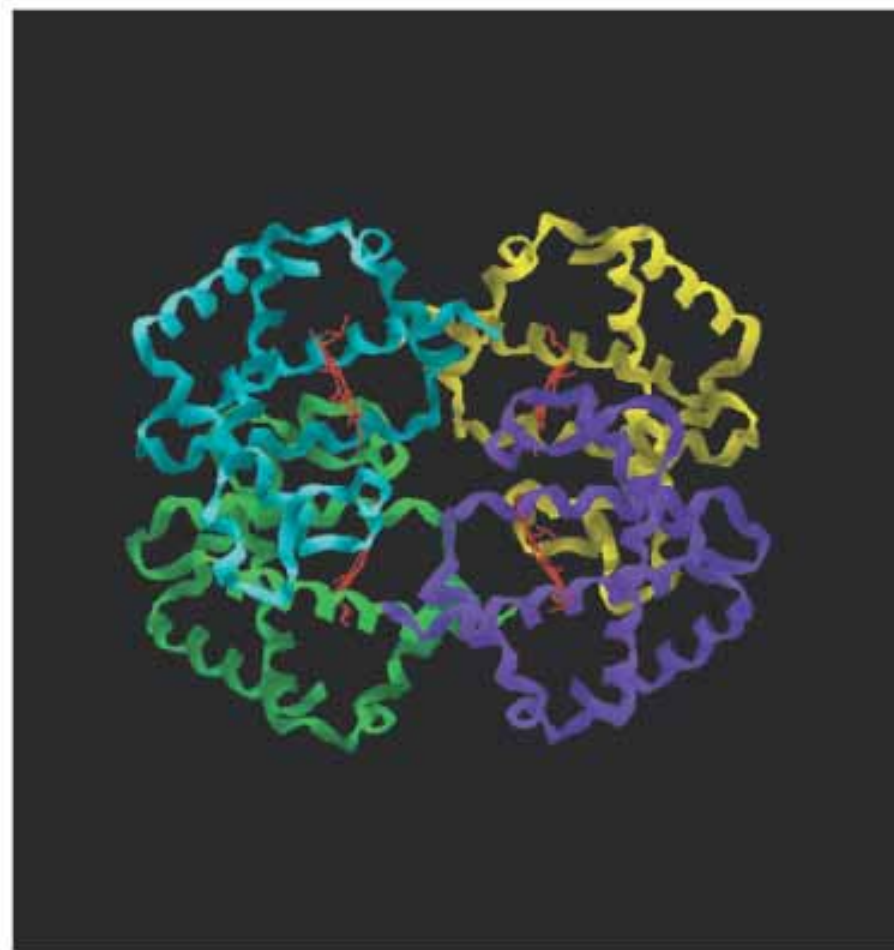
Quaternary Protein Structure

- ***Quaternary protein structure***: The way in which two or more polypeptide sub-units associate to form a single three-dimensional protein unit. Non-covalent forces are responsible for quaternary structure essential to the function of proteins.

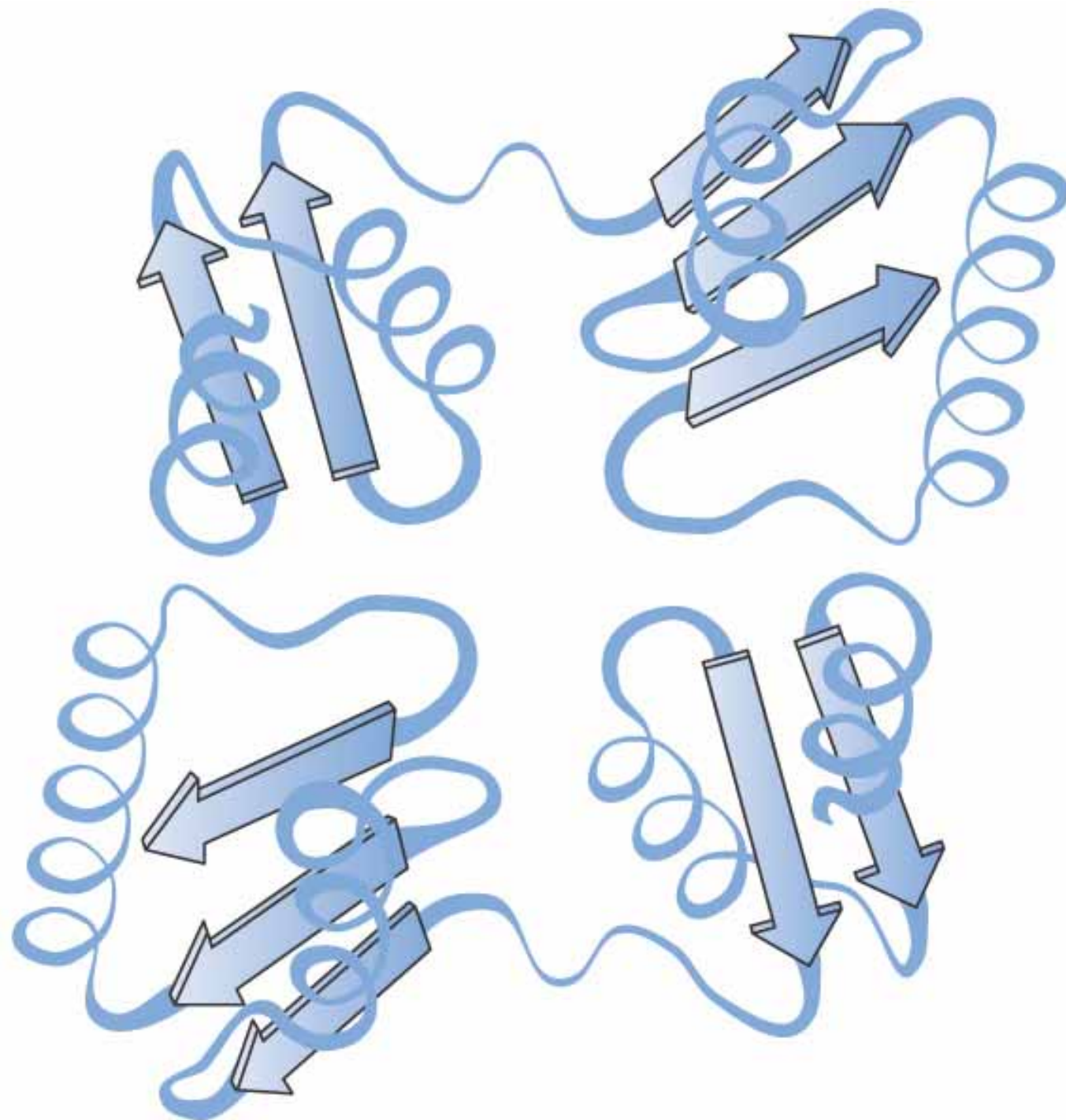


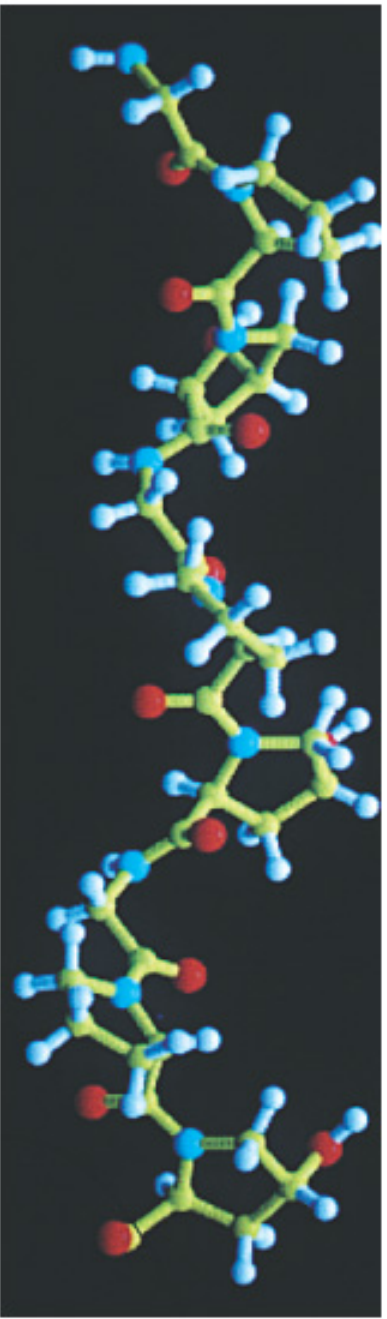


(a)

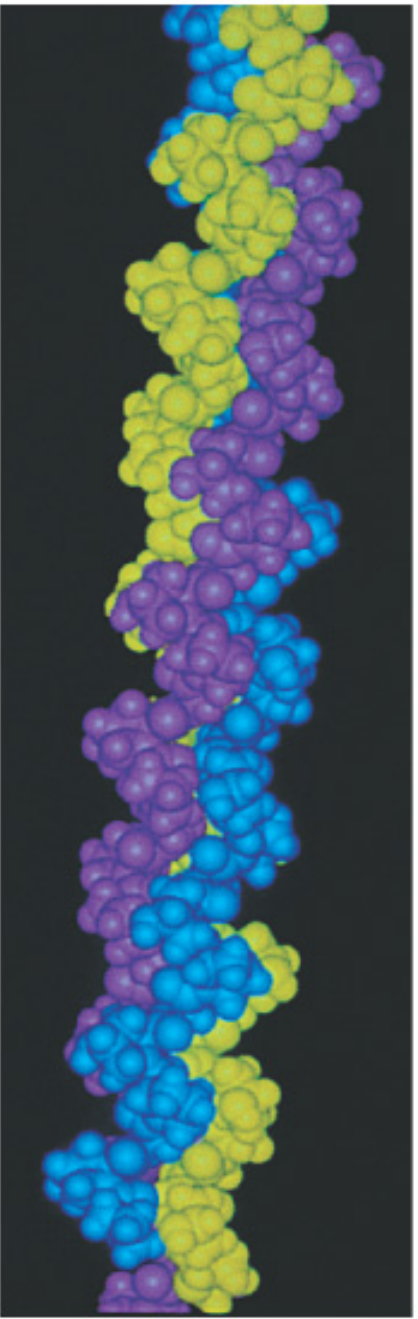


(b)

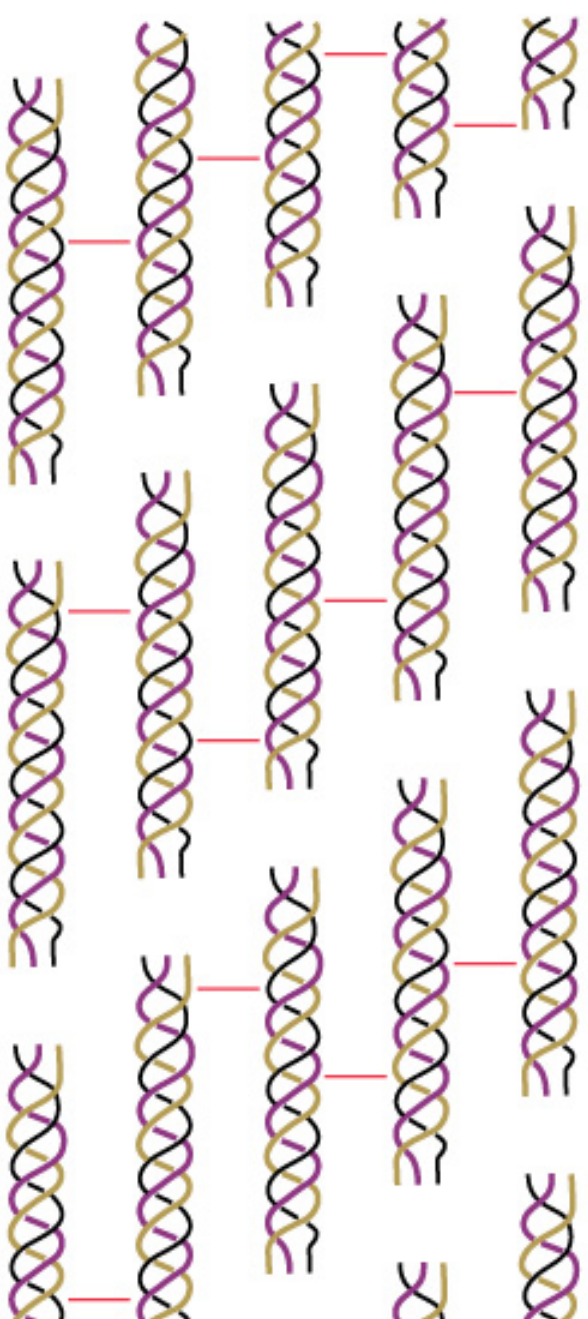




(a)



(b)



(c)

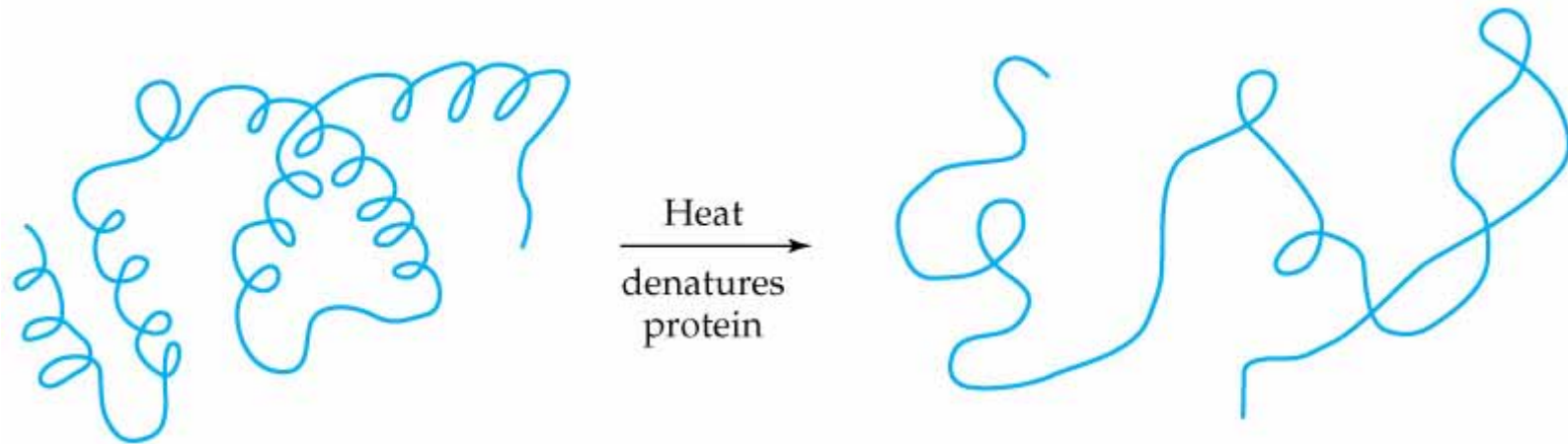
Chemical Properties of Proteins

- *Protein hydrolysis:* In protein hydrolysis, peptide bonds are hydrolyzed to yield amino acids. This is reverse of protein formation.





- *Protein denaturation*: The loss of secondary, tertiary, or quaternary protein structure due to disruption of non-covalent interactions and or disulfide bonds that leaves peptide bonds and primary

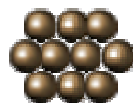
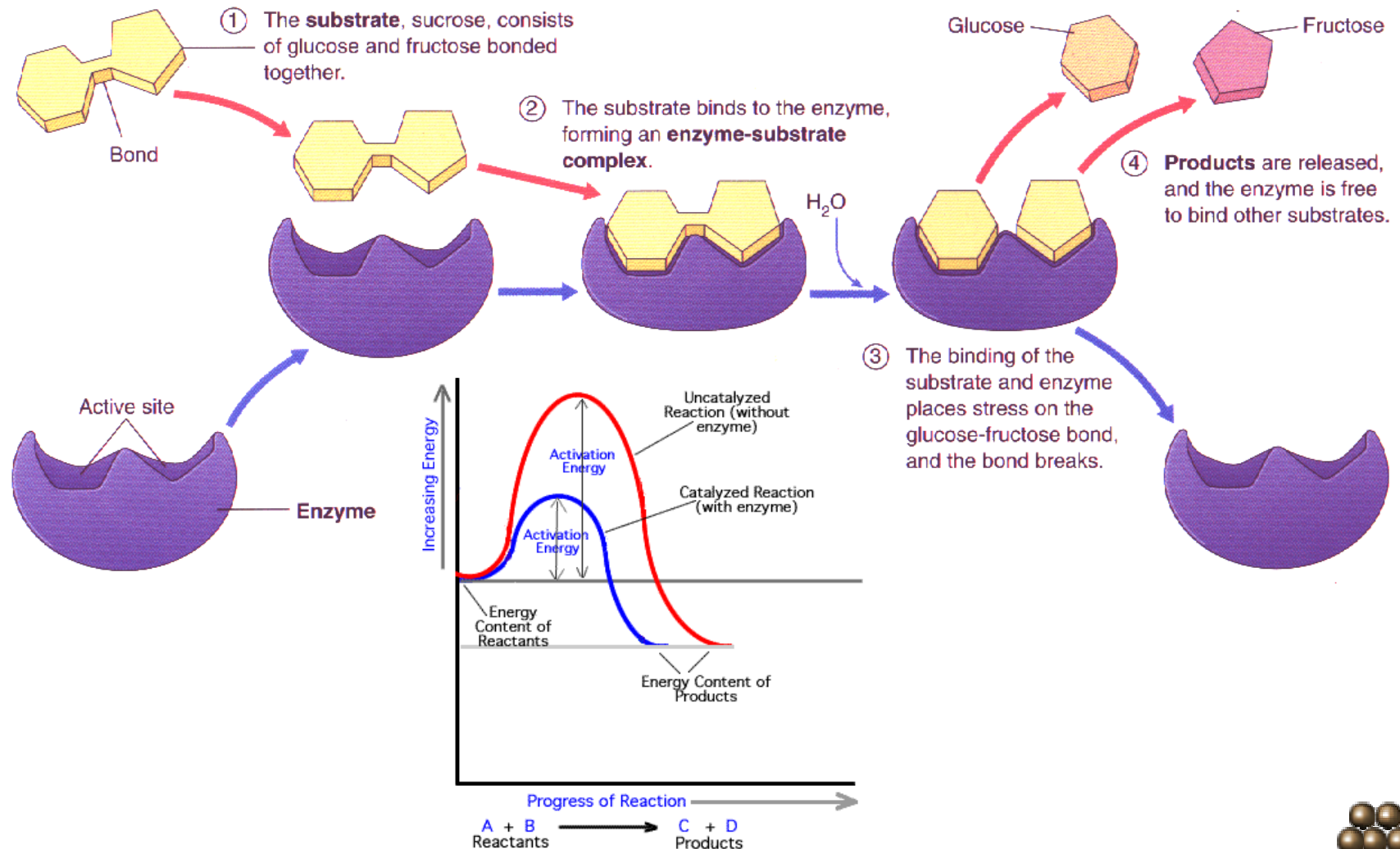


Catalysis by Enzymes

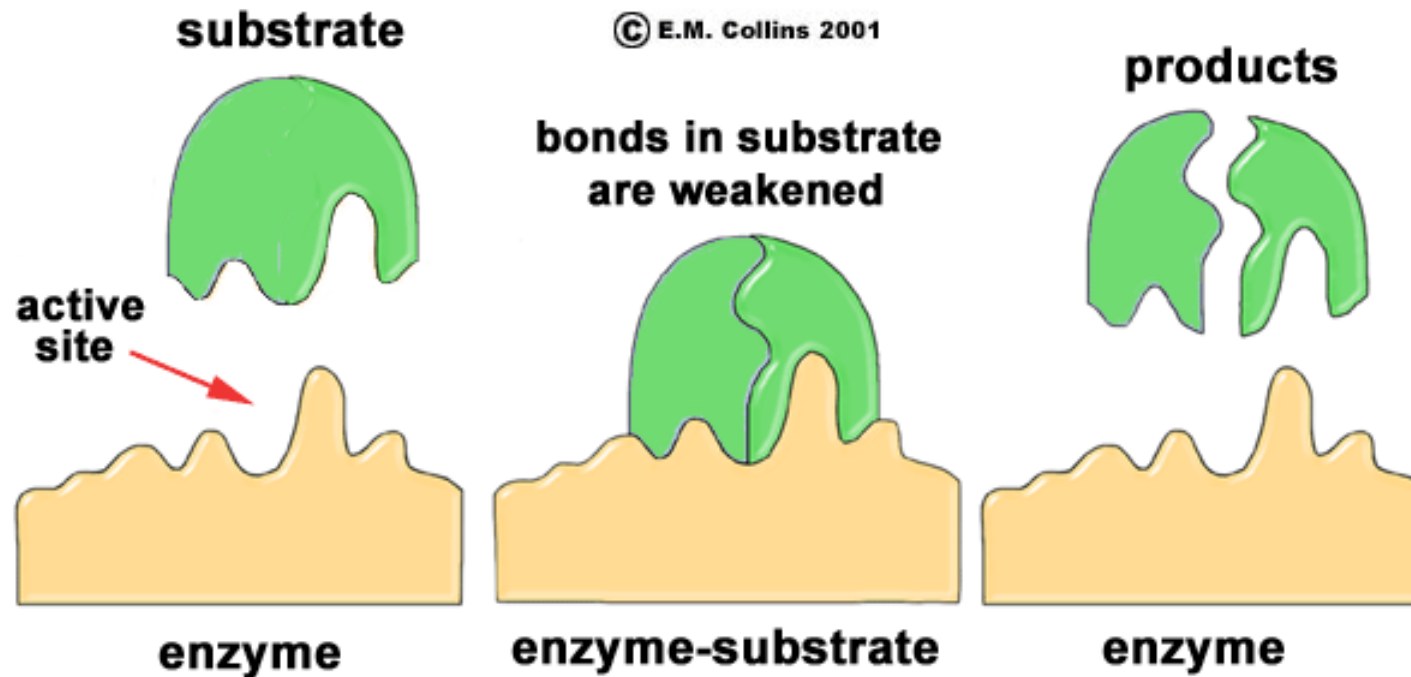
- ***Enzyme*** A protein that acts as a catalyst for a biochemical reaction.



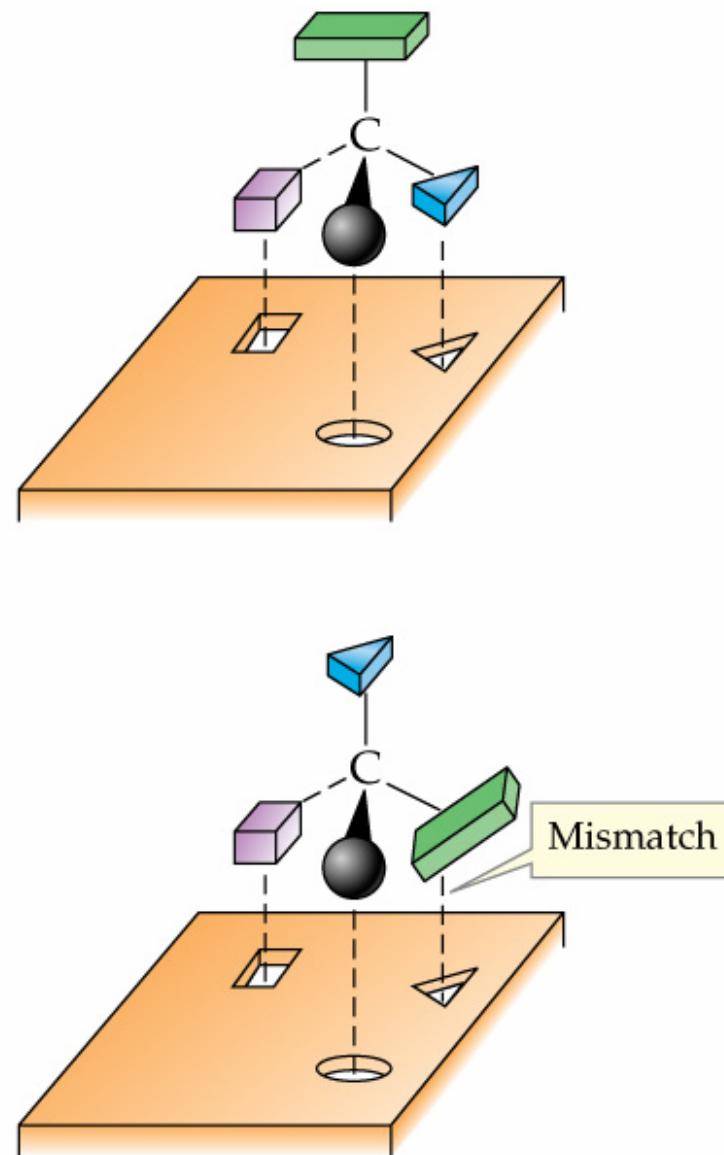
Enzymatic Reaction



Specificity



The specificity of an enzyme for one of two enantiomers is a matter of fit. One enantiomer fits better into the active site of the enzyme than the other enantiomer. Enzyme catalyzes reaction of the enantiomer that fits better into the active site of the enzyme.

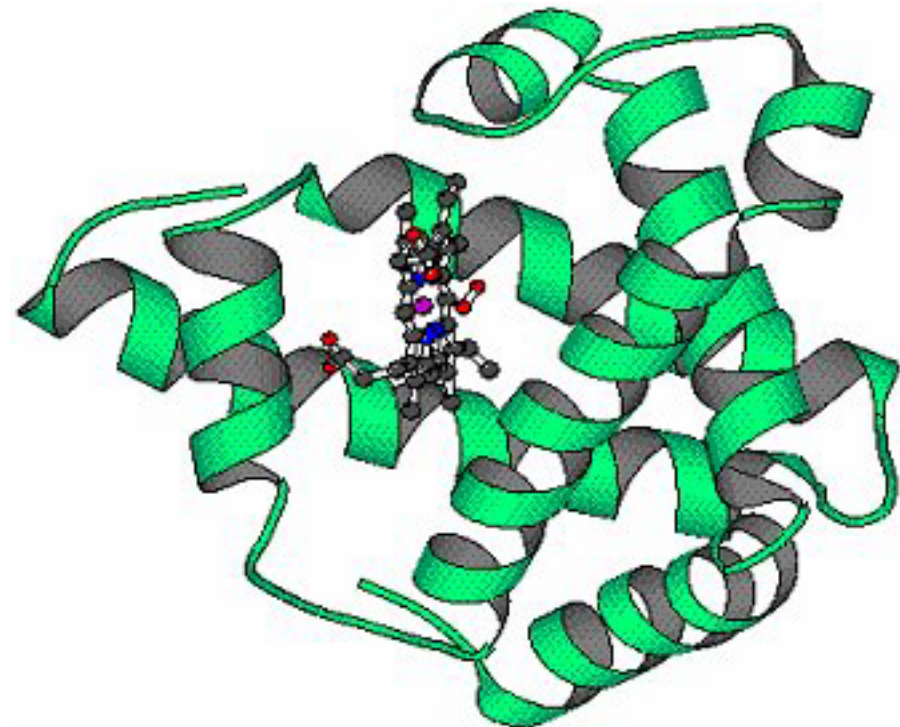
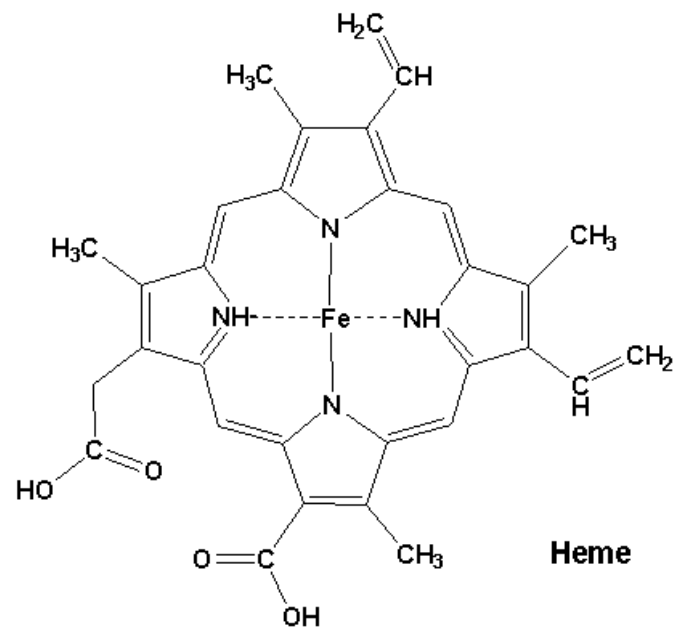
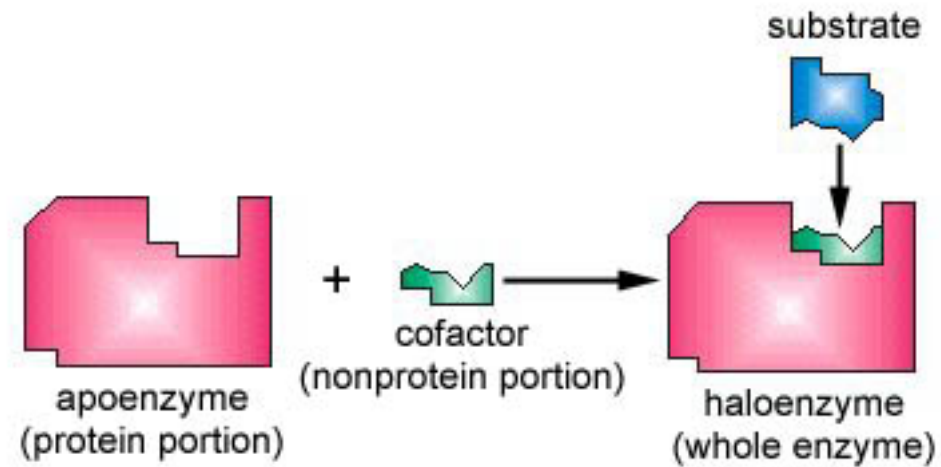


Enzyme Cofactors

- Many enzymes are conjugated proteins that require **nonprotein** portions known as ***cofactors***.
- Some cofactors are metal ions, others are nonprotein **organic molecules** called ***coenzymes***.
- An enzyme may require a metal-ion, a coenzyme, or both to function.



Cofactor



- Cofactors provide additional chemically active functional groups which are not present in the side chains of amino acids that made up the enzyme.
- Metal ions may anchor a substrate in the active site or may participate in the catalyzed reaction.



How Enzyme Work

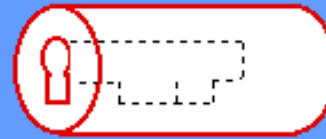
- Two modes are invoked to represent the interaction between substrate and enzymes. These are:
- ***Lock-and-key model***: The substrate is described as fitting into the active site as a key fit into a lock.
- ***Induced-fit-model***: The enzyme has a flexible active site that changes shape to accommodate the substrate and facilitate the reaction.



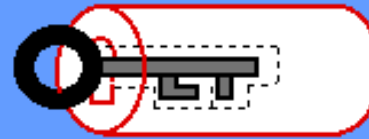
Lock and Key Analogy



key = substrate



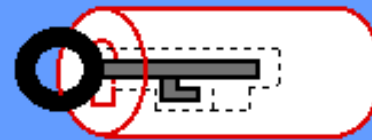
lock = enzyme



correct fit,
will react

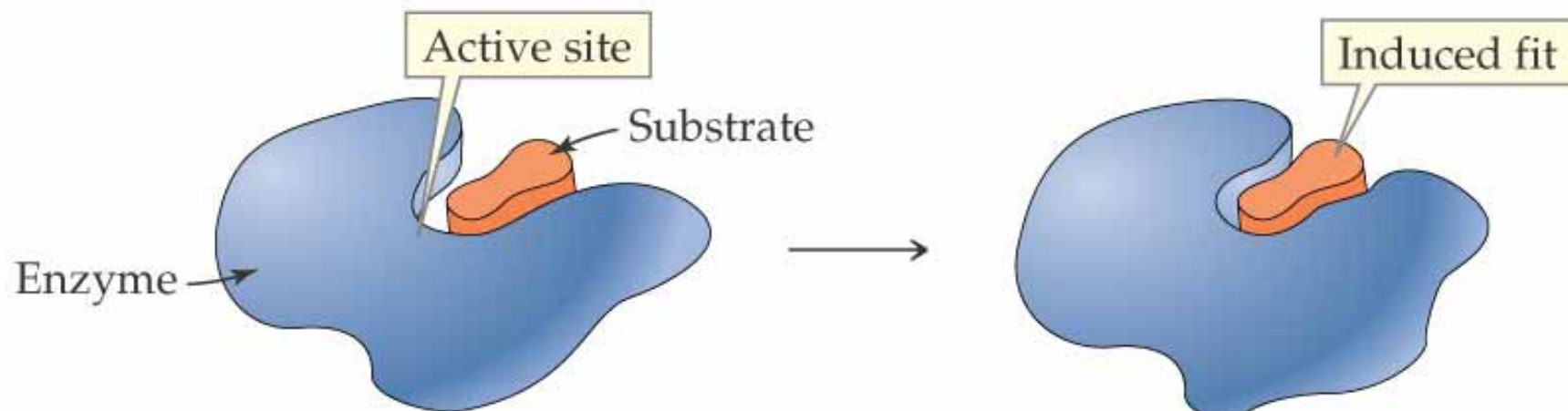


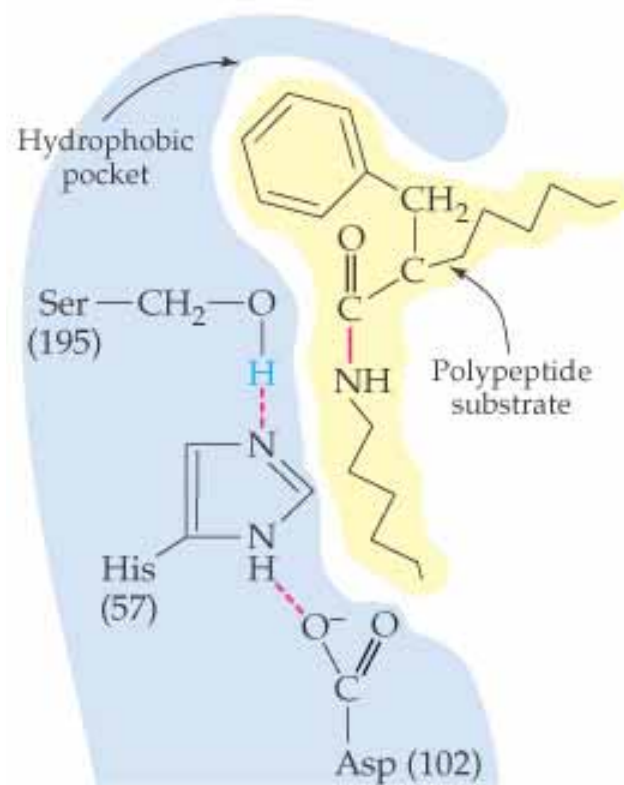
incorrect substrate



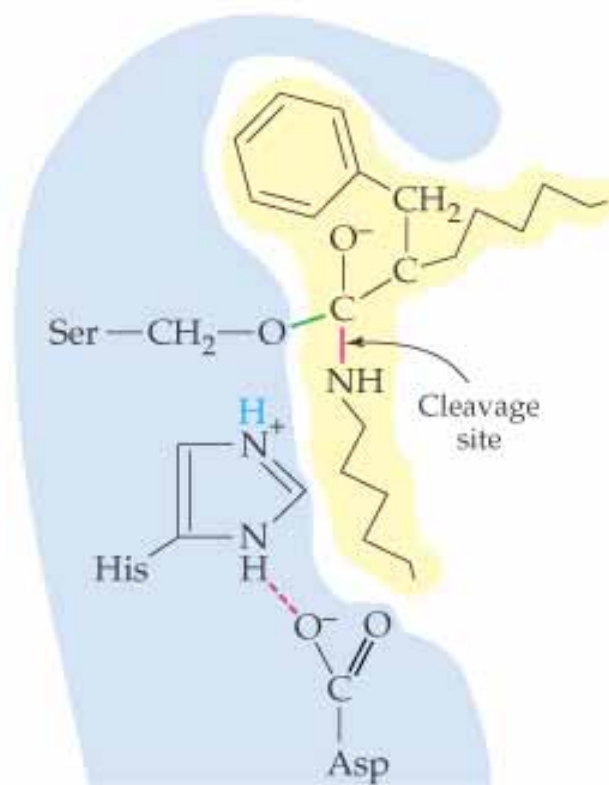
no reaction

C. Ophardt, c. 2003

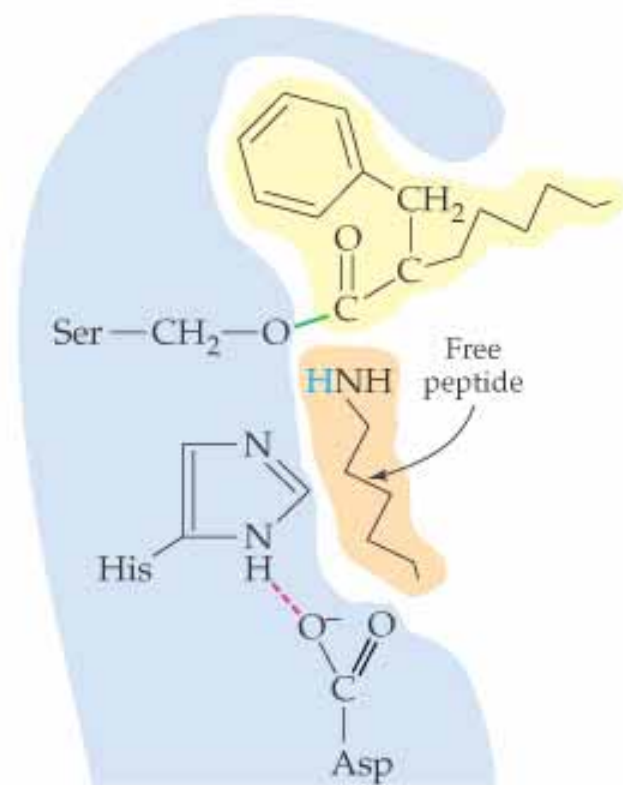




(a)



(b)



(c)

19.5 Effect of Concentration on Enzyme Activity

- Variation in concentration of enzyme or substrate alters the rate of enzyme catalyzed reactions.
- *Substrate concentration:* At low substrate concentration, the reaction rate is directly proportional to the substrate concentration. With increasing substrate concentration, the rate drops off as more of the active sites are occupied.



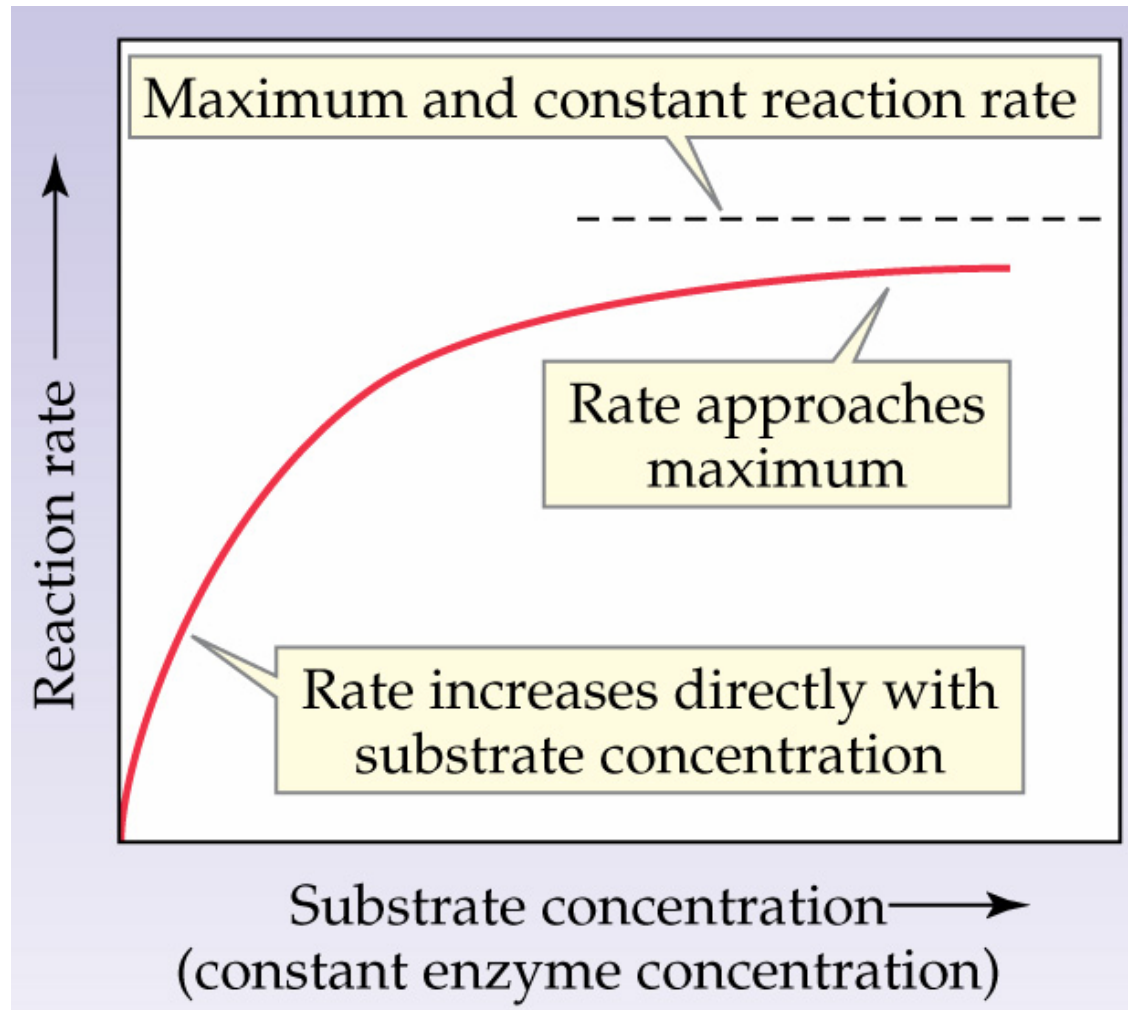
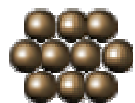
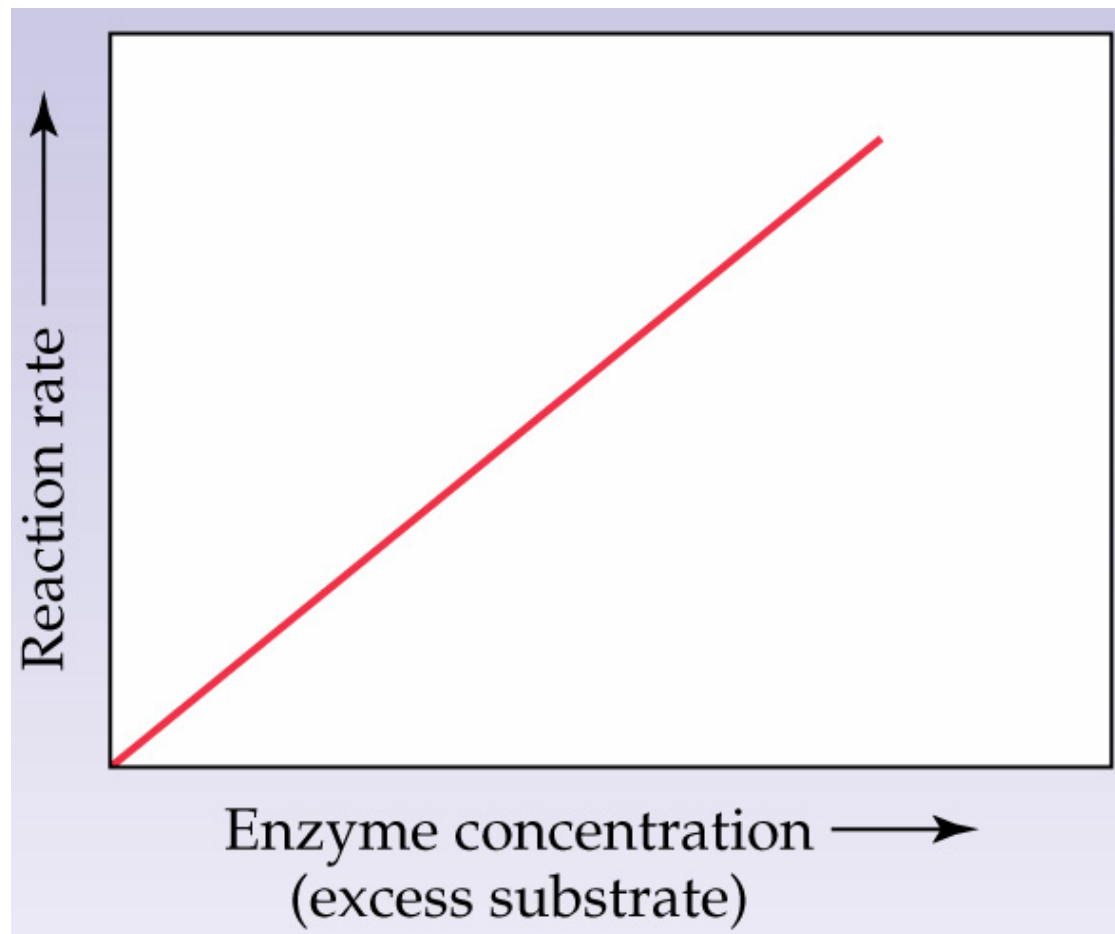


Fig 19.5 Change of reaction rate with substrate concentration when enzyme concentration is constant.



- *Enzyme concentration:* The reaction rate varies directly with the enzyme concentration as long as the substrate concentration does not become a limitation, Fig 19.6 below.



19.6 Effect of Temperature and pH on Enzyme Activity

- Enzymes maximum catalytic activity is highly dependent on temperature and pH.
- Increase in temperature increases the rate of enzyme catalyzed reactions. The rates reach a maximum and then begins to decrease. The decrease in rate at higher temperature is due to denaturation of enzymes.



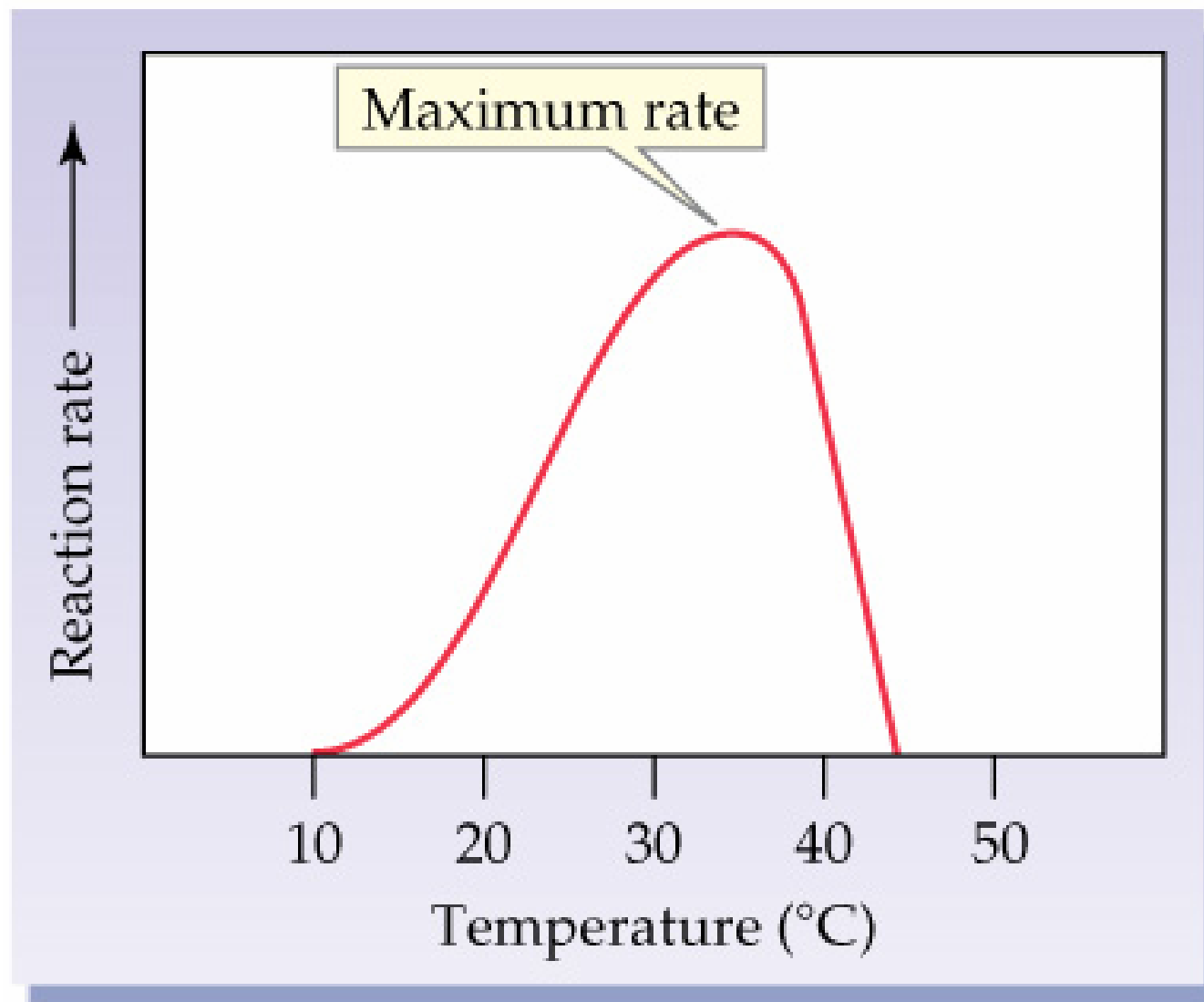
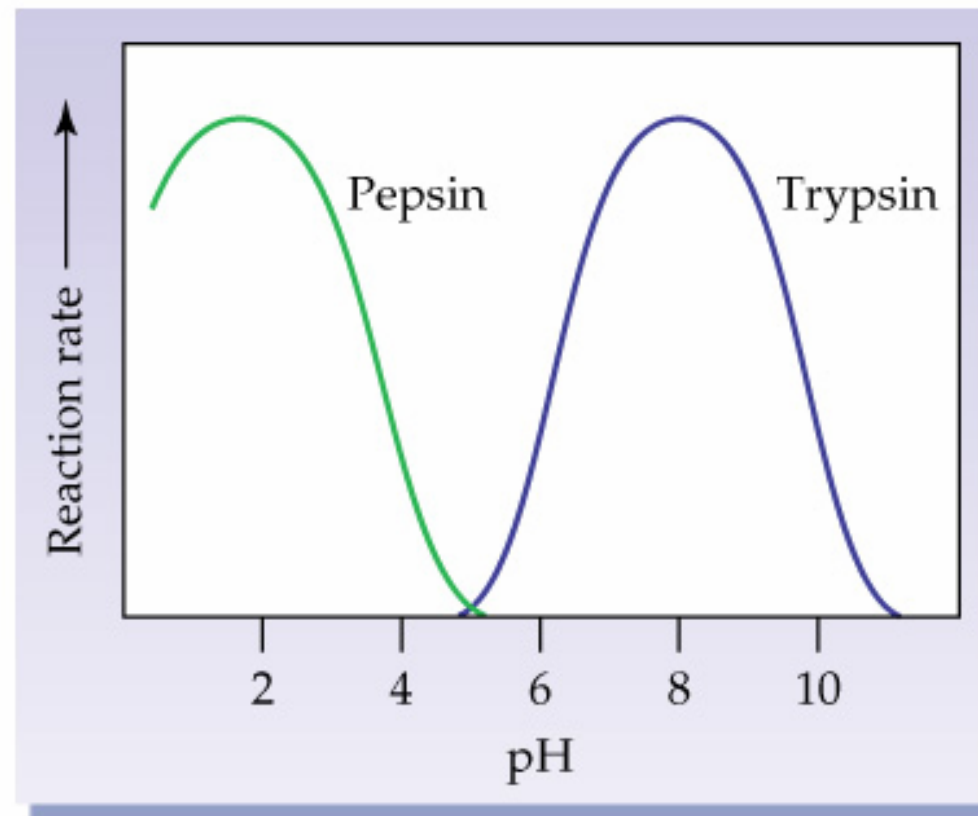


Fig 19.7 (a) Effect of temperature on reaction rate



- Effect of pH on Enzyme activity: The catalytic activity of enzymes depends on pH and usually has a well defined optimum point for maximum catalytic activity Fig 19.7 (b) below.



19.7 Enzyme Regulation: Feedback and Allosteric Control

- Concentration of thousands of different chemicals vary continuously in living organisms which requires regulation of enzyme activity.
- Any process that starts or increase the activity of an enzyme is ***activation***.
- Any process that stops or slows the activity of an enzyme is ***inhibition***.

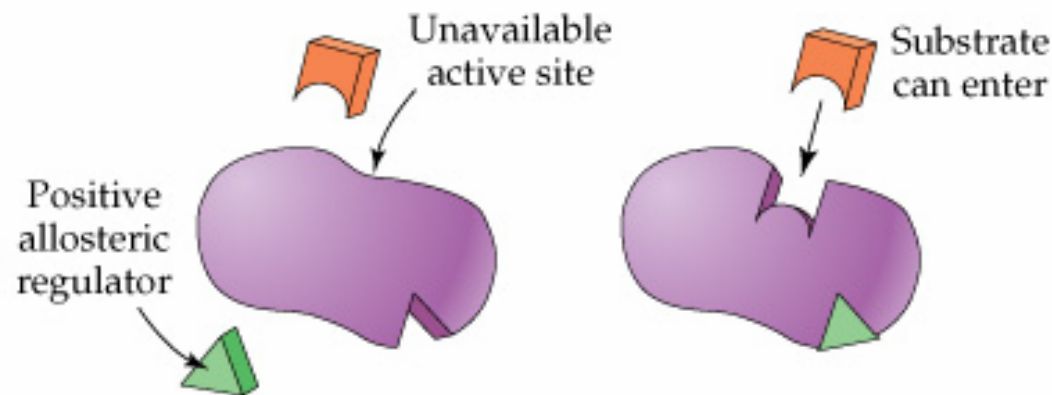


Two of the mechanism

- **Feedback control:** Regulation of an enzyme's activity by the product of a reaction later in a pathway.
- **Allosteric control:** Activity of an enzyme is controlled by the binding of an activator or inhibitor at a location other than the active site. Allosteric controls are further classified as positive or negative.
 - A positive regulator changes the activity site so that the enzyme becomes a better catalyst and rate accelerates.
 - A negative regulator changes the activity site so that the enzyme becomes less effective catalyst and rate slows down.

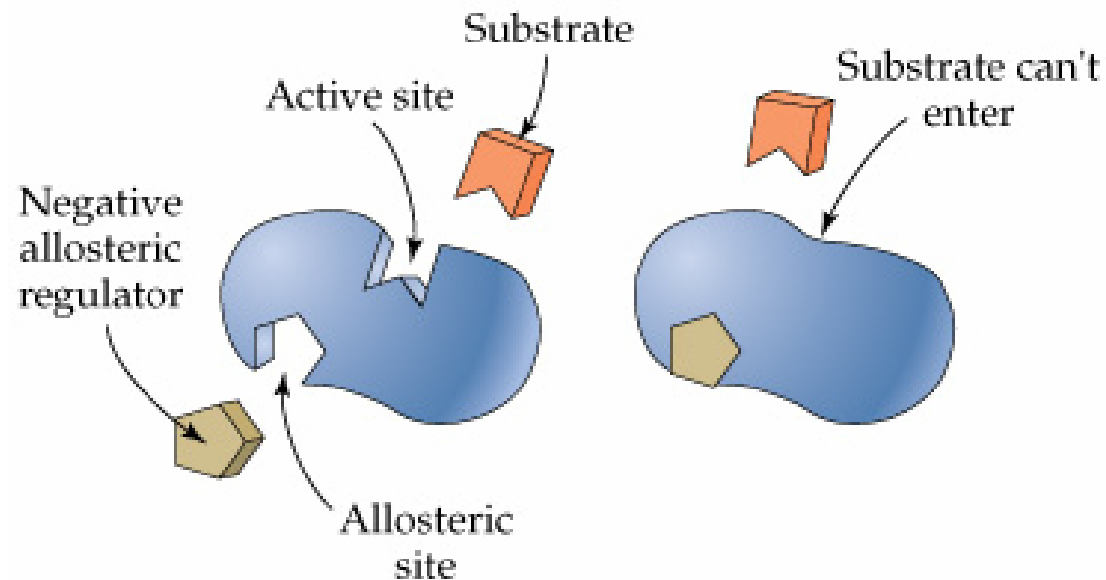


Positive allosteric control

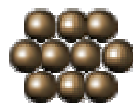


A positive regulator changes the activity site so that the enzyme becomes a better catalyst and rate accelerates.

Negative allosteric control



A negative regulator changes the activity site so that the enzyme becomes less effective catalyst and rate slows down.



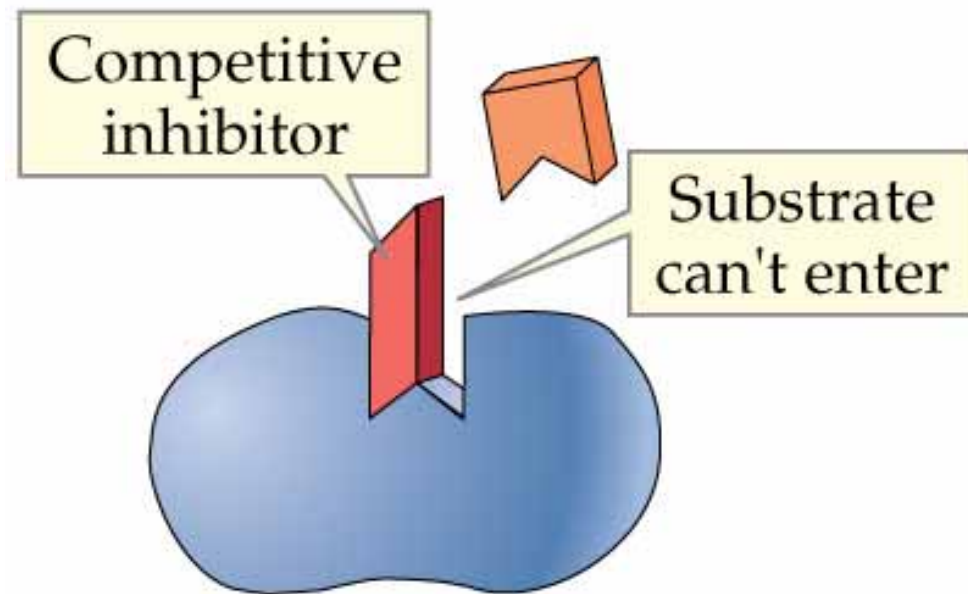
19.8 Enzyme Regulation: Inhibition

- The inhibition of an enzyme can be *reversible* or *irreversible*.
- In *reversible inhibition*, the inhibitor can leave, restoring the enzyme to its uninhibited level of activity.
- In *irreversible inhibition*, the inhibitor remains permanently bound to the enzyme and the enzyme is permanently inhibited.



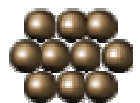
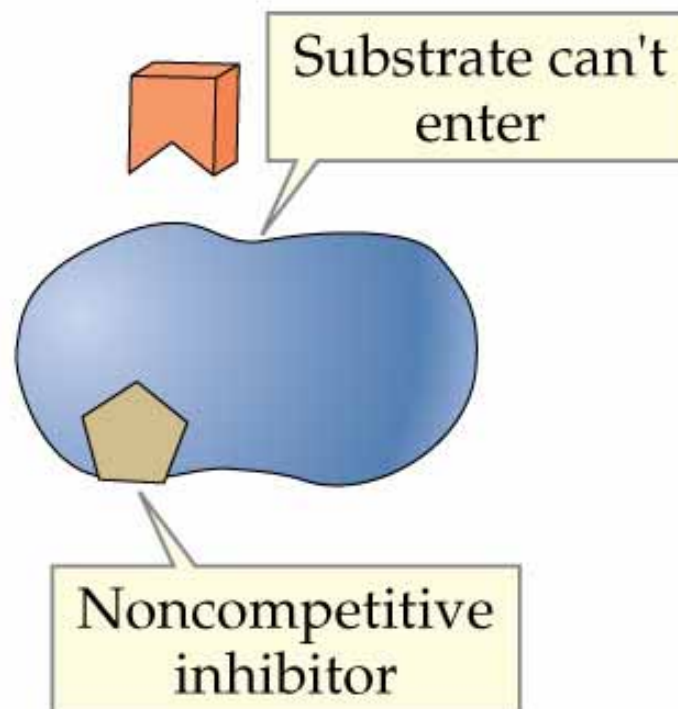
- Inhibitions are further classified as:
- *Competitive inhibition* if the inhibitor binds to the active site.

Competitive inhibition

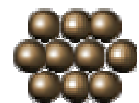
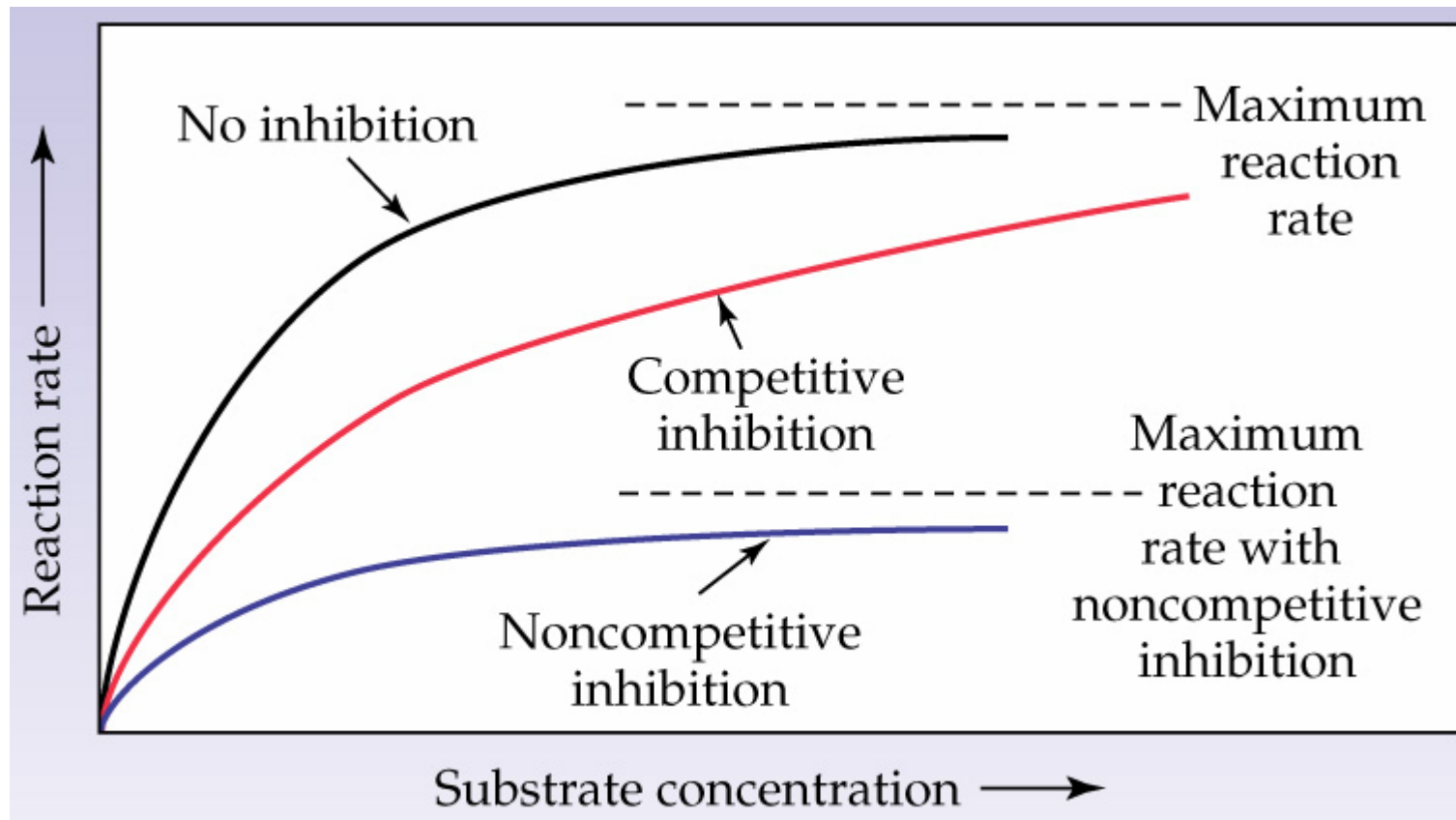


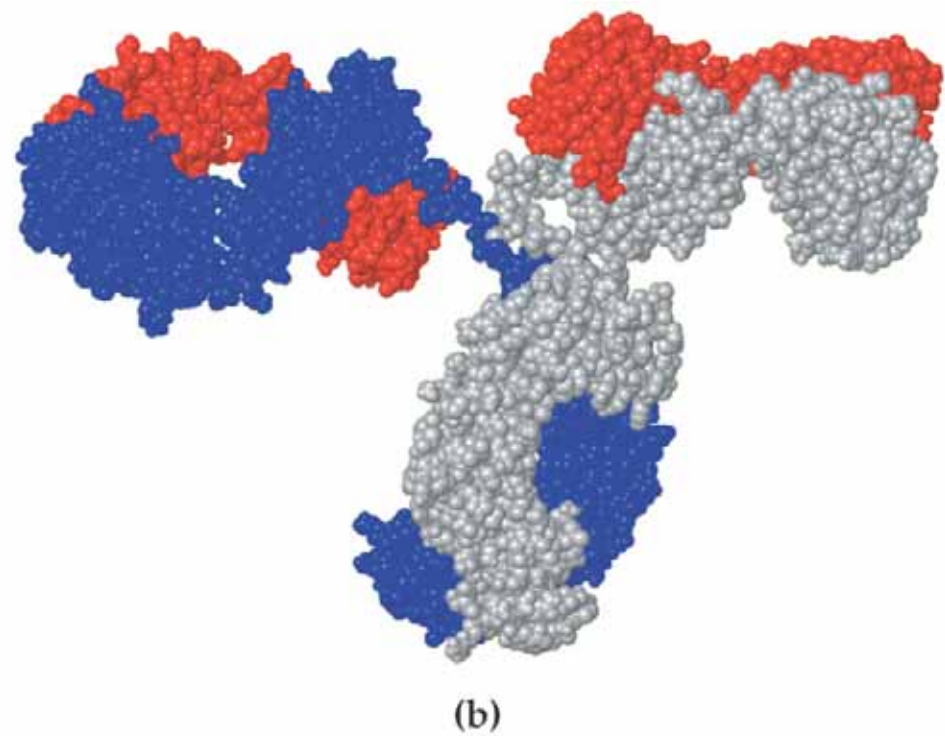
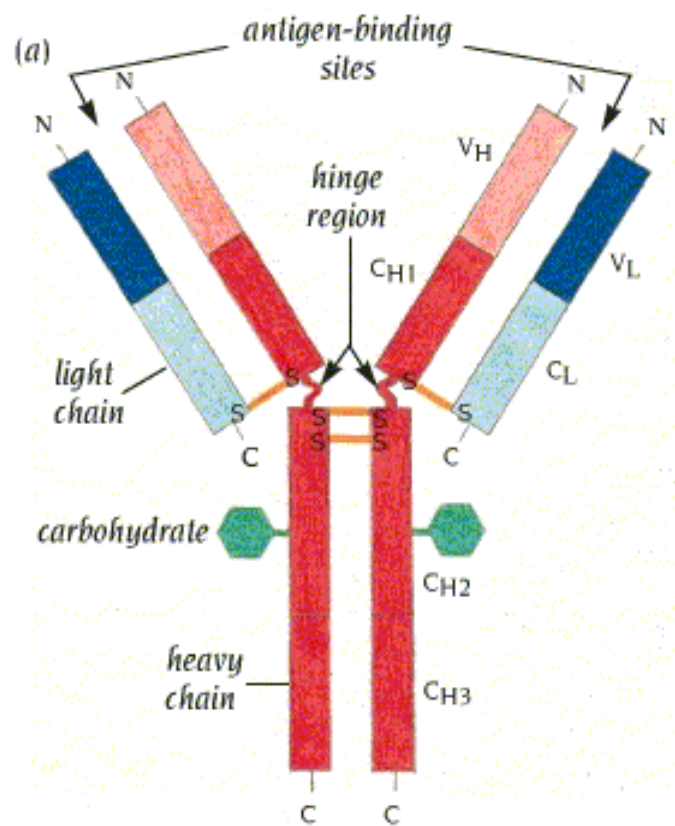
- *Noncompetitive inhibition*, if the inhibitor binds elsewhere and not to the active site.

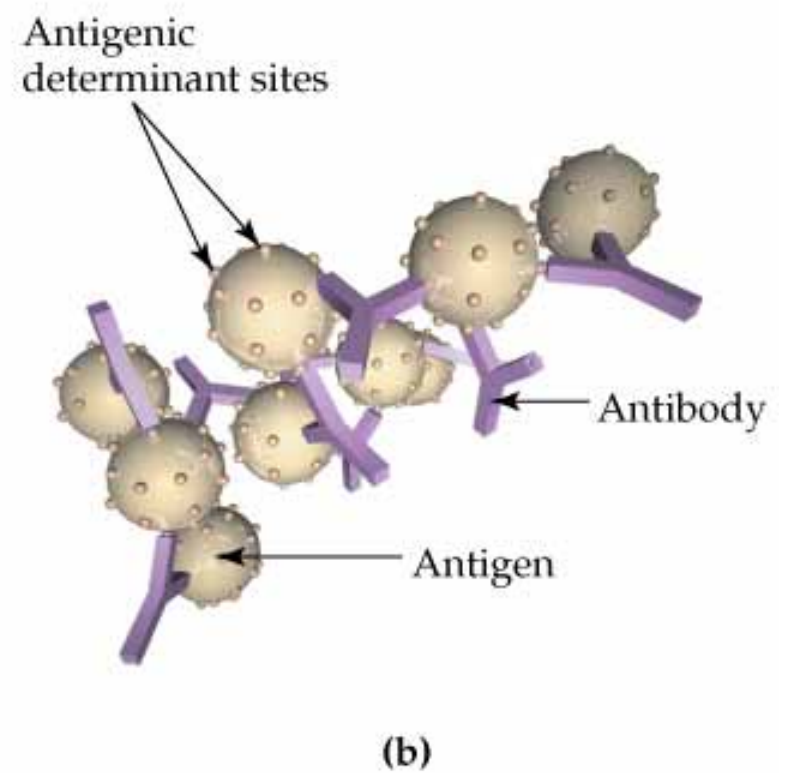
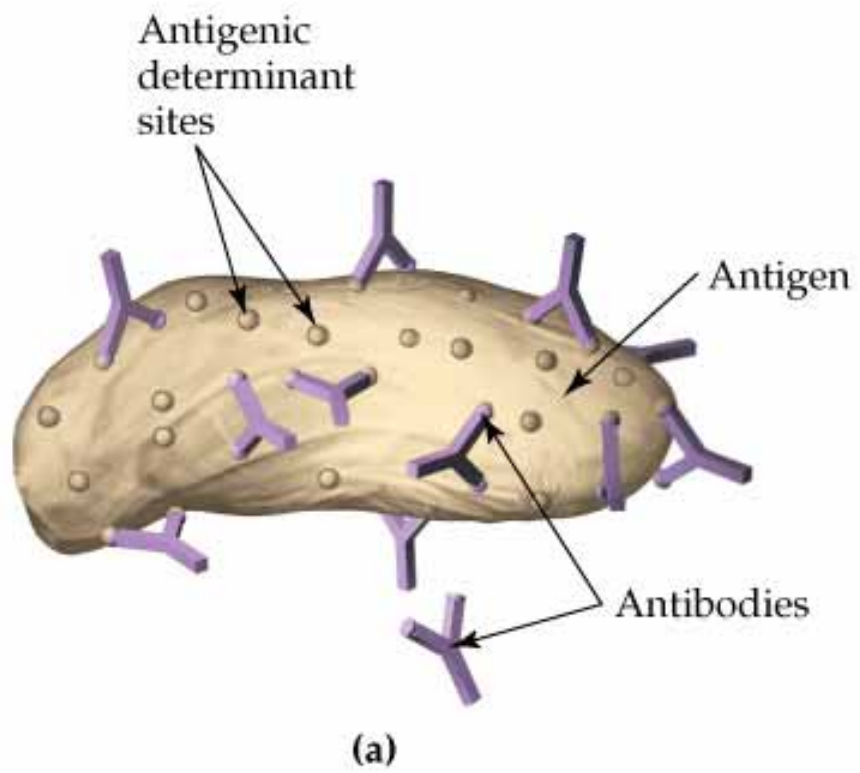
Noncompetitive inhibition



- The rates of enzyme catalyzed reactions with or without a competitive inhibitor are shown in the Fig 19.9 below.







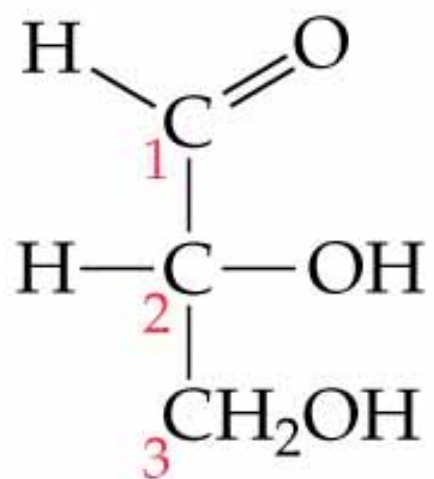
An Introduction to Carbohydrates

- *Carbohydrates* are a large class of naturally occurring polyhydroxy aldehydes and ketones.
- Monosaccharides also known as simple sugars, are the simplest carbohydrates containing 3-7 carbon atoms.
- sugar containing an aldehydes is known as an aldose.
- sugar containing a ketones is known as a ketose.

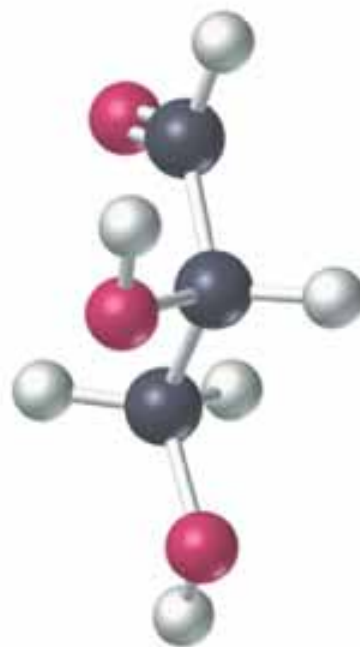
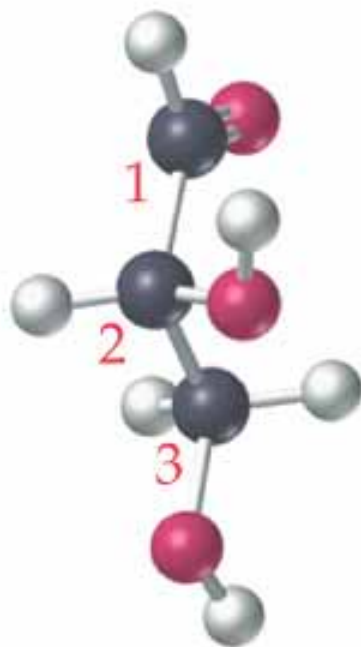


- The number of carbon atoms in an aldose or ketose may be specified as by tri, tetr, pent, hex, or hept. For example, glucose is aldohexose and fructose is ketohexose.
- Monosaccharides react with each other to form disaccharides and polysaccharides.
- Monosaccharides are chiral molecules and exist mainly in cyclic forms rather than the straight chain.

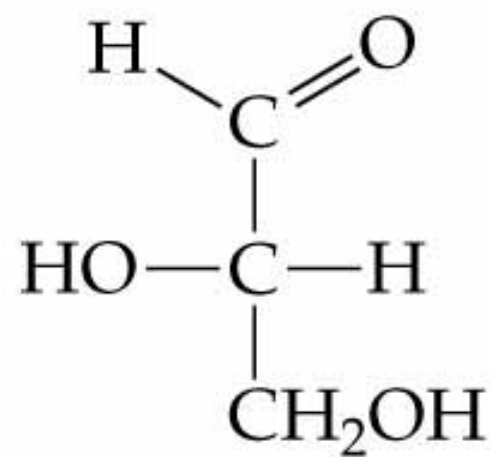


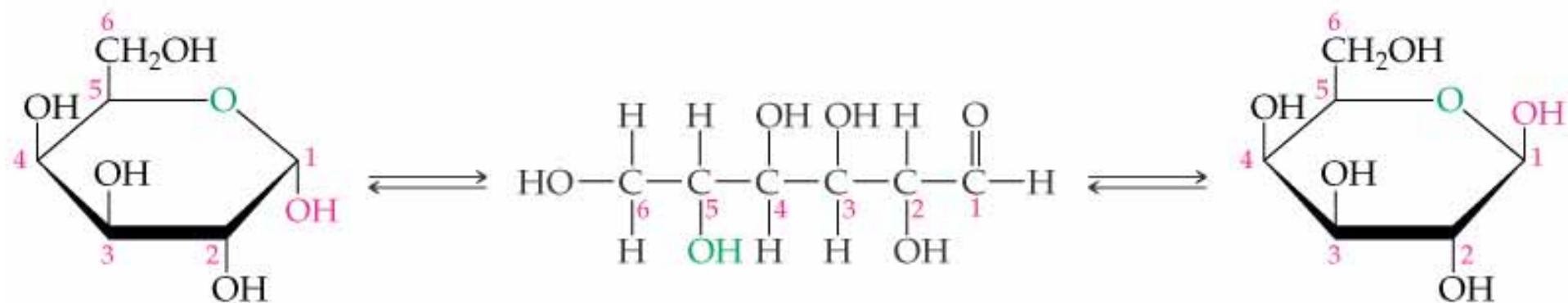


D-Glyceraldehyde
Right-handed



L-Glyceraldehyde
Left-handed





α -D-Galactose

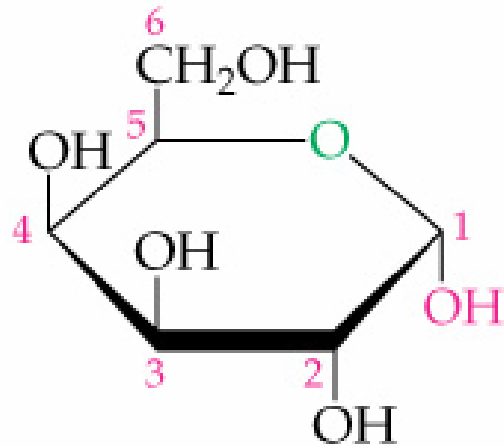


Open-chain galactose

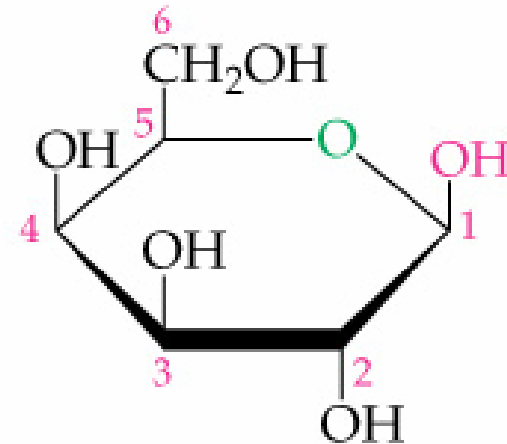


β -D-Galactose

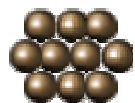
- *Anomers:* Cyclic sugars that differ only in positions of substituents at the hemiacetal carbon; the α -form has the -OH group on the opposite side from the $\text{-CH}_2\text{OH}$; the β -form has the -OH group on the same side as the $\text{-CH}_2\text{OH}$ group.



α -D-Galactose

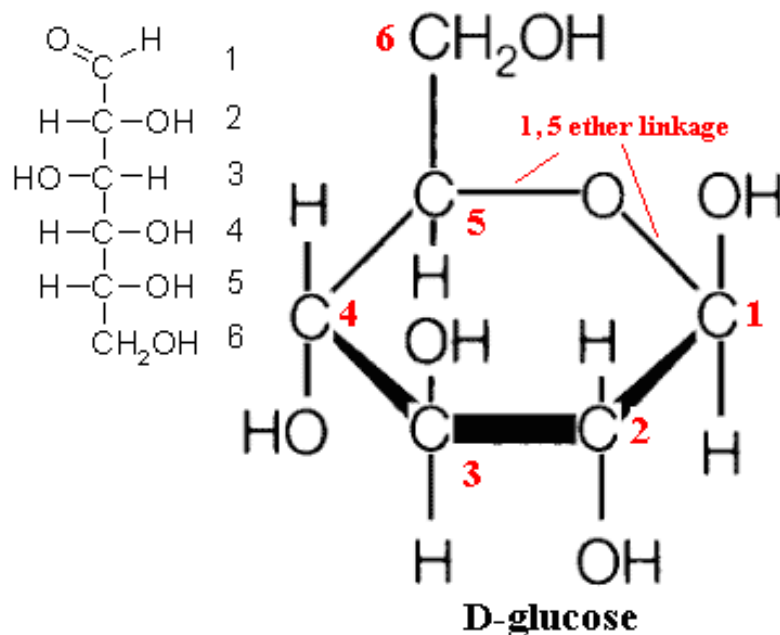


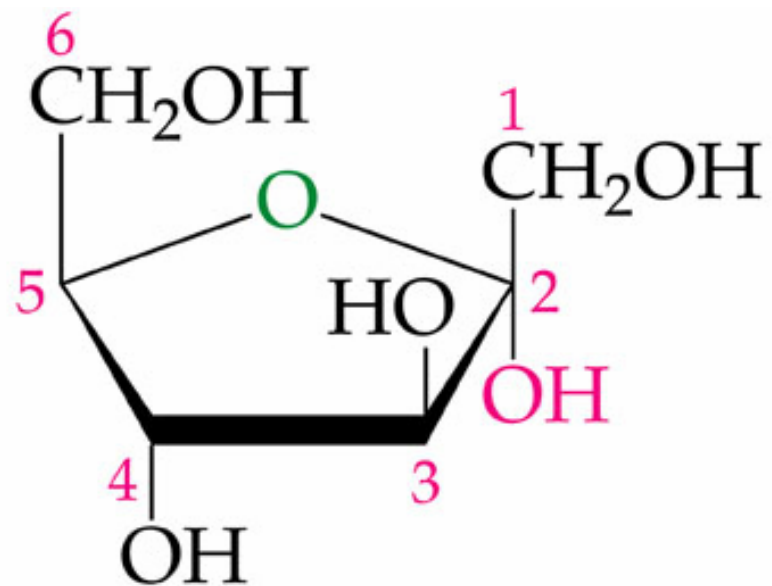
β -D-Galactose



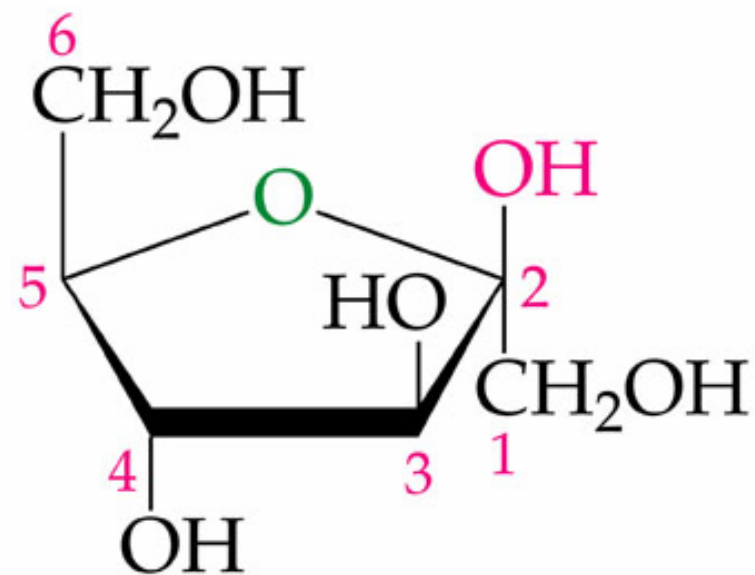
Some Important Monosaccharides

Monosaccharides are generally high-melting, white, crystalline solids that are soluble in water and insoluble in nonpolar solvents. Most monosaccharides are sweet tasting, digestible, and nontoxic.

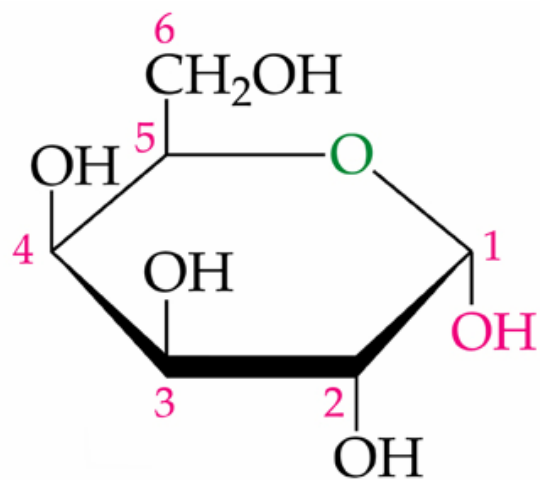




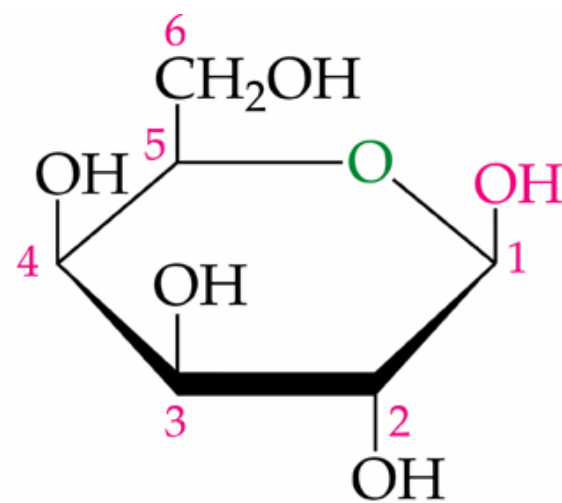
α -D-Fructose



β -D-Fructose



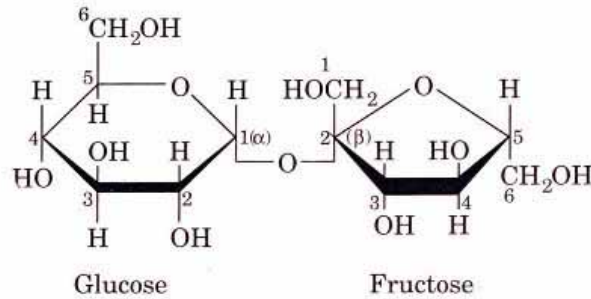
α -D-Galactose



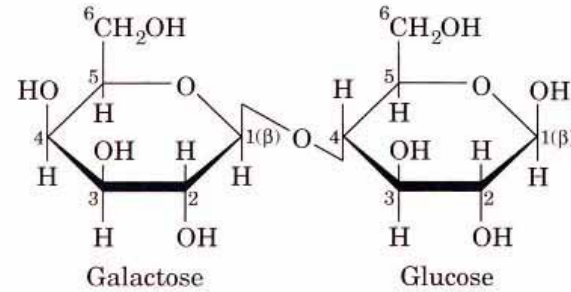
β -D-Galactose



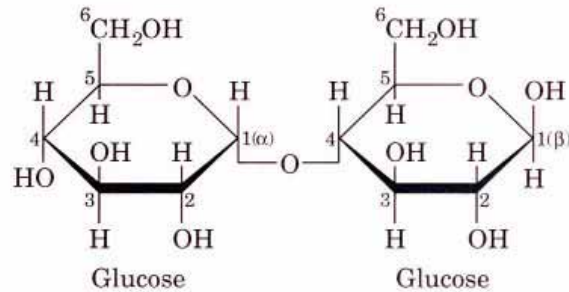
Some Common Disaccharides



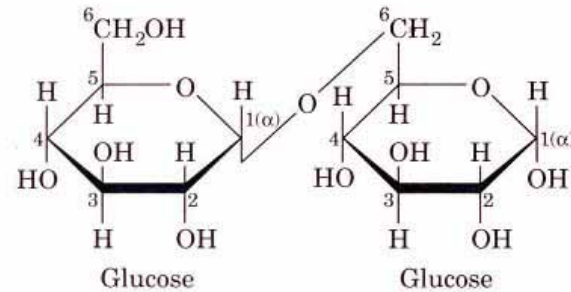
Sucrose



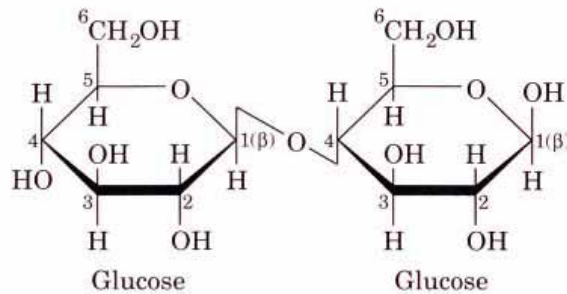
Lactose



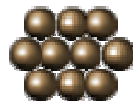
Maltose



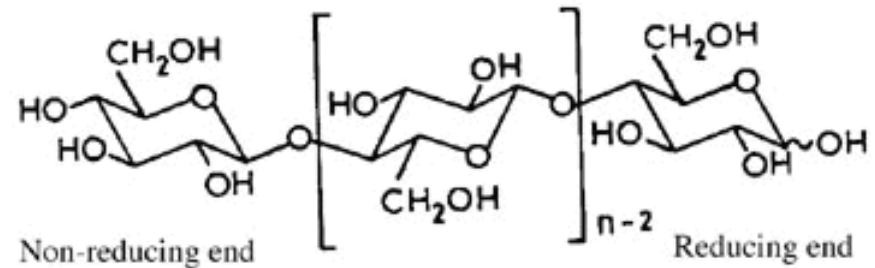
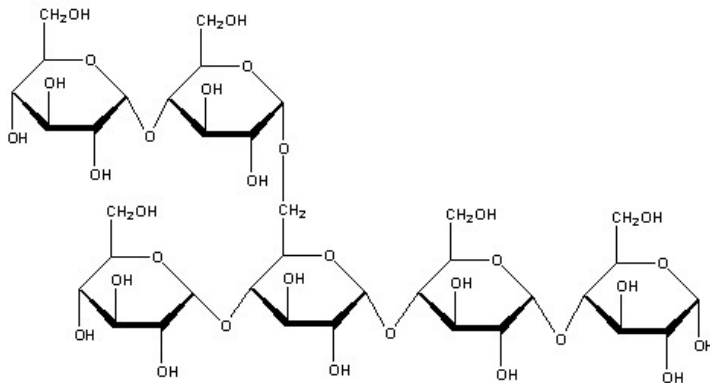
Isomaltose



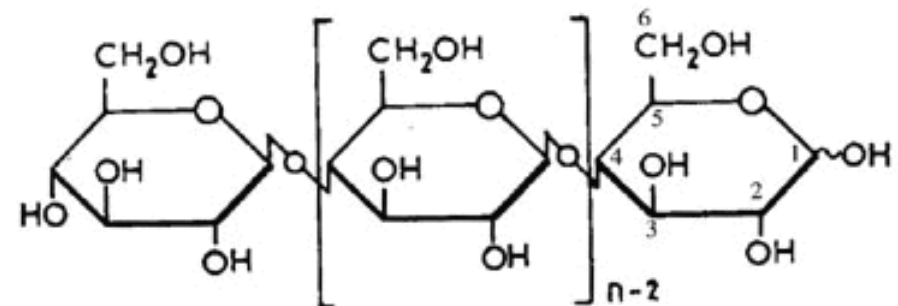
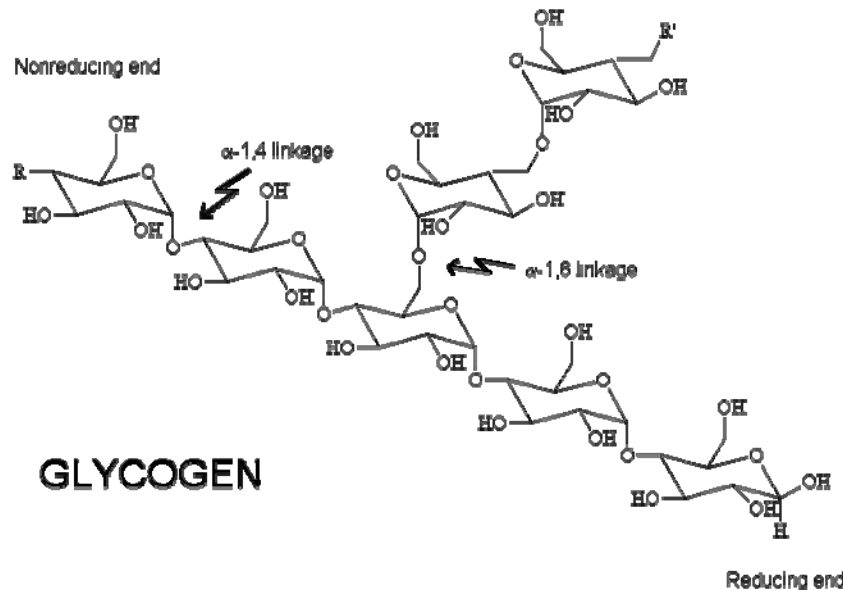
Cellobiose



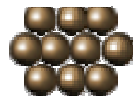
Polysaccharides



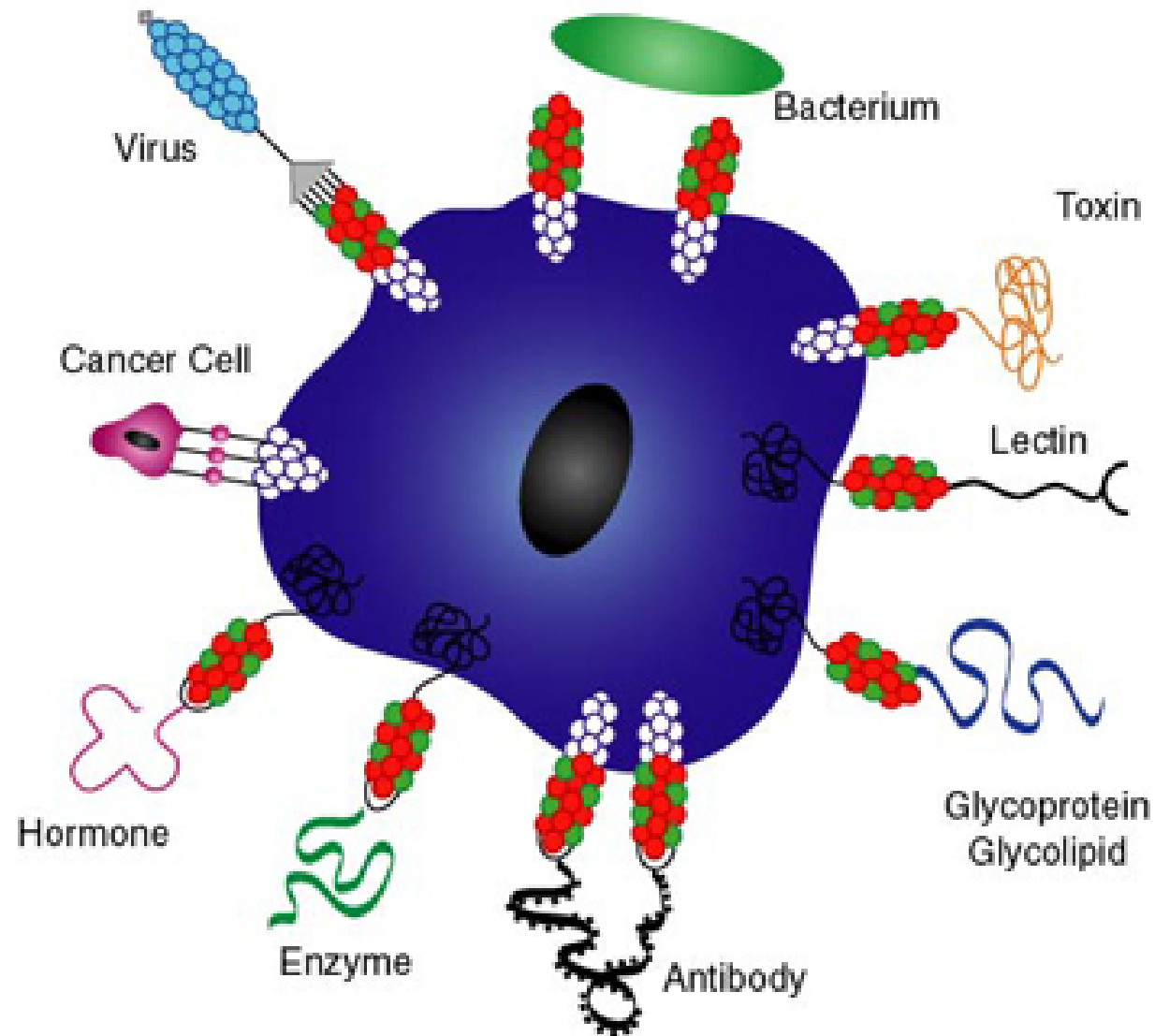
Sometimes shown as



Cellulose

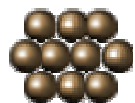
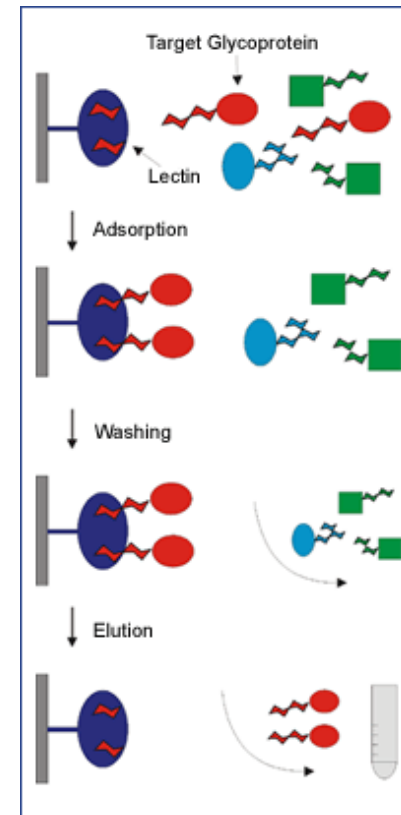
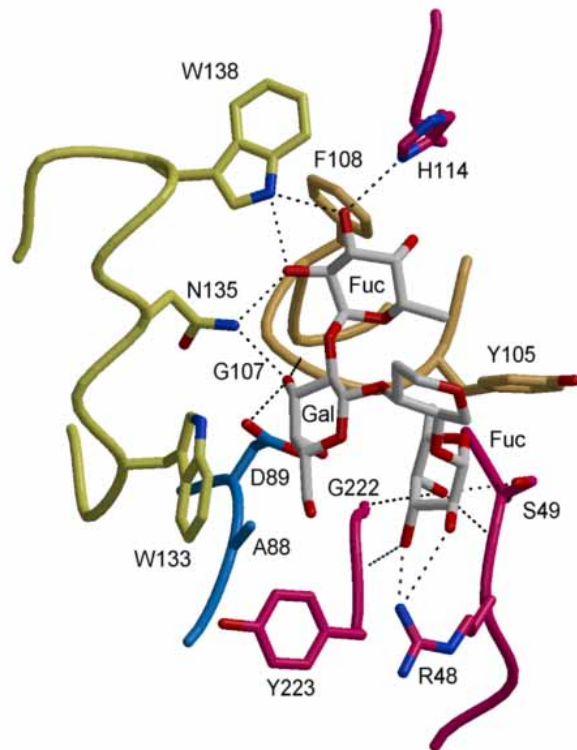


Cell-Surface Carbohydrates Involved in Molecular Recognition

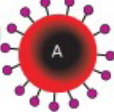
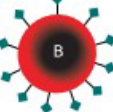
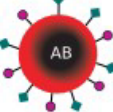










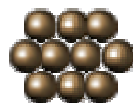
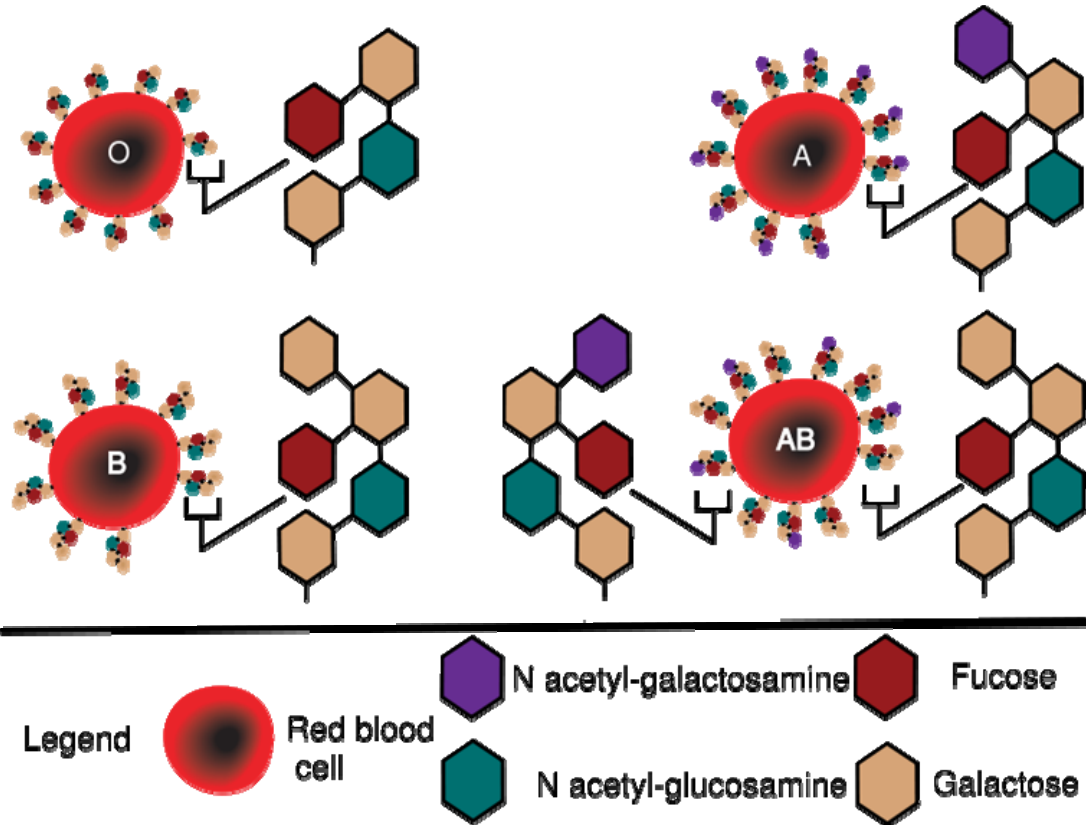
Lectin

Lectins are sugar-binding proteins which are highly specific for their sugar moieties. They typically play a role in biological recognition phenomena involving cells and proteins. For example, some bacteria use lectins to attach themselves to the cells of the host organism during infection.

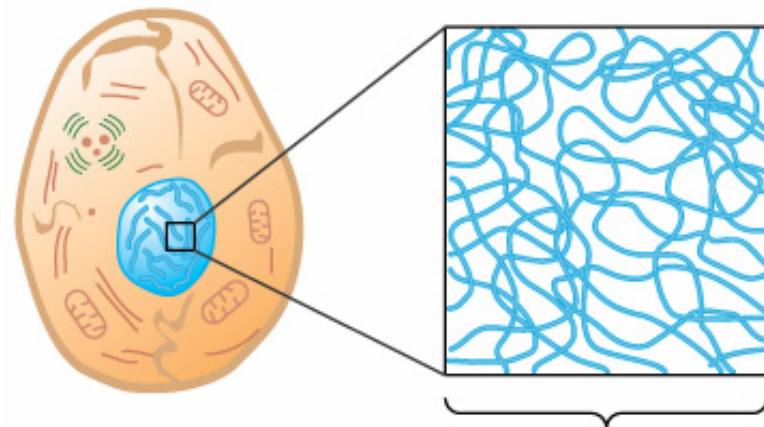


Blood Type

| | Group A | Group B | Group AB | Group O |
|---------------------|--|--|---|--|
| Red blood cell type |  |  |  |  |
| Antibodies present |  Anti-B |  Anti-A | None |  Anti-A and Anti-B |
| Antigens present | A antigen  | B antigen  | A and B antigens   | No antigens |

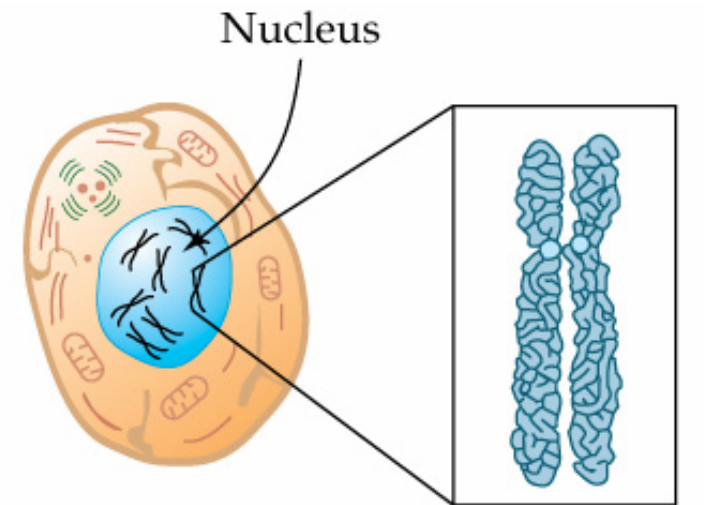


DNA



Nondividing
cell

Chromatin
in nucleus

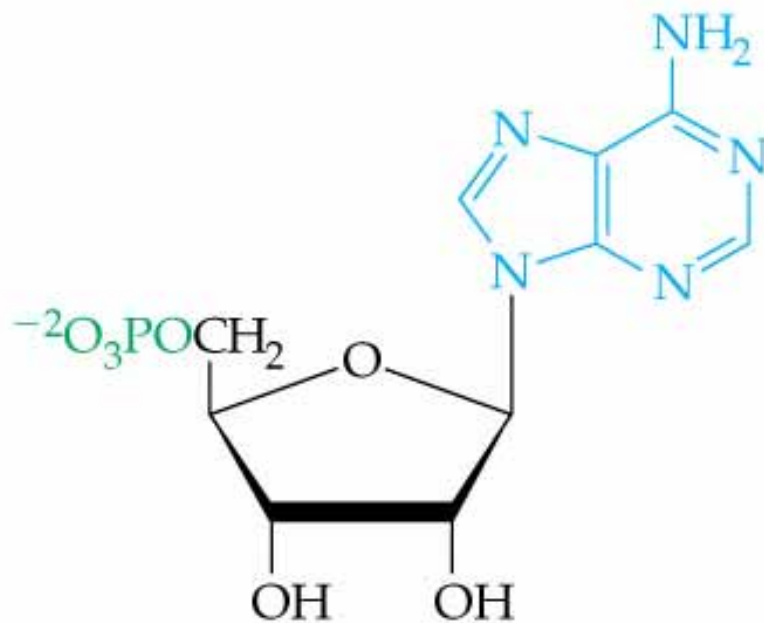


Cell prepared
for division

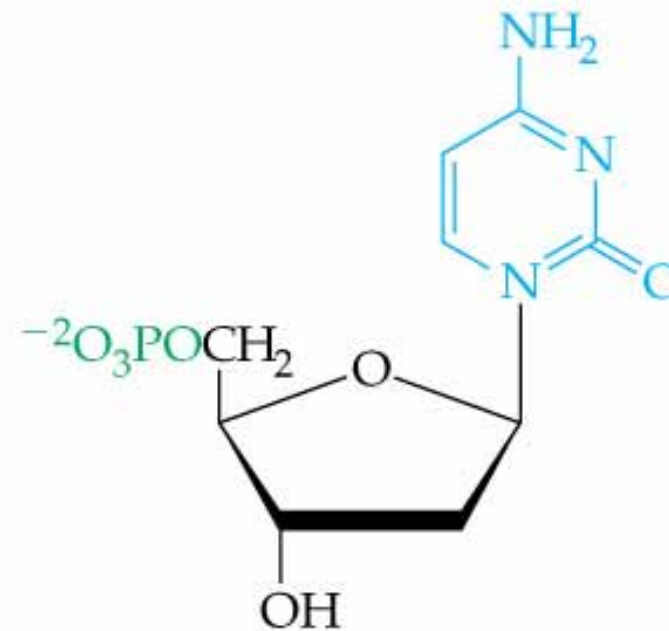
Visible
chromosome



- In RNA, the sugar is ribose.
- In DNA, the sugar is deoxyribose.



Adenosine 5'-monophosphate (AMP)
(a ribonucleotide)

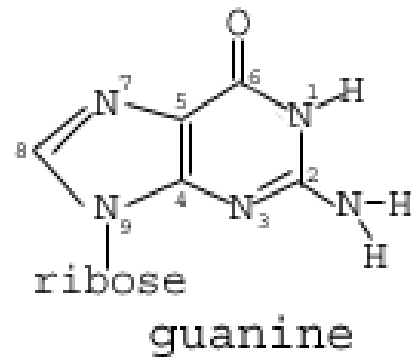
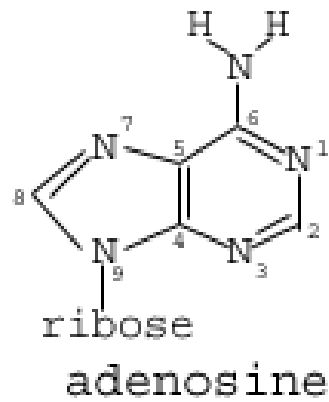


Deoxycytidine 5'-monophosphate (dCMP)
(a deoxyribonucleotide)

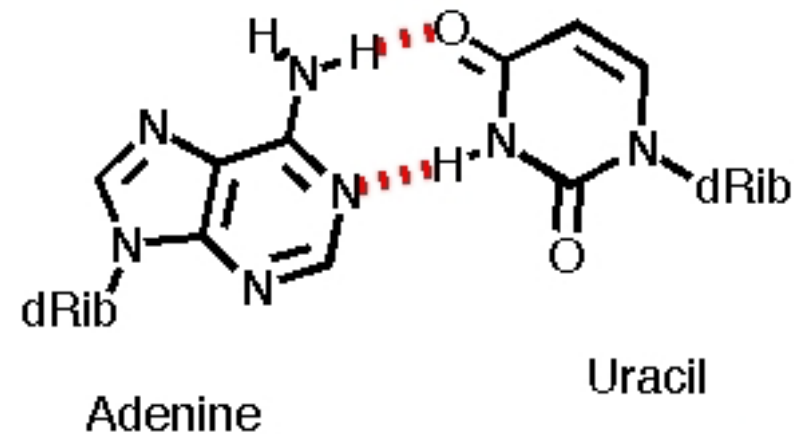
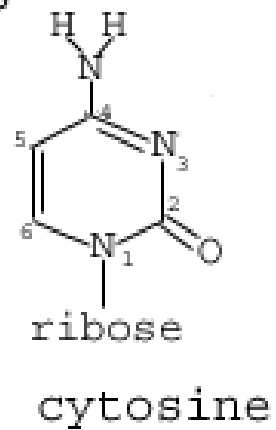
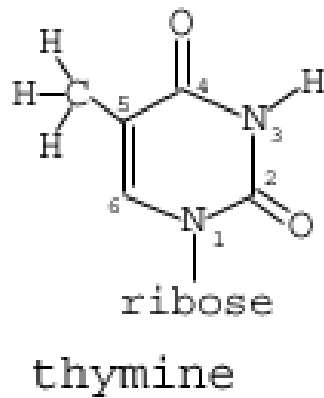


Base

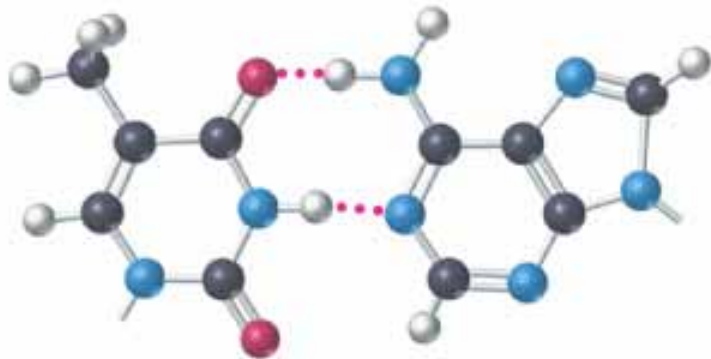
Purines



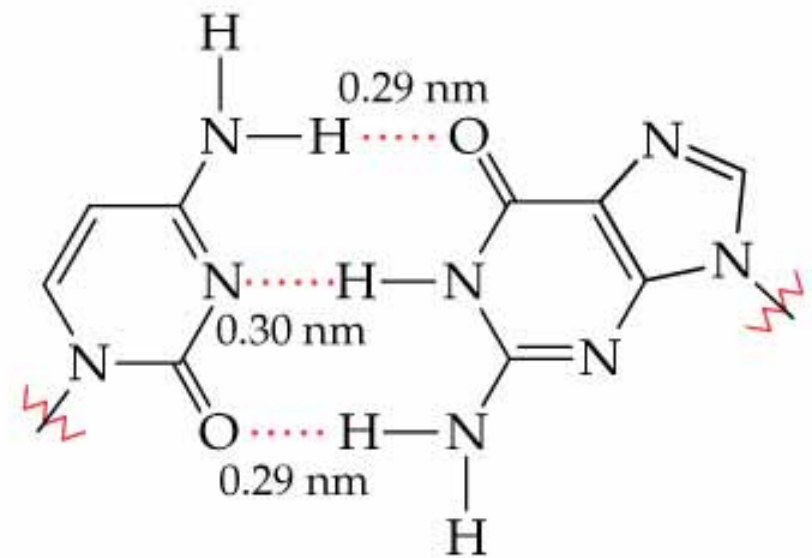
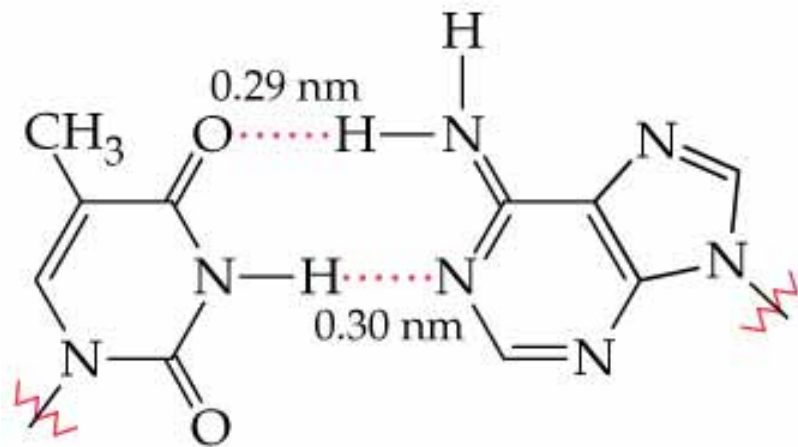
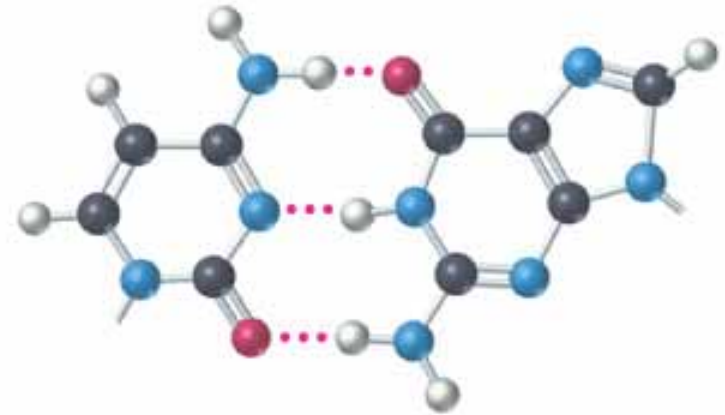
Pyrimidines

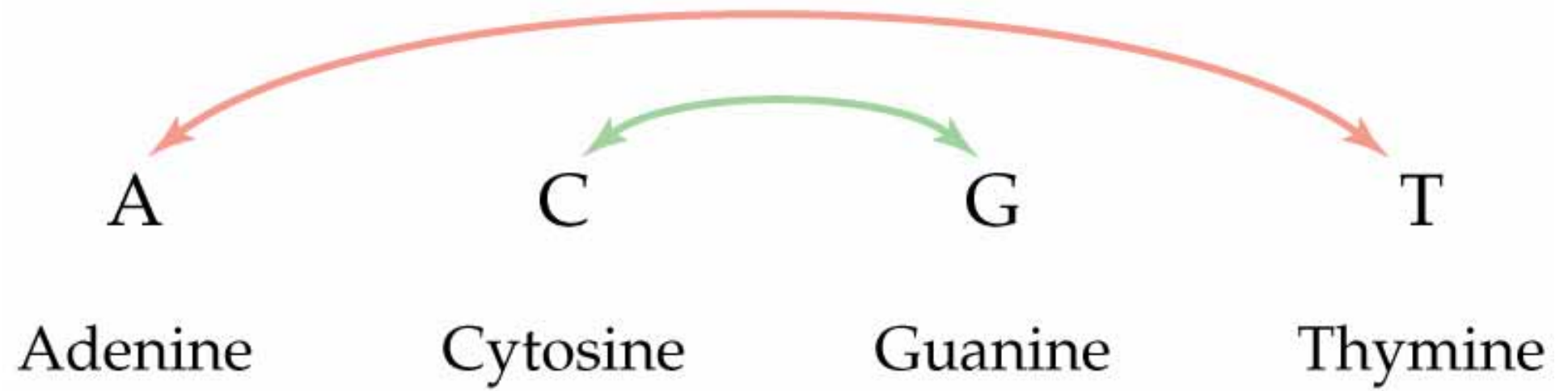


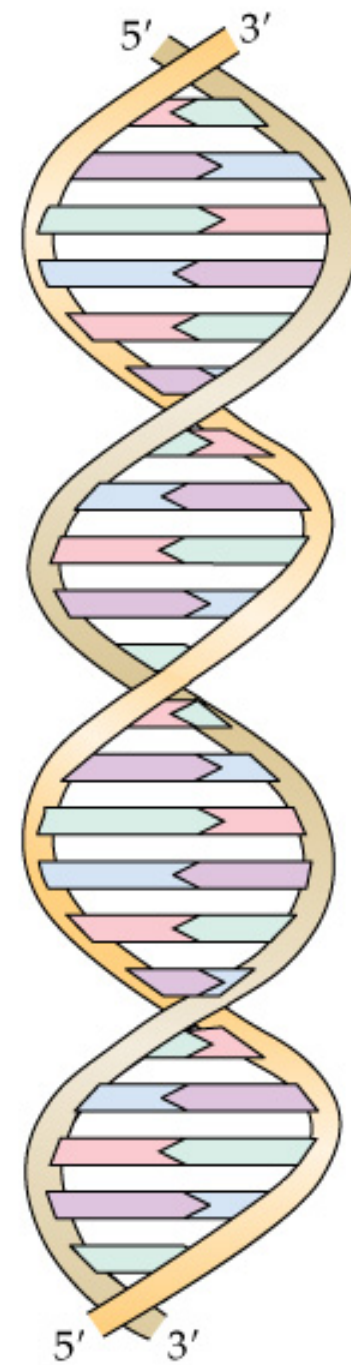
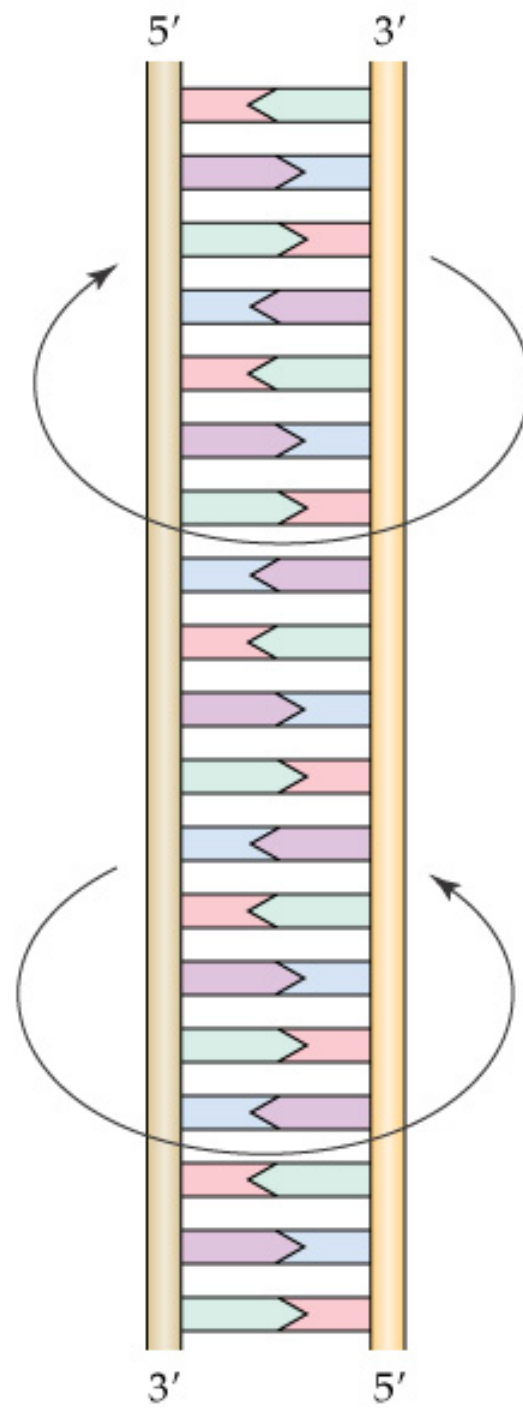
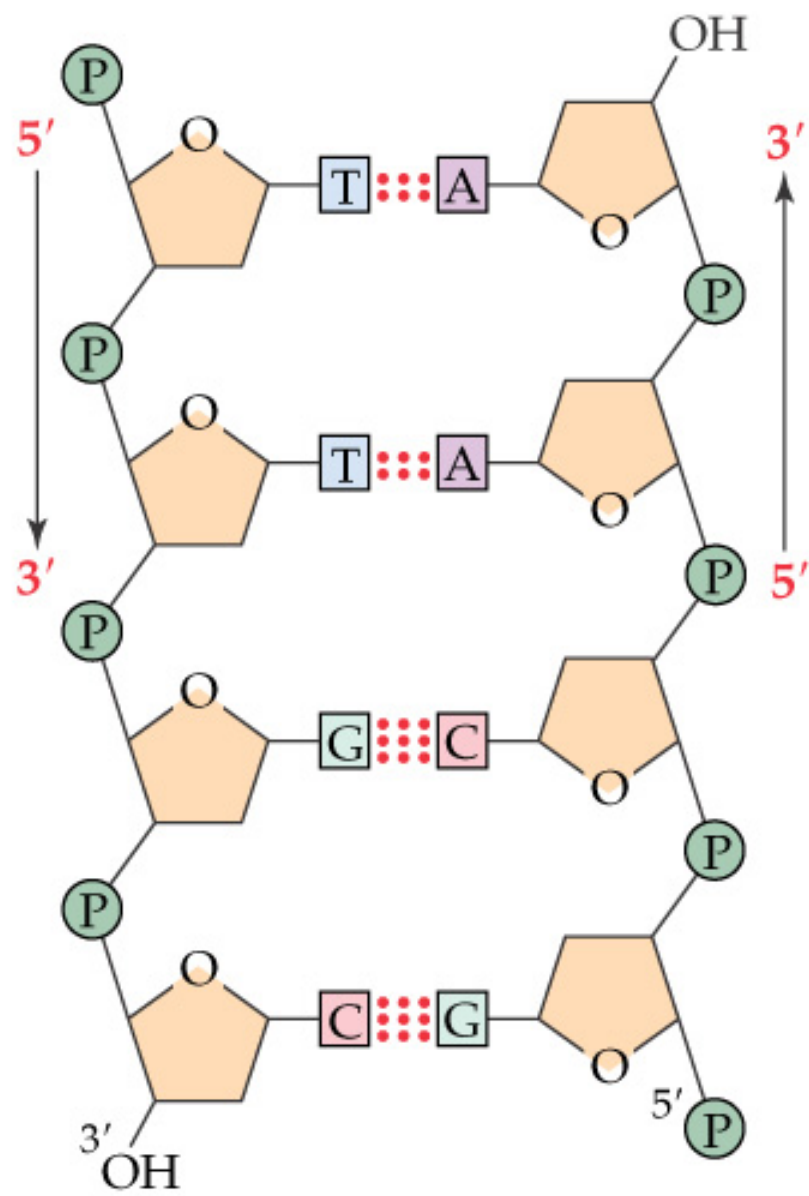
Thymine-Adenine

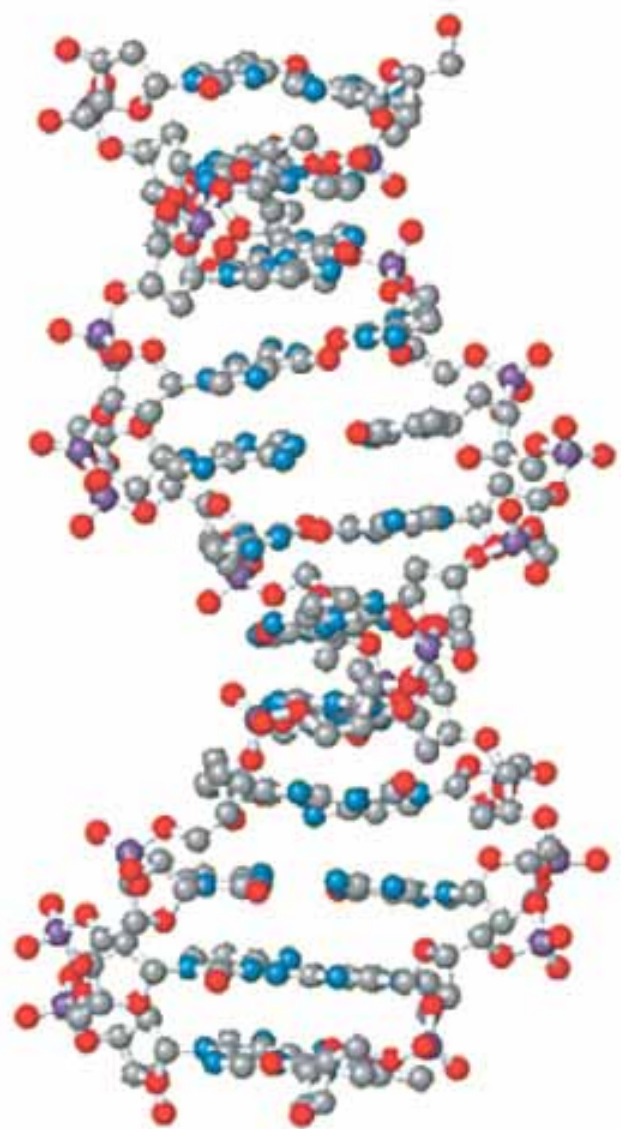


Cytosine-Guanine

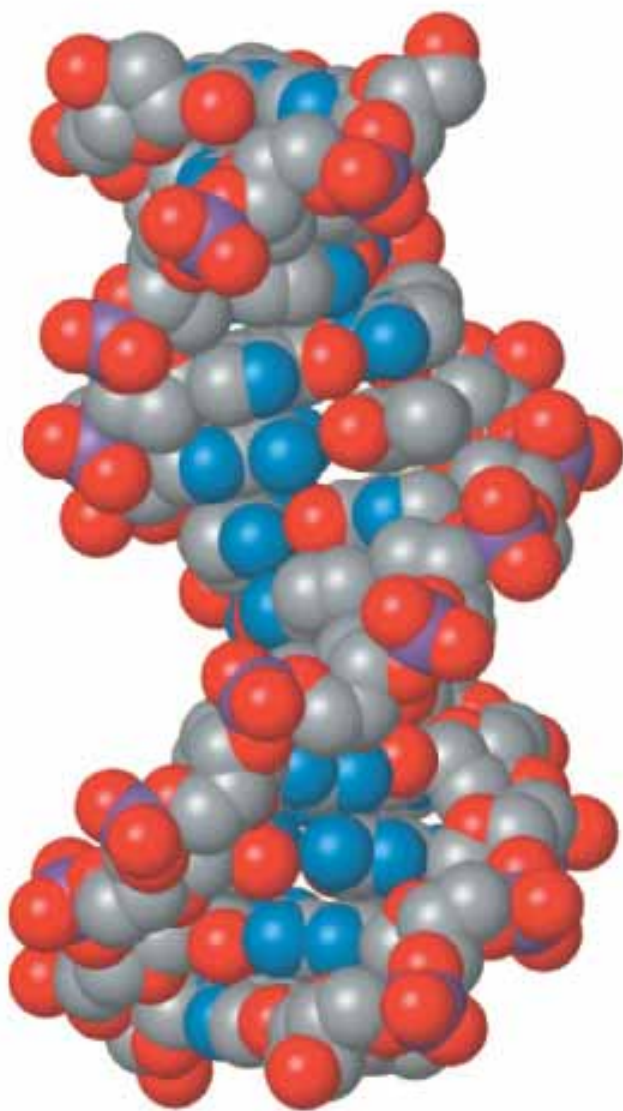




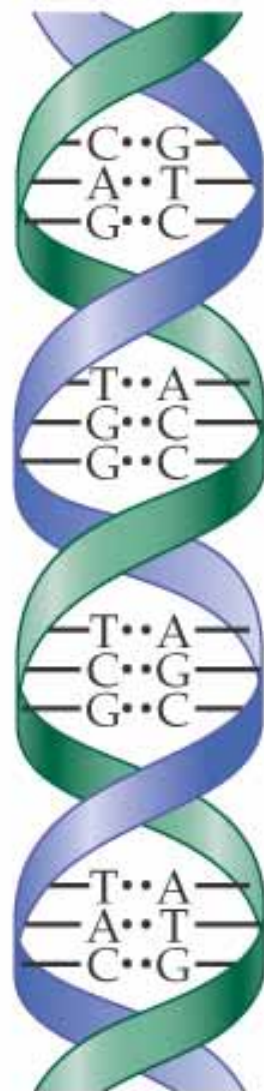




(a)

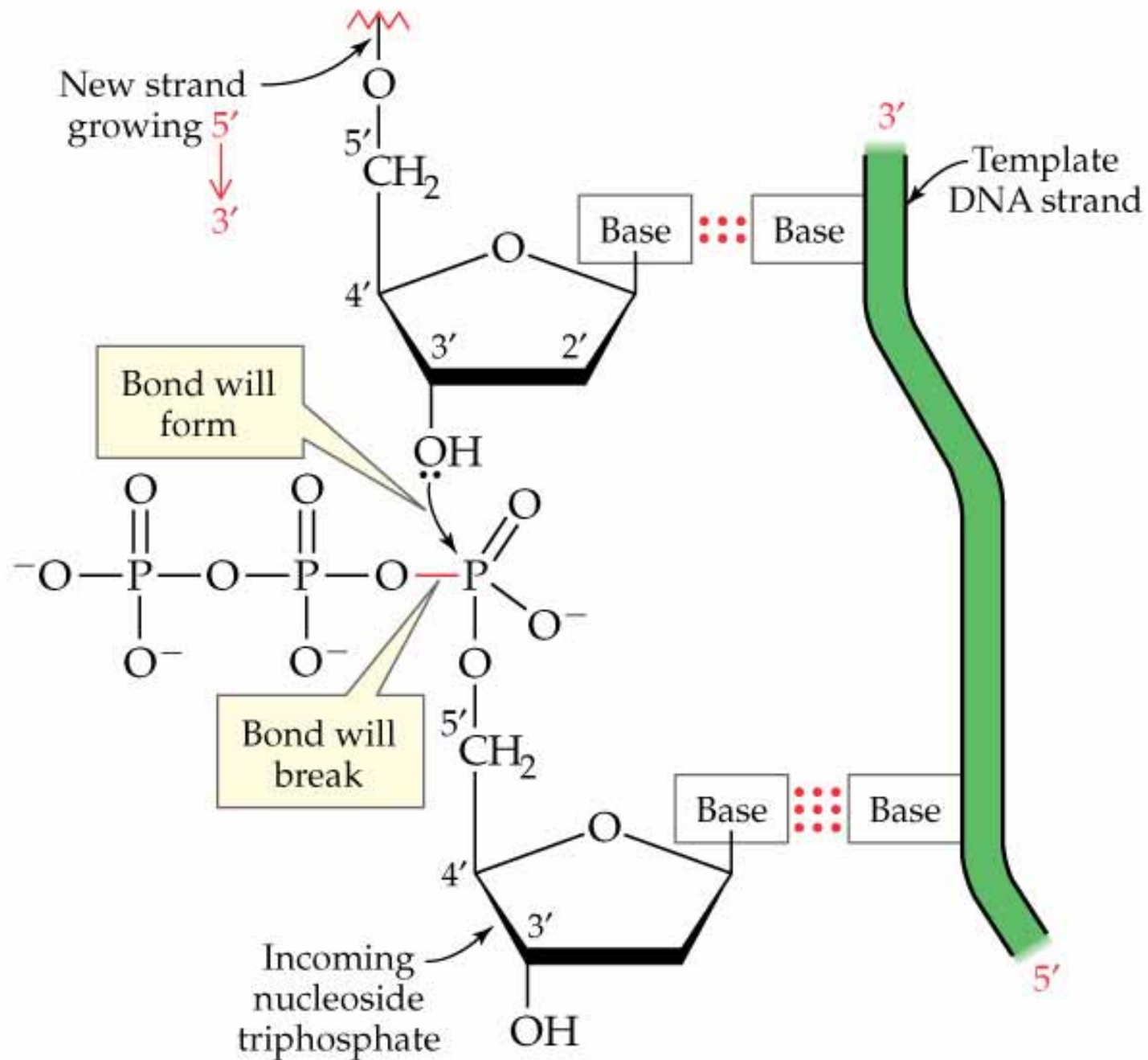


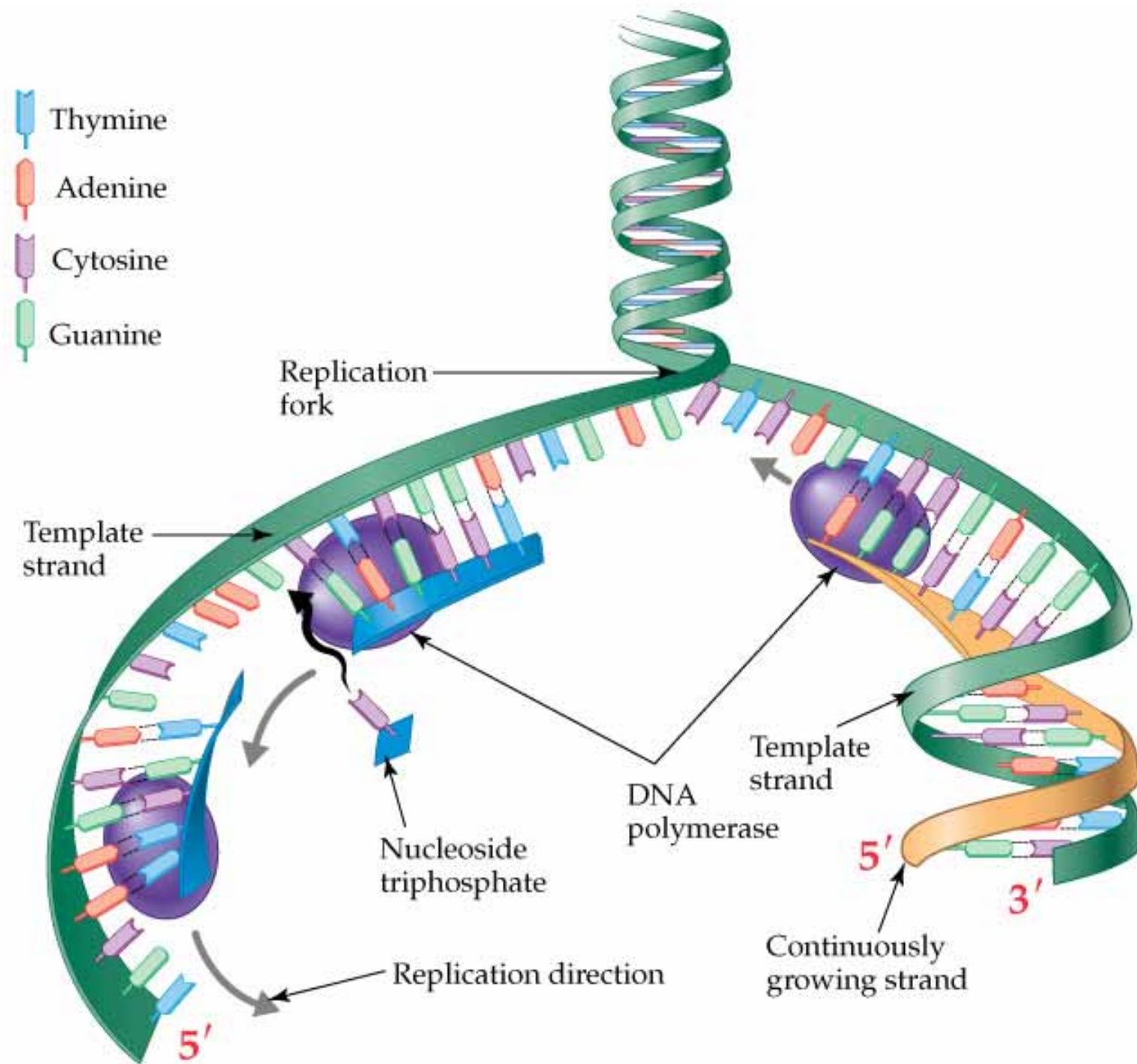
(b)

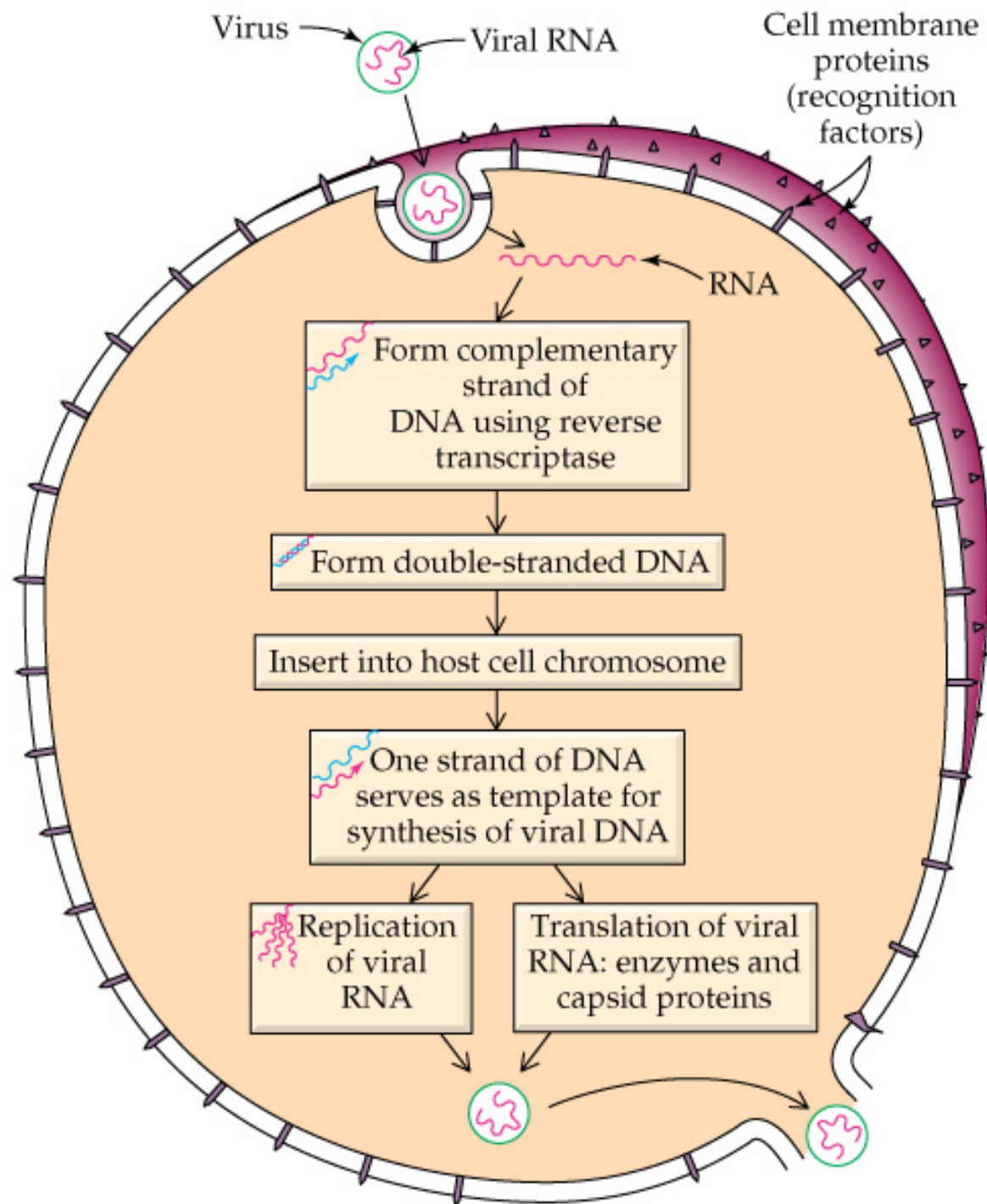


(c)

Bond formation in DNA replication







Cell nucleus



DNA

Transcription



mRNA

- The following three RNA make it possible for the encoded information carried by the DNA to be put to use in the synthesis of proteins.

- Ribosome RNA***: The granular organelles in the cell where protein synthesis takes place. These organelles are composed of protein and ribosomal RNA (rRNA).

- Messenger RNA (mRNA)***: The RNA that carries the code transcribed from DNA and directs protein synthesis.

- Transfer RNA (tRNA)***: The smaller RNA that delivers amino acids one by one to protein chains growing at ribosomes. Each tRNA recognizes and carries only one amino acid.



